Diss. ETH No. 18269

Porous Materials and Capsules from Particle-Stabilized Emulsions

A dissertation submitted to the

Swiss Federal Institute of Technology Zurich

for the degree of

Doctor of Sciences

presented by

Ilke Akartuna

Dipl. Ing. TUHH
born on January 22, 1979
Turkey

accepted on the recommendation of

Prof. Dr. Ludwig J. Gauckler, examiner
Prof. Dr. Erich J. Windhab, co-examiner

Zurich, 2009

Acknowledgments

Adrian Marberger, André R. Studart, Anna Evans, Anthony Palladino, Barbara Scherrer, Basil Thalmann, Boris Iwanovsky, Christina Pecnik, David Magias-Alguacil, Elena Tervoort, Erich J. Windhab, Fabian Fischer, Felix Schuler, Frank T. Filser, Gabor Csucs, Gary Messing, Hakan Hakkı Atasoy, Ilhan A. Aksay, Irène Urbánek, Iwan Schenker, Jérôme Zemp, Joanna C. H. Wong, Joëlle Hofstetter, Lars Fleig, Lea Nowack, Lorenz J. Bonderer, Ludwig J. Gauckler, Mischa Müller, My Family, Nicolas Walpen, Peter Kocher, Pierre Elsener, Pierrick Prétat, Oleg Lukin, René Kopetschny, Yasmina Ries.

Table of Contents

Summary

Emulsions stabilized through the adsorption of colloidal particles at the liquid-liquid interface have been of interest in a wide variety of applications ranging from pharmaceutical and food products to cosmetic and agricultural applications. Particle stabilized-emulsions often contain a limited concentration of particles. Thus, the aim of this thesis was to develop a simple and general approach for the preparation of stable particle-stabilized emulsions through the in situ surface modification of a high concentration of particles with different surface chemistries, and then the application of these emulsions as templates for the fabrication of colloidal capsules and macroporous materials.

Oil-in-water and water-in-oil emulsions are efficiently stabilized using colloidal inorganic particles. The adsorption of initially hydrophilic particles to the oil-water interface is induced by adjusting the particle wetting behaviour in the liquid media through the adsorption of short amphiphilic molecules. Short amphiphiles are shown to be appropriate molecules for the in situ hydrophobization of high concentration of particles. Different types of emulsions are formed by changing the liquid phase in which the particles are originally dispersed and surface modified. In addition to the emulsions stabilized with surface modified inorganic particles, highly stable water-in-oil emulsions are prepared upon adsorption of polymeric colloidal particles at the oil-water interface. The adsorption of polymeric particles at the oil-water interface is accomplished by adjusting the wetting of the particles by the two immiscible liquids. To elucidate the mechanisms taking place during emulsification, the conditions required for particle adsorption at the liquid-liquid interface and for the stabilization of different type of emulsions using the same particles in different liquids are investigated in detail. The final microstructure of oil-water mixtures are tailored by adjusting the initial composition of emulsions. The use of high concentration of particles leads to enhanced stability of particle-stabilized emulsions.

Emulsions stabilized by colloidal particles with different surface chemistries exhibit solid-like behaviour with a viscoelastic character and pronounced yield stress.

The rheological properties of particle-stabilized emulsions and the dependence of these properties on the initial composition of emulsions are investigated to explain the possible mechanisms that determine the final droplet size of emulsions. To evaluate the interrelation between the composition and the rheology of emulsions, a model is applied to the experimental emulsion data. In agreement with the model, the final droplet size of emulsions is controlled by the interfacial tension of the suspension-oil interface, the viscosity of emulsions, and the shear rate during mixing.

Dilution of such highly stable emulsions results in wet colloidal capsules with single layer of particles in the outer shell. Close-packed particle shell surrounding each droplet provide the structural rigidity of the capsules and enable drying of wet capsules into semi-permeable, hollow capsules. The permeability of the capsules can be controlled by the interstices between the particles. Particle locking at the interface using polymers or ionic species further allows adjusting the mechanical strength and the permeability of the dry capsules.

The long term stability and viscoelastic character of particle-stabilized emulsions also allow shaping of the emulsions using conventional technologies, and drying and sintering of the emulsions directly into macroporous materials in the absence of any chemical reaction. The microstructure and the porosity of porous materials are tailored by changing the composition of the original emulsions. Sintering of emulsions stabilized by polymeric particles enable the preparation of porous polymers from a variety of polymeric particles including intractable polymers. The solid macroporous ceramics obtained from emulsions stabilized with inorganic particles exhibit variety of microstructures ranging from homogeneous to hierarchical pore structures. The incorporation of a third phase such as air into oil-in-water emulsions results in porous structures exhibiting pore sizes at length scales differing by one order of magnitude. Tailoring the pore structure in different length scales enables the fabrication of porous ceramics with porosities up to 96% and compressive strengths up to 13 MPa.

Zusammenfassung

Emulsionen, die durch die Adsorption von kolloidalen Partikel auf der flüssig-flüssig Grenzfläche stabilisiert sind, sind interessant für viele Anwendungen: von Arzneimitteln und Nährungsmitteln bis hin zu Kosmetikprodukten und agrarwirtschaftliche Anwendungen. Die partikelstabilisierten Emulsionen enthalten häufig eine limitierte Partikelkonzentration. Deshalb war das Ziel dieser Doktorarbeit eine einfache und allgemeine Methode zu entwickeln um die Herstellung der stabilen partikelstabilisierten Emulsionen durch eine in situ Oberflächenmodifikation der höheren Partikelkonzentration mit einer unterschiedlichen Oberflächenchemie zu ermöglichen, und dann die Anwendung dieser Emulsionen als Vorlage für die Herstellung von kolloidalen Kapseln und makroporösen Materialen.

Öl-in-Wasser und Wasser-in-Öl Emulsionen werden effektiv mit den kolloidalen anorganischen Partikel stabilisiert. Die Adsorption der anfangs hydrophilen Partikel auf der Öl-Wasser Grenzfläche wird durch Anpassung des Partikelbenetzungsverhaltens im flüssigen Medium durch die Adsorption von kurzen amphiphilen Molekülen induziert. Kurze Amphiphile sind geeignete Moleküle für die in situ Hydrophobisierung von Partikel in hohen Konzertrationen. Unterschiedliche Emulsionstypen werden durch die Veränderung der flüssigen Phase erhalten, in welcher die Partikel ursprünglich dispergiert sind und deren Oberfläche modifiziert ist. Zusätzlich zu den Emulsionen, die mit oberflächenmodifizierten anorganischen Partikel stabilisiert sind, wurden hochstabile Wasser-in-Öl Emulsionen durch die Adsorption von polymeren Kolloidpartikel auf der Öl-Wasser Grenzfläche hergestellt. Die Adsorption der polymeren Kolloidpartikel auf der Öl-Wasser Grenzfläche wird durch Anpassung des Partikelbenetzungsverhaltens mit zwei unmischbaren Flüssigkeiten durchgeführt. Um den Mechanismus der Emulgierung aufzuklären, wurden die Konditionen für die Adsorption der Partikel auf der flüssig-flüssig Grenzfläche und für die Stabilisierung der unterschiedlichen Emulsionstypen mit denselben Partikel in unterschiedlichen Flüssigkeiten ausführlich untersucht. Die finalen Mikrostrukturen der Öl-Wasser Mischungen werden durch Anpassen der Emulsionsanfangszusammensetzung

bestimmt. Die Verwendung von hochkonzentrierten Partikel führt zu verbesserter Stabilität der partikelstabilisierten Emulsionen.

Emulsionen, die mit Kolloidpartikel unterschiedlicher Oberflächenchemie stabilisiert sind, zeigen ein Festkörper-ähnliches Verhalten mit einem viskoelastischen Charakter und einem ausgeprägten Fliessspannung. Die rheologischen Eigenschaften der partikelstabilisierten Emulsionen und die Abhängigkeit dieser Eigenschaften von der Anfangskomposition der Emulsionen wurden untersucht, um den möglichen Mechanismus, welcher die Endtropfengrösse der Emulsionen bestimmt zu erklären. Um die Zusammenhang zwischen der Rezeptur und der Rheologie der Emulsionen zu evaluieren, wurde ein Modell auf die experimentellen Emulsionsdaten angewendet. In Übereinstimmung mit dem Modell, wird die Endtropfengrösse der Emulsionen durch die Oberflächenspannung der Suspension-Öl Grenzfläche, die Viskosität der Emulsionen, und die Schergeschwindigkeit während des Mischens kontrolliert.

Verdünnung der hochstabilen Emulsionen führt zu nass kolloidalen Kapseln mit einer einzigen Partikelschicht in der äusseren Hülle. Die dichtgepackten Partikel-schichten um jedes Tröpfchen liefern die Struktursteifigkeit der Kapseln und ermöglichen das Trockenen der nassen Kapseln zu halbdurchlässigen Hohlkapseln. Die Durchlässigkeit der Kapseln kann durch die Fuge zwischen den Partikeln kontrolliert werden. Das Verbinden von Partikel auf der Grenzfläche durch Polymere oder ionische Spezies ermöglicht das Anpassen der mechanischen Festigkeit und der Durchlässigkeit der trockenen Kapseln.

Die Langzeitstabilität und der Viskoelastizitätcharakter der partikelstabilisierten Emulsionen ermöglichen auch die Formgebung der Emulsionen mit konventionellen Technologien, sowie das Trocknen und Sintern der Emulsionen direkt zu makroporösen Materialien ohne irgendeiner chemischen Reaktion. Das Gefüge und die Porosität der porösen Materialien werden durch die Veränderung des Aufbaus der ursprünglichen Emulsionen reguliert. Das Sintern der Emulsionen, die mit den Polymerpartikel stabilisiert sind, ermöglicht die Herstellung von porösen Polymeren anhand einer breiten Auswahl an Polymerpartikeln - einschliesslich unlöslichen Polymeren. Die festen makroporösen Keramiken, die von aus den anorganischen partikelstabilisierten Emulsionen hergestellt werden, zeigen eine breite Vielfalt an Mikrostrukturen - von homogenen bis hierarchischen Porenstrukturen. Die Beimischung einer dritten Phase

wie Luft in Öl-in-Wasser Emulsionen ergibt poröse Strukturen mit Poren, deren Länge um eine Grössenordnung variieren kann. Das Kontrollieren der Porenstruktur in unterschiedlichen Längestufen ermöglicht die Herstellung von porösen Keramiken mit Porositäten bis 96% und Druckfestigkeiten bis 13 MPa.

1 Introduction

The processing technology of ceramics is an important aspect of ceramic engineering which enables the fabrication of ceramic products with different size, shape, composition, structure, and cost. The properties and functions of ceramics are very much dependent on their chemical composition and microstructure. To control these features and minimize the microstructural defects, processing of ceramics through the consolidation of colloidal particle suspensions have been subject of research and development [1].

Tailoring the surface chemistry of colloidal particles and controlling the interactions between particles enable the fabrication of more reliable ceramics. Several colloidal processing routes such as slip casting, tape casting/screen printing, pressure filtration, osmotic consolidation, centrifugal consolidation, aqueous injection molding, gel casting, direct coagulation casting, spray pyrolysis, and robocasting have been developed in response to a variety of applications which require different material properties and functions [2, 3].

In addition to dense ceramics, porous ceramics are also required by an increasing number of applications such as filtration of molten metals, high-temperature thermal insulation, support for catalytic reactions, filtration of particulates from diesel engine exhaust gases, and filtration of hot corrosive gases in various industrial processes [4, 5]. These applications take advantage of the low thermal mass, low thermal conductivity, controlled permeability, high surface area, low density, high specific strength, and low dielectric constant of porous ceramics.

The properties of porous ceramics are highly influenced by their chemical composition and microstructure. Porosity, pore morphology and size distribution of the porous structures can be tailored for a certain application by the processing route used for the production of the porous ceramic. Similar to the production of dense ceramics, several processing methods based on colloidal routes have been developed for the preparation of macroporous ceramics. Among these methods, replica, direct foaming, and sacrificial template methods have become the most widely applied approaches [5-7].

The replica technique involves the impregnation of a cellular structure made of polymer, coral, or wood with a ceramic slurry or a precursor solution and pyrolysis of the template material to produce a macroporous ceramic exhibiting the same structure as the original porous material. This technique has been mainly used for the fabrication of uniform cellular open-cell (reticulate) ceramic structures.

In contrast to replica method, direct foaming method is based on the incorporation of a gaseous phase into a ceramic suspension or a sol and sintering of dry foams to produce macroporous ceramics. Direct foaming techniques allow formation of either open or closed cell ceramics with dense struts. Wet foams are usually stabilized by surface active agents such as long-chain amphiphilic molecules and proteins to prevent disproportionation and coalescence. However, due to the low adsorption energy of surface active molecules at the gas–liquid interface, wet foams collapse within a few hours after foaming. The stability of foam bubbles against collapse is achieved by setting the foam thorough the addition of gelling and cross linking agents to the wet foam [8, 9] or condensation of metal hydroxides and alkoxides [10, 11]. As an alternative to the surfactant-stabilized direct foaming techniques, colloidal particles have recently been used for the stabilization of gas bubbles [7, 12]. Unlike surface active molecules, particles adsorbed at the gas-liquid interface were observed to impede the drainage, coalescence, and disproportionation [13].

The sacrificial template method involves incorporation of a fugitive phase such as starch, carbon, salts, and polymer beads into ceramic particle assemblies or ceramic precursors and subsequent extraction of these phases upon pyrolysis or leaching to generate pores within the final structure. This technique allows formation of either open or closed cell macroporous ceramics. The time consuming extraction steps and the extensive amount of gaseous by-products generated during extraction of the organic phases can be overcome using liquid fugitive phases such as water, supercritical carbon dioxide, and volatile oils, which can be evaporated or sublimated at milder conditions without emitting toxic gases. The main advantage of the sacrificial template method is the possibility of adjusting the porosity, pore size and pore morphology of the porous ceramic independently just by changing the size and the amount of the fugitive materials.

The incorporation of volatile oils as sacrificial phases by means of emulsion templates has been a versatile approach to produce macroporous materials. The emulsion templating method is based on preparation of emulsions with inorganic

precursors in the continuous phase and subsequent removal of the dispersed droplets by drying and heat treatment.

Due to the high liquid-liquid interfacial area, emulsions are thermodynamically unstable systems. They often undergo coalescence, Ostwald ripening, and phase separation processes. Stabilization of emulsions is normally achieved through the adsorption of surface active long-chain amphiphiles or proteins at the liquid-liquid interface [14, 15]. However, due to the weak attachment of these molecules at interfaces, emulsions usually collapse during the removal of the liquid phases. Therefore, the emulsion microstructure is usually consolidated thorough the gelation of the continuous phase via sol-gel processes. The consolidation of the emulsions with sol-gel transitions usually leads to formation of macroporous monoliths with porosities up to 92% and pore sizes ranging from a few hundred nanometers to a few micrometers. While sol-gel based emulsion templating enables the production of highly porous ceramics with wide range of pore sizes, the examples of porous structures have been mainly limited to the well-defined chemical compositions such as silica [16-22] and titania [16, 17, 23, 24].

Alternatively, colloidal particles adsorbed at liquid interfaces have also been used to stabilize emulsions [25-27] and produce macroporous ceramics after drying [28, 29]. Stabilization of emulsions by solid particles offers advantages over surfactant-stabilized systems due to the increased emulsion stability achieved in the presence of solid particles against coalescence and Oswald ripening [27, 30, 31]. The effectiveness of particles against destabilization mechanisms descends from the irreversible adsorption of particles to the oil-water interface, which results from the high energy of attachment of particles to the interface [27, 30-33]. As a consequence of irreversible adsorption, particles forming dense films around the dispersed droplets hinder coalescence and resist Ostwald ripening. Furthermore, three-dimensional network of particles as a result of particle-particle interactions in the continuous phase brings additional stabilization against coalescence [30].

This enhanced stability of emulsions achieved with particles allows for the consolidation of the emulsion microstructure without requiring gelation or any other chemical reactions. Macroporous ceramics obtained from particle-stabilized emulsions may exhibit interconnected cells ranging from 5 to 50 μm in size [28].

Besides bulk macroporous ceramics, formation of solid shell of close packed colloidal particles at the interface of emulsion droplets has also led to fabrication of

semi-permeable capsules [34-39]. Such capsules have become increasingly important for the efficient encapsulation and delivery of living cells or active agents in food processing, pharmaceutical and agricultural industries, and biomedicine [40-44].

Emulsion droplets produced by mechanical mixing [34, 35, 37] or microfluidic devices [39, 45] can be harvested to produce colloidal wet capsules as a result of the enhanced emulsion stability achieved in the presence particles. In addition to wet capsules, dry hollow capsules can also be prepared upon evaporation of the liquid phases [35, 46-49]. Fabrication of dry capsules often requires strengthening of the particle shells to prevent capsule rupture under the high capillary forces developed during drying. Thus, the particles at the interface are locked together to adjust the elasticity of the capsule wall [35, 38, 48, 50, 51]. The permeability of capsules is usually defined by the interstices between the colloidal particles and can be tuned by changing the particle size and/or controlling the extent of particle locking at the interface [35, 37].

Emulsion templating method has been successfully applied to produce bulk macroporous ceramics and semi-permeable capsules. The high stability of particle-stabilized emulsions has allowed for a better control over the microstructure of materials as compared to other approaches based on surfactant-stabilized mixtures. However, stabilization of emulsions has been so far limited to particles whose surface wettability can be tailored through prior chemical treatments such as silanization of silica particles, or capping ligands sophisticatedly designed for iron oxide nanoparticles. The use of inorganic particles with tailored properties should enable the manufacture of novel materials with unique functionalities, including biocompatibility, high-temperature resistance, high strength, and magnetic response. Hence, a general method to tailor the surface chemistry and control the processing of inorganic particles of different size and surface chemistry into macroporous ceramics and semi-permeable functional inorganic capsules is yet to be developed.

The aim of this thesis is to develop a new simple and general method to produce macroporous ceramics and semi-permeable inorganic capsules from particle-stabilized emulsions by tailoring the surface chemistry of metal oxide particles of various sizes and chemical compositions. The method relies on short amphiphilic molecules for the surface modification of a wide range of inorganic particles. Short amphiphilic molecules with a head group showing high affinity towards the particle surface are selected for the in situ surface hydrophobization of initially hydrophilic metal oxide particles. The high solubility and critical micelle concentrations of short amphiphiles in

the liquid phase allows the surface modification of high concentrations of submicrometer-sized particles of various surface chemistries. In situ hydrophobization with short amphiphiles renders the particles partially hydrophobic, favoring their adsorption at the oil-water interface. Particles adsorbed at the interface lead to the formation of remarkably stable emulsions, which can be characterized with a viscoelastic behavior. The long-term stability and the viscoelastic behavior of the particle-stabilized emulsions enable their processing into porous structures of various shapes using conventional shaping technologies without requiring any further gelation or strengthening reaction. Thus, particle-stabilized emulsions can be directly dried and sintered to obtain macroporous ceramics of various porosity levels, pore morphologies and pore size ranges.

In addition to bulk macroporous ceramics, this simple approach presented here has also allowed for the production of large quantities of functional semi-permeable wet and dry capsules through the stabilization of emulsions with inorganic particles of various sizes, chemical compositions, and functionalities.

In the following chapters, the versatility of the method will be illustrated using examples of emulsions, macroporous ceramics, and colloidal capsules produced by colloidal alumina, silica, and iron oxide particles as well as polymeric particles.

1.1 References

1. *9th International Ceramic Processing Science and Symposium*. 2006. Florida, USA: John Wiley & Sons.

2. Lange, F. F., *Powder processing science and technology for increased reliability*. J. Am. Ceram. Soc., 1989, 72(1), 3-15.

3. Lewis, J. A., *Colloidal processing of ceramics*. J. Am. Ceram. Soc., 2000, 83(10), 2341-2359.

4. Ishizaki, K., Komarneni, S., Nanko, M., *Porous Materials: Process Technology and Applications*. 1998, Dordrecht, Kluwer Academic Publishers.

5. Scheffler, M., Colombo, P., *Cellular Ceramics: Structure, Manufacturing, Properties and Applications*. 2005, Weinheim, Wiley - VCH.

6. Colombo, P., *Conventional and novel processing methods for cellular ceramics*. Philos. Trans. Roy. Soc. A, 2006, 364, 109-124.

7. Studart, A. R., Gonzenbach, U. T., Tervoort, E., Gauckler, L. J., *Processing routes to macroporous ceramics: A review*. J. Am. Ceram. Soc., 2006, 89(6), 1771-1789.

8. Sepulveda, P., *Gelcasting foams for porous ceramics*. Am. Ceram. Soc. Bull., 1997, 76(10), 61-65.

9. Green, D. J., Colombo, P., *Cellular ceramics: Intriguing structures, novel properties, and innovative applications*. MRS Bull., 2003, 28(4), 296-300.

10. Wu, M., Fujiu, T., Messing, G. L., *Synthesis of cellular inorganic materials by foaming sol-gels.* J. Non-Crystalline Solids, 1990, 121(1-3), 407-412.

11. Fujiu, T., Messing, G. L., Huebner, W., *Processing and properties of cellular silica synthesized by foaming sol-gels.* J. Am. Ceram. Soc., 1990, 73(1), 85-90.

12. Gonzenbach, U. T., Studart, A. R., Tervoort, E., Gauckler, L. J., *Macroporous ceramics from particle-stabilized wet foams.* J. Am. Ceram. Soc., 2007, 90(1), 16-22.

13. Gonzenbach, U. T., Studart, A. R., Tervoort, E., Gauckler, L. J., *Ultrastable particle-stabilized foams.* Angew. Chem. Int. Ed., 2006, 45(21), 3526-3530.

14. Becher, P., *Emulsions: Theory and Practice*. 3rd ed. 2001, Washington, D.C., American Chemical Society. 513.

15. Myers, D., *Surfaces, Interfaces and Colloids: Principles and Applications*. 1991, Weinheim, VCH Publishers.

16. Imhof, A., Pine, D. J., *Ordered macroporous materials by emulsion templating.* Nature, 1997, 389(6654), 948-951.

17. Imhof, A., Pine, D. J., *Uniform macroporous ceramics and plastics by emulsion templating.* Adv. Mater., 1998, 10(9), 697-700.

18. Yi, G.-R., Yang, S.-M., *Microstructures of porous silica prepared in aqueous and nonaqueous emulsion templates.* Chem. Mater., 1999, 11(9), 2322-2325.

19. Sen, T., Tiddy, G. J. T., Casci, J. L., Anderson, K. R., *Macro-cellular silica foams: Synthesis during the natural creaming process of an oil-in-water emulsion.* Chem. Commun., 2003, 2182-2183.

20. Sen, T., Tiddy, G. J. T., Casci, J. L., Anderson, M. W., *Meso-cellular silica foams, macro-cellular silica foams and mesoporous solids: A study of emulsion mediated synthesis.* Microporous Mesoporous Mater., 2005, 78, 255-263.

21. Carn, F., Colin, A., Achard, M.-F., Deleuze, H., Sellier, E., Birot, M., Backov, R., *Inorganic monoliths hierarchically textured via concentrated direct emulsion and micellar templates.* J. Mater. Chem., 2004, 14(9), 1370-1376.

22. Carn, F., Colin, A., Schmitt, V., Leal Calderon, F., Backov, R., *Soft matter, sol-gel process and external magnetic field to design macrocellular silica scaffolds.* Colloids Surf., A, 2005, 263, 341-346.

23. Manoharan, V. N., Imhof, A., Thorne, J. D., Pine, D. J., *Photonic crystals from emulsion templates.* Adv. Mater., 2001, 13(6), 447-450.

24. Imhof, A., Pine, D. J., *Preparation of titania foams.* Adv. Mater., 1999, 11(4), 311-314.

25. Ramsden, W., *Separation of solids in the surface-layers of solutions and suspensions (Observations on surface-membranes, bubbles, emulsions, and mechanical coagulation). Preliminary account.* Proc. Roy. Soc. London, 1903, 72, 156-164.

26. Pickering, S. U., *Emulsions.* J. Chem. Soc., 1907, 91, 2001-2021.

27. Aveyard, R., Binks, B. P., Clint, J. H., *Emulsions stabilised solely by colloidal particles.* Adv. Colloid Interface Sci., 2003, 100-102, 503-546.

28. Binks, B. P., *Macroporous silica from solid stabilized emulsion templates.* Adv. Mater., 2002, 14(24), 1824-1827.

29. Arditty, S., Schmitt, V., Giermanska-Kahn, J., Leal Calderon, F., *Materials based on solid-stabilized emulsions.* J. Colloid Interface Sci., 2004, 275(2), 659-664.

30. Binks, B. P., *Particles as surfactants-Similarities and differences.* Curr. Opin. Colloid Interface Sci., 2002, 7(1-2), 21-41.

31. Hunter, T. N., Pugh, R. J., Franks, G. V., Jameson, G. J., *The role of particles in stabilising foams and emulsions.* Adv. Colloid Interface Sci., 2008, 137(2), 57-81.

32. Pieranski, P., *Two-dimensional interfacial colloidal crystals.* Phys. Rev. Lett., 1980, 45(7), 569-572.

33. Levine, S., Bowen, B. D., Partridge, S. J., *Stabilization of emulsions by fine particles I. Partitioning of particles between continuous phase and oil/water interface.* Colloids Surf., 1989, 38(2), 325-343.

34. Velev, O. D., Furusawa, K., Nagayama, K., *Assembly of latex particles by using emulsion droplets as templates. 1. Microstructured hollow spheres.* Langmuir, 1996, 12(10), 2374-2384.

35. Dinsmore, A. D., Hsu, M. F., Nikolaides, M. G., Marquez, M., Bausch, A. R., Weitz, D. A., *Colloidosomes: Selectively permeable capsules composed of colloidal particles.* Science, 2002, 298, 1006-1009.

36. Hsu, M. F., Nikolaides, M. G., Dinsmore, A. D., Bausch, A. R., Gordon, V. D., Chen, X., Hutchinson, J. W., Weitz, D. A., Marquez, M., *Self-assembled shells composed of colloidal particles: Fabrication and characterization.* Langmuir, 2005, 21, 2963-2970.

37. Duan, H., Wang, D., Sobal, N. S., Giersig, M., Kurth, D. G., Möhlwald, H., *Magnetic colloidosomes derived from nanoparticle interfacial self-assembly.* Nano Lett., 2005, 5(5), 949-952.

38. Noble, P. F., Cayre, O. J., Alargova, R. G., Velev, O. D., Paunov, V. N., *Fabrication of "Hairy" colloidosomes with shells of polymeric microrods.* J. Am. Chem. Soc., 2004, 126, 8092-8093.

39. Subramaniam, A. B., Abkarian, M., Stone, H. A., *Controlled assembly of jammed colloidal shells on fluid droplets.* Nat. Mater., 2005, 4, 553-556.

40. Gibbs, B. F., Kermasha, S., Alli, I., Mulligan, C. N., *Encapsulation in the food industry: A review.* Int. J. Food Sci. Nutr., 1999, 50(3), 213-224.

41. Gouin, S., *Microencapsulation: Industrial appraisal of existing technologies and trends.* Trends Food Sci. Technol., 2004, 15(7-8), 330-347.

42. Chaikof, E. L., *Engineering and material considerations in islet cell transplantation.* Annu. Rev. Biomed. Eng., 1999, 1(1), 103-127.

43. Park, J. K., Chang, H. N., *Microencapsulation of microbial cells.* Biotechnol. Adv., 2000, 18(4), 303-319.

44. Madene, A., Jacquot, M., Scher, J., Desobry, S., *Flavour encapsulation and controlled release - A review.* Int. J. Food Sci. Technol., 2006, 41(1), 1-21.

45. Lee, D., Weitz, D. A., *Double emulsion-templated nanoparticle colloidosomes with selective permeability.* Adv. Mater., 2008, 20(18), 3498-3503.

46. Croll, L. M., Stöver, H. D. H., *Formation of tectocapsules by assembly and cross-linking of poly(divinylbenzene-alt-maleic anhydride) spheres at the oil-water interface.* Langmuir, 2003, 19, 5918-5922.

47. Skaff, H., Lin, Y., Tangirala, R., Breitenkamp, K., Böker, A., Russell, T. P., Emrick, T., *Crosslinked capsules of quantum dots by interfacial assembly and ligand crosslinking.* Adv. Mater., 2005, 17(17), 2082-2086.

48. Kim, S. H., Heo, C. J., Lee, S. Y., Yi, G. R., Yang, S. M., *Polymeric particles with structural complexity from stable immobilized emulsions.* Chem. Mater., 2007, 19(19), 4751-4760.

49. Kim, J.-W., Fernandez-Nievest, A., Dan, N., Utada, A. S., Marquez, M., Weitz, D. A., *Colloidal assembly route for responsive colloidosomes with tunable permeability*. Nano Lett., 2007, 7(9), 2876-2880.

50. Gordon, V. D., Chen, X., Hutchinson, J. W., Bausch, A. R., Marquez, M., Weitz, D. A., *Self-assembled polymer membrane capsules inflated by osmotic pressure*. J. Am. Chem. Soc., 2004, 126, 14117-14122.

51. Bon, S. A. F., Cauvin, S., Colver, P. J., *Colloidosomes as micron-sized polymerisation vessels to create supracolloidal interpenetrating polymer network reinforced capsules*. Soft Matter, 2007, 3(2), 194-199.

2 Stabilization of Oil-in-Water Emulsions by Colloidal Particles Modified with Short Amphiphiles*

Abstract

Emulsions stabilized through the adsorption of colloidal particles at the liquid-liquid interface have long been used and investigated in a number of different applications. The interfacial adsorption of particles can be induced by adjusting the particle wetting behaviour in the liquid media. Here, we report a new approach to prepare stable oil-in-water emulsions by tailoring the wetting behaviour of colloidal particles in water using short amphiphilic molecules. We illustrate the method using hydrophilic metal oxide particles initially dispersed in the aqueous phase. The wettability of such particles in water is reduced by an in situ surface hydrophobization that induces particle adsorption at oil-water interfaces. We evaluate the conditions required for particle adsorption at the liquid-liquid interface and discuss the effect of the emulsion initial composition on the final microstructure of oil-water mixtures containing high concentrations of alumina particles modified with short carboxylic acids. This new approach for emulsion preparation can be easily applied to a variety of other metal oxide particles.

---

* *I. Akartuna, A. R. Studart, E. Tervoort, U. T. Gonzenbach, and L. J. Gauckler, Langmuir, 2008, 24 (14), 7161-7168.*

2.1 Introduction

Emulsions are of great practical interest due to their widespread use in pharmaceutical, food, cosmetic, paint, and ink products. In many of these applications the stability of emulsions is of utmost importance to keep their properties over long periods of time [1].

However, emulsions often undergo coalescence, Ostwald ripening, and phase separation processes. Stable emulsions are normally prepared by adsorbing surface active molecules like long-chain surfactants, amphiphilic polymers, lipids, and proteins at the liquid-liquid interface. These molecules lower the energy required for droplet formation and enhance the stability of emulsions by providing a steric/electrostatic barrier against droplet coalescence [1, 2].

Alternatively, Ramsden [3] and Pickering [4] have shown more than a century ago that solid particles adsorbed at liquid-liquid interfaces can also be used for the stabilization of so-called Pickering emulsions. As opposed to surface active molecules, interfacially adsorbed particles lower the system free energy by reducing the liquid-liquid interfacial area [5, 6].

Stabilization of emulsions by solid particles usually leads to increased stability against coalescence and Ostwald ripening in comparison to surfactant-stabilized systems [6, 7]. The effectiveness of particles against these destabilization processes stems from their strong adsorption to the liquid-liquid interface [5]. The energy of attachment of particles at interfaces can be several orders of magnitude higher than thermal energy, which ultimately leads to irreversible interfacial adsorption [6-8]. The adsorption energy increases monotonically with increasing contact angles (θ) and proportionally with $(1 \pm \cos\theta)^2$, reaching a maximum at $\theta = 90°$ [6].

Besides a strong adsorption at the interface, the stabilization of emulsions also requires that the adsorbed particles impede thinning of the liquid film between droplets. In contrast to the adsorption energy, earlier studies have shown that the highest resistance against film thinning is achieved for particles forming contact angles approaching 0 and 180° [9, 10].

Considering these opposite trends, optimum contact angles (θ) between 70 and 86°, and between 94 and 110° have been suggested for the stabilization of oil-in-water and water-in-oil emulsions, respectively, using interfacially adsorbed particles [10]. Under

such conditions, particles should be able to sterically hinder the coalescence of droplets over long periods of time, which has been experimentally confirmed in a number of recent studies [6, 11-16].

The stabilization of liquid-liquid interfaces with colloidal particles allows for the preparation of emulsions in the absence of hazardous and toxic surfactants, which is particularly important in health care and pharmaceutical products. In addition to emulsion stabilization, the adsorption of colloidal particles on liquid droplets has also been exploited to produce solid-coated capsules (or colloidosomes) that can be used for the encapsulation of chemicals, drugs, fragrances, food, nutrients, and cells [17-21]. Alternatively, particle-stabilized emulsions can be dried and sintered to produce macroporous materials used as bio-scaffolds, low-weight structures, separation membranes, and others [22-25].

Particle-stabilized emulsions can be prepared by tailoring the wettability of colloidal particles in the liquid media, so that their adsorption at the liquid-liquid interface is favored. As mentioned above, particles with intermediate wettability ($70 < \theta < 86°$ or $94 < \theta < 110°$) are expected to be the most suitable for emulsion stabilization. Different approaches have been used to tailor the particle wettability within this range, by for instance (1) in situ modifying the particle surface via the adsorption of long-chain amphiphilic molecules (surfactants/co-surfactants) [11, 17, 26-32], (2) varying the lyophobicity (hydrophobicity) of inorganic particles through prior chemical surface treatments (e.g., silanization of silica particles) [7, 16, 33-42] or (3) using polymeric particles exhibiting hydrophilic charge carriers on the surface (e.g., modified latex particles) [17, 19, 43-47].

These methods have been successfully applied to adjust the wetting behavior of particles in liquids. However, emulsions prepared using such approaches often contain a limited concentration of particles (typically < 5 vol%), despite the fact that higher concentrations are known to increase emulsion stability [7, 12, 14, 36, 48, 49]. Even though low particle concentrations are advantageous in some applications, the enhanced stability achieved at high concentrations is particularly important for the further processing of emulsions into macroporous materials [50]. The low concentration of stabilizing particles used so far in Pickering emulsions might be related to the extensive particle agglomeration normally observed at high solids concentration, which ultimately inhibits particle adsorption at the liquid-liquid interface. Agglomeration occurs due to the low wettability of particles in the liquid continuous phase. In the case of particles modified with long amphiphiles, the formation of micelles and other amphiphile

aggregated structures in the aqueous phase might reduce the amount of free amphiphiles available for adsorption on the particle surface, limiting the concentration of modified particles in the emulsion. The development of a general and simple approach for the surface modification of a high concentration of particles exhibiting a wide range of surface chemistries should be of advantage in several applications.

Here, we describe a simple and versatile approach for the preparation of stable Pickering emulsions through the in situ surface modification of a high concentration of particles with different surface chemistries. In contrast to the aforementioned methods, our approach relies on short amphiphilic molecules for the in situ surface hydrophobization of initially hydrophilic particles. The short amphiphiles exhibit high solubility and critical micelle concentrations in water, enabling the surface modification of up to 40 vol% of submicrometer-sized particles of various surface chemistries. The initial hydrophilic nature of the colloidal particles allows for the homogeneous dispersion of high concentrations of particles prior to surface modification. In this article, we illustrate this novel approach using mainly alumina powder and carboxylic acids as colloidal particles and short amphiphiles, respectively. Amphiphiles suitable for the modification of particles with different surface chemistries than alumina are also investigated to illustrate the versatility of the method.

2.2 Materials and methods

2.2.1 Materials

Experiments were performed using the following metal oxides: (1) α-Al_2O_3 powder (Ceralox HPA-0.5, 99.99 % Al_2O_3, Sasol North America Inc., Tucson, AZ, USA) with average particle diameter, d_{50}, of 200 nm, specific surface area of 10 m^2/g, and density of 3.98 g/cm^3; (2) Al_2O_3 powder, a mixture of 70 % δ- and 30 % γ-phase (Nanophase Technologies Co., Romeoville, IL, USA) with d_{50} of 65 nm, specific surface area of 38 m^2/g, and density of 3.6 g/cm^3 (hereafter referred to as δ-Al_2O_3), (3) SiO_2 powder (grade Snowtex ZL, Nissan Chemical, Houston, TX, USA) with d_{50} ~ 80 nm, specific surface area of 25 m^2/g, and density of 2.1 g/cm^3, and (4) Fe_3O_4 powder (>98 % Fe_3O_4, Nanostructured & Amorphous Materials, Inc., Houston, TX; USA) with d_{50} of 20-30 nm, specific surface area of 60 m^2/g, and density of 4.95 g/cm^3.

Octane (97 % pure, boiling temperature T_b = 125 °C, Acros Organics, Belgium) was used as received for the preparation of the emulsions. The short amphiphilic molecules used for particle modification were acetic acid, propionic acid, valeric acid, and propyl gallate (> 99.7 %, > 99 %, > 99 % pure, > 98 %, respectively, Sigma-Aldrich Chemie GmbH, Germany), formic acid, butyric acid, hexyl amine, and octyl gallate (> 98 % pure, > 99.5 %, > 98 % pure, and > 99 % pure, respectively, Fluka AG, Buchs, Switzerland). Double deionized water with an electrical resistance of 18 MΩcm was used in the experiments (Nanopure, Barnstead, USA). Hydrochloric acid (HCl, 2 M) and sodium hydroxide (NaOH, 1 M) solutions (Titrisol, Fluka AG, Buchs, Switzerland) were used to adjust the pH.

2.2.2 Preparation of suspensions

The preparation of aqueous colloidal suspensions varied according to the amphiphiles and metal oxide particles used. In the case of α-alumina and δ-alumina to be modified with carboxylic acids, suspensions were prepared by first adding 58 and 30 vol% of powder, respectively, into deionized water. During addition of α-alumina powder the suspension pH was maintained at values below 5 by adding small aliquots of 2 N HCl solution, whereas in the case of δ-alumina a pH of approximately 5 was obtained without addition of acidic solutions. For α- and δ-alumina particles to be modified with short alkyl gallates, powders were added to aqueous solutions containing, respectively, 30 and 5 mmol/L of propyl gallate at pH 9.9. The pH of both suspensions was maintained at 9.9 by adding 1 N NaOH and/or 2 N HCl dropwise. In the case of silica particles, suspensions with 45 vol% solids were prepared by adding silica powder directly to deionized water without any pH adjustment. For iron oxide particles, 10 vol% solid suspensions were prepared by adding particles to 44 mmol/L aqueous octyl gallate solutions at pH 9.9. The pH adjustment was done by adding 1 N NaOH and/or 2 N HCl dropwise.

In order to de-agglomerate and homogeneously disperse the colloidal particles in the aqueous phase, suspensions were ball-milled in polyethylene bottles for 22 h using alumina milling balls (10 mm diameter) for α-alumina suspensions and zirconia balls (5, 10 and 20 mm diameter) for δ-alumina, iron oxide, and silica suspensions. In all cases a ball/powder weight ratio of 2.5 was used. After the ball-milling procedure, the pH values of the α-alumina, δ-alumina, silica, and iron oxide suspensions were ~5.5, 5.5,

~8.3, and 10.2, respectively. The ball-milled suspensions were transferred to a glass beaker prior to amphiphile addition. The surface modifier was dissolved in water and the resulting aqueous solution was added dropwise to the suspension under magnetic stirring. In the case of iron oxide particles, stirring was performed mechanically. The pH of the suspensions was subsequently adjusted to 4.75 and 9.9 for particles modified with short carboxylic acids and alkyl gallates, respectively, by adding 1 – 4 N NaOH and/or 2 N HCl dropwise. In the case of silica suspensions, no pH adjustment was needed, resulting in a final pH in the range of 10.2 – 10.4. Finally, additional water was added to dilute the suspensions to the desired solids content.

2.2.3 Interfacial tension measurements

The oil-water interfacial tension was assessed using the pendant drop method (PAT1, Sinterface Technologies, Berlin, Germany). Measurements were performed by forming a pendant drop of amphiphile aqueous solutions or amphiphile-containing suspensions inside an oil-filled quartz cell (2.8 × 3.0 × 3.3 cm^3). The amphiphile aqueous solutions were prepared by adding pure propionic, butyric, or valeric acids to double deionized water, whereas the amphiphile-containing suspensions were prepared at solids content of 35 vol% alumina using the ball-milling procedure described above. In order to eliminate the effect of oil impurities on the interfacial tension analysis, octane was columned twice through chromatographic alumina prior to these experiments. The measurements were performed using purified oil saturated with amphiphiles. Detailed information on the concentration of amphiphiles used to prepare the saturated oil is given in the Chapter 11.1. For the preparation of saturated oil, the amphiphiles were mixed with the oil and the resulting solution was stirred for 1 h to achieve equilibrium conditions. The interfacial tension analysis was performed for 1000 s at a constant temperature of 22 °C. Fixed drop volumes of 35 and 15 mm^3 were used for drops of amphiphile aqueous solutions and amphiphile-containing suspensions, respectively.

2.2.4 Preparation and characterization of oil-in-water emulsions

After the preparation of suspensions with the desired solids and amphiphile contents, the suspensions were transferred to 1 L polyethylene beakers to which the oil phase was added. Emulsification was performed by vigorously stirring the suspension

and the oil phase for 3 min, unless mentioned otherwise, using a household mixer at full power (Multimix 350 W, Braun, Spain). It is important to note that the particle concentration indicated throughout this study refers to the solids content in the initial aqueous suspension and is not based on the emulsion total volume.

The droplet size distribution of the resulting emulsion was evaluated using an optical microscope in transmission mode (Polyvar MET, Reichert-Jung, Austria) connected to a digital camera (DC 300, Leica, Switzerland). Five pictures were taken randomly from different spots of the same sample. The droplet size was measured with the linear intercept method using the software Lince (TU Darmstadt, Germany). Confocal laser microscopy was also performed to confirm the adsorption of surface modified particles at the oil-water interface. The preparation of samples for confocal microscopy is described in Chapter 11.1.

2.3 Results and discussion

2.3.1 Particle modification and adsorption at the oil-water interface

The adsorption of particles to the oil-water interface to form particle-stabilized emulsions was induced by surface modifying the initially hydrophilic particles in the aqueous phase. In the case of alumina particles, surface modification was accomplished at pH 4.75 using carboxylic acids containing less than eight carbon atoms.

The adsorption of particles at the oil-water interface after surface modification was investigated by measuring the interfacial tension between octane and an aqueous suspension containing 35 vol% of surface modified particles. The interfacial tension results are shown in Figure 2.1 for suspensions prepared with various concentrations of propionic, butyric, and valeric acids. The addition of increasing amounts of such short amphiphiles to the colloidal suspensions decreases the oil-water interfacial tension from 51.4 mN/m to values as low as 27 mN/m. Figure 2.1 shows that the reduction in interfacial tension upon amphiphile addition is more pronounced for molecules with longer hydrocarbon tail. An initial concentration of 140 mmol/L of propionic acid is required to reduce the oil-water interfacial tension to about 65 % of its initial value (33.5 mN/m), whereas in the case of longer valeric acid molecules the concentration needed to reach this condition is decreased to approximately 30 mmol/L.

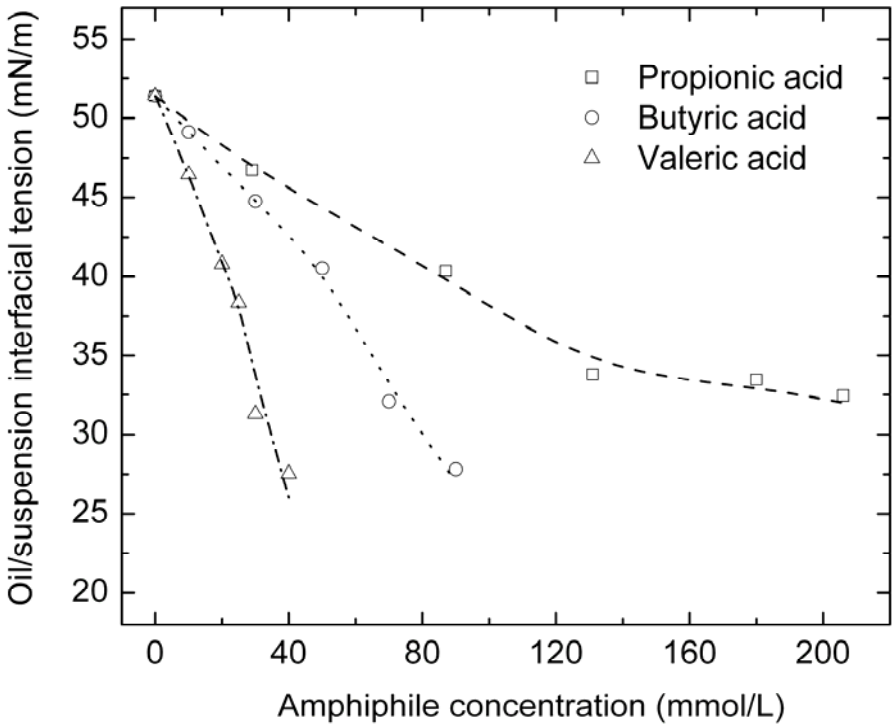

Figure 2.1: Interfacial tension between octane and aqueous suspensions prepared with 35 vol% alumina particles and various concentrations of propionic, butyric, and valeric acids at pH 4.75.

The observed decrease in interfacial tension may result from the adsorption of surface modified particles and/or free amphiphilic molecules at the oil-water interface. The reduction of the overall interfacial tension due to the adsorption of modified particles results from the replacement of a high-energy oil-water interfacial area by less energetic solid-oil and solid-water interfacial areas [5, 6].

In order to account for the individual contributions of modified particles and free amphiphiles to the decrease in interfacial tension shown in Figure 2.1, we evaluated the interfacial tension of the oil-water interface in the presence of free amphiphilic molecules alone. This was accomplished by measuring the interfacial tension between octane and a drop of aqueous solutions containing amphiphile concentrations corresponding to the amount of molecules non-adsorbed on the particle surface (from reference 51[51]). The results are depicted in Figure 2.2 for various initial concentrations of propionic, butyric, and valeric acids.

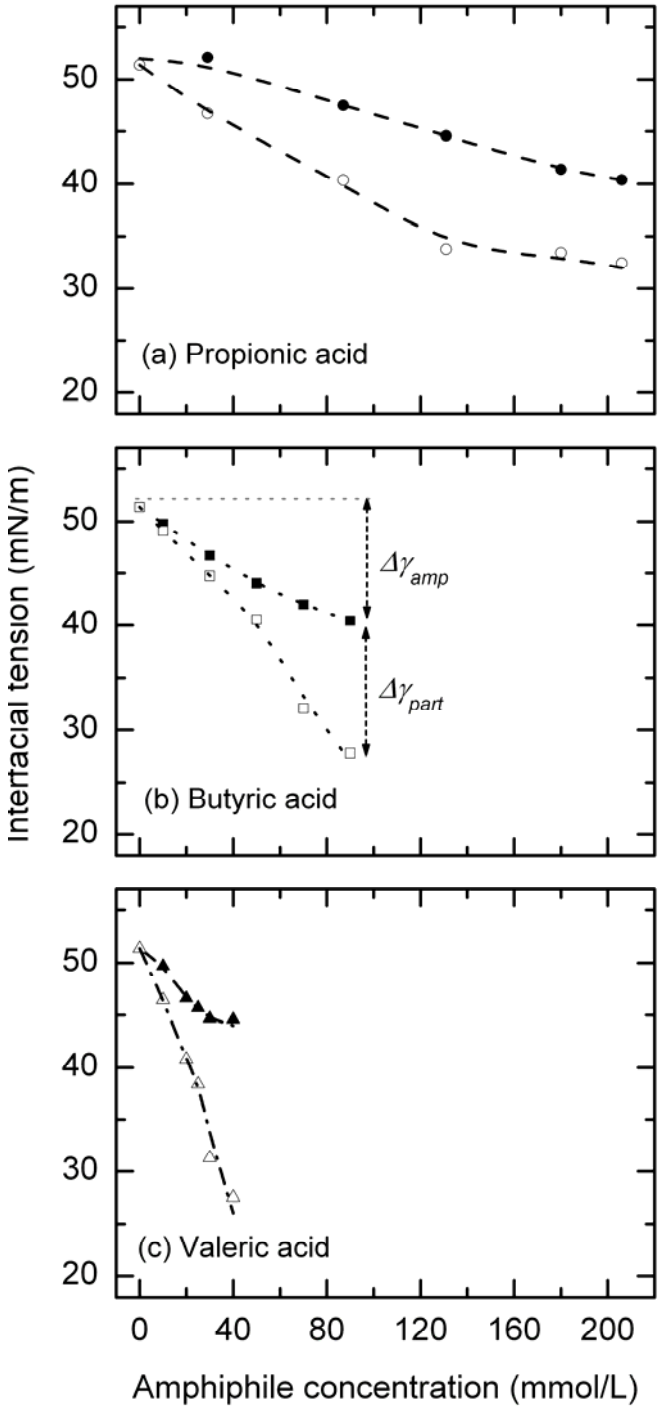

Figure 2.2: Interfacial tension between (1) octane and 35 vol% alumina suspensions prepared with various initial concentrations of carboxylic acids (a, b, and c, open symbols) at pH 4.75 and (2) octane and aqueous solutions containing solely the amount of amphiphiles that does not adsorb on the particle surface (free) at the initial concentrations indicated in the graph (a, b, and c, full symbols) at pH 4.75. The individual contributions of free amphiphiles ($\Delta\gamma_{amp}$) and modified particles ($\Delta\gamma_{part}$) to the overall decrease in interfacial tension is indicated in graph b for a butyric acid initial concentration of 90 mmol/L as an example.

Figure 2.2 shows that both free amphiphiles and surface modified particles contribute to the decrease in the oil-water interfacial tension. The decrease in interfacial tension is more pronounced for longer amphiphiles and for higher initial amphiphile concentrations. The more hydrophobic nature of longer amphiphiles favors the adsorption of free molecules and modified particles at the oil-water interface, resulting in lower interfacial tension values. Higher initial concentrations of amphiphiles, on the other hand, increase the amount of amphiphiles adsorbed on the particle surface, as well as the concentration of free amphiphiles in the liquid phase. The higher amount of amphiphiles on the surface enhances the hydrophobicity of particles, favoring their adsorption at the interface and a reduction of the oil-water interfacial tension. Additionally, the increased concentration of free amphiphiles in the aqueous solution enhances the amount of amphiphilic molecules adsorbed at the interface, further decreasing the oil-water interfacial tension.

Interestingly, in the case of butyric and valeric acids, the interface tension resulting from modified particles decreases significantly above a certain critical amphiphile concentration. For concentrations above this threshold value, particles are presumably too hydrophobic to remain in the aqueous phase and therefore adsorb massively to the oil-water interface. A similar behavior was observed for amphiphile-coated particles adsorbed at air-water interfaces in recent related studies [51, 52].

It is important to note that a fraction of the free amphiphiles initially present in the aqueous phase of oil-water mixtures can also diffuse into the oil phase of the mixture. The partition of the amphiphiles initially dissolved in the aqueous phase depends strongly on the oil to water volume ratio of the mixture (see Chapter 11.1). The oil to water volume ratio used in the pendant drop apparatus is considerably higher than that encountered in the emulsions investigated here. Taking this into account, the interfacial tension measurements discussed above were carried out using an oil phase partially saturated with carboxylic acids in order to reproduce the partition of amphiphiles that occurs in the wet emulsion formulations. Further details on the partition of the amphiphiles and on the procedure used to saturate the oil phase are given in Chapter 11.1.

2.3.2 In situ particle-stabilized emulsions

Particle-stabilized emulsions exhibiting a variety of microstructures were obtained by vigorous mechanical shearing the initial aqueous suspensions containing

short amphiphiles. Since air bubbles could also be incorporated into the system during shearing, microstructures containing both air bubbles and oil droplets in various proportions were obtained when the oil volume fraction was varied between 0 and 72 vol%, as illustrated in Figure 2.3 (triangles) for mixtures prepared with 35 vol% alumina suspensions (dashed line corresponding to a fixed particle to water volume ratio of 0.54). Note that the oil volume fraction here refers to the oil concentration with respect to total emulsion volume (water + particles + oil).

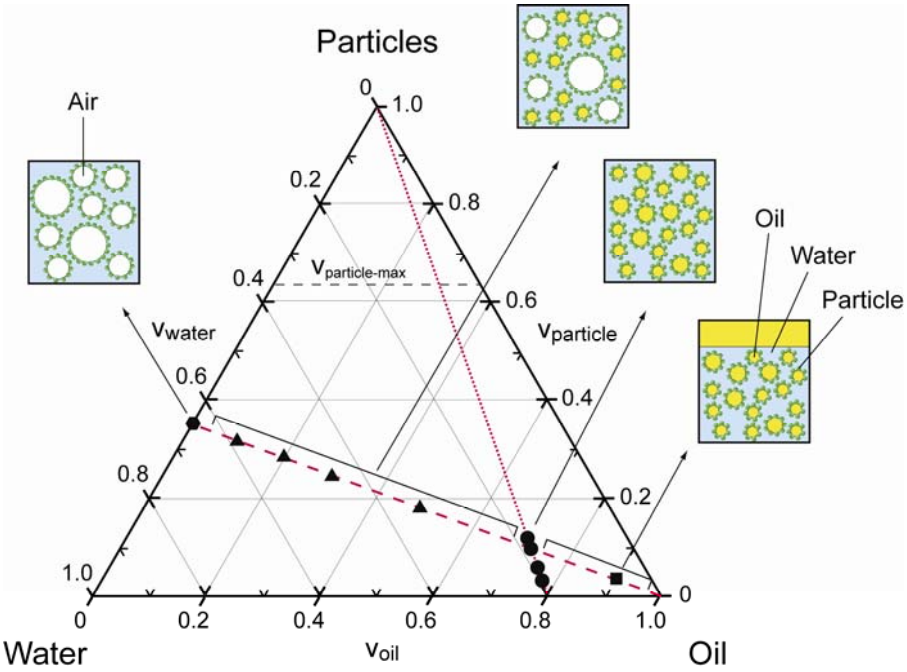

Figure 2.3: Compositional diagram indicating the particle-oil-water formulations evaluated in this study and the resulting microstructures of the mixtures obtained. The volume fractions of water, oil, and particles are indicated by v_{water}, v_{oil}, and $v_{particles}$, respectively. The dashed line indicates the compositions prepared at a constant particle concentration of 35 vol% in the suspension, which corresponds to a particle to water volume ratio of 0.54. The dotted line shows the emulsions prepared at a fixed oil to water volume ratio of 4. $v_{particle-max}$ refers to the maximum particle concentration that can be achieved in the system assuming random particle packing. The circles indicate the compositions investigated in more detail in this work.

In the absence of oil, mechanical shearing of 35 vol% alumina suspensions resulted in the particle-stabilized foams described in recent studies [51, 52]. Oil volume fractions higher than 70 vol% led to emulsions containing solely oil droplets as

dispersed phase in the aqueous suspension. For suspensions containing 35 vol% particles, the maximum volume fraction of oil that could be incorporated in the emulsion was approximately 72 vol%. Oil additions beyond this value resulted in emulsions with a phase-separated layer of oil on top of the emulsified mixture (Figure 2.3).

In this study, we investigated emulsions containing solely oil droplets as dispersed phase. Compositions were prepared at a fixed oil to water volume ratio of 4, which is represented by the dotted line in the diagram shown in Figure 2.3. Such fixed oil to water ratio leads to oil volume fractions between 70.6 and 77.3 vol% when the particle concentration in the initial suspension is varied from 15 to 40 vol% (circles in Figure 2.3). This particle concentration range corresponds to a particle to water volume ratio varying from 0.18 (15 vol% in water) to 0.67 (40 vol% in water). Mixtures containing both oil droplets and air bubbles dispersed in a continuous suspension will be discussed in detail in a following publication.

The adsorption of free amphiphiles and surface modified particles at the oil-water interface enabled the preparation of remarkably stable emulsions (Figure 2.4). The as-prepared emulsions exhibited viscoelastic behavior with a high yield stress typical for compressed emulsions [53]. Slight dilution of the as-prepared mixture with the continuous water phase (~ 1 vol%) enables the preparation of fluid emulsions that can be easily poured or used for dip coating, spin coating, or spray deposition on substrates. Therefore, the rheological properties of the emulsion can be tuned according to their specific application by adjusting the volume fraction of the continuous phase after emulsification.

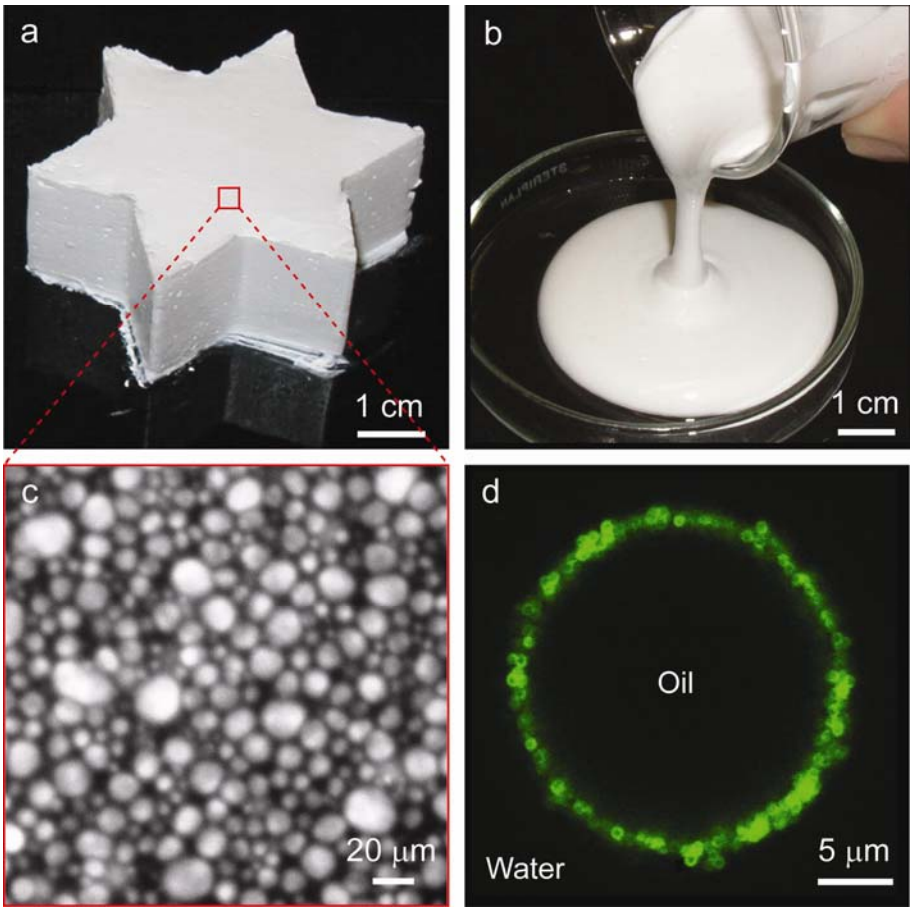

Figure 2.4: Oil-in-water emulsions stabilized by in situ modified colloidal particles. Images a and b show alumina-stabilized wet emulsions exhibiting tunable rheological behavior: (a) strongly elastic (compressed) emulsions obtained after mechanical shearing, (b) fluid emulsion obtained after increasing the continuous water phase by 1 vol% in case of the emulsion shown in (a). The optical micrograph in (c) exhibits a typical microstructure of such wet emulsions. (d) A confocal scanning laser micrograph of an oil droplet coated with modified silica particles in water. The solid-coated oil droplet was obtained after dilution of an oil-in-water emulsion stabilized by silica particles modified with hexyl amine. The image clearly shows the adsorption of monosized fluorescent silica particles (spheres with green fluorescent ring) at the oil-water interface.

The amphiphile concentrations required in the initial suspension to achieve complete emulsification depends on the amphiphile tail length, as indicated in Figure 2.5 for the case of emulsions prepared from 35 vol% alumina suspensions at pH 4.75. In this case, emulsification was achieved using carboxylic acids with one to five carbons at initial concentrations in the aqueous phase ranging from 10 to 250 mmol/L depending on the amphiphile.

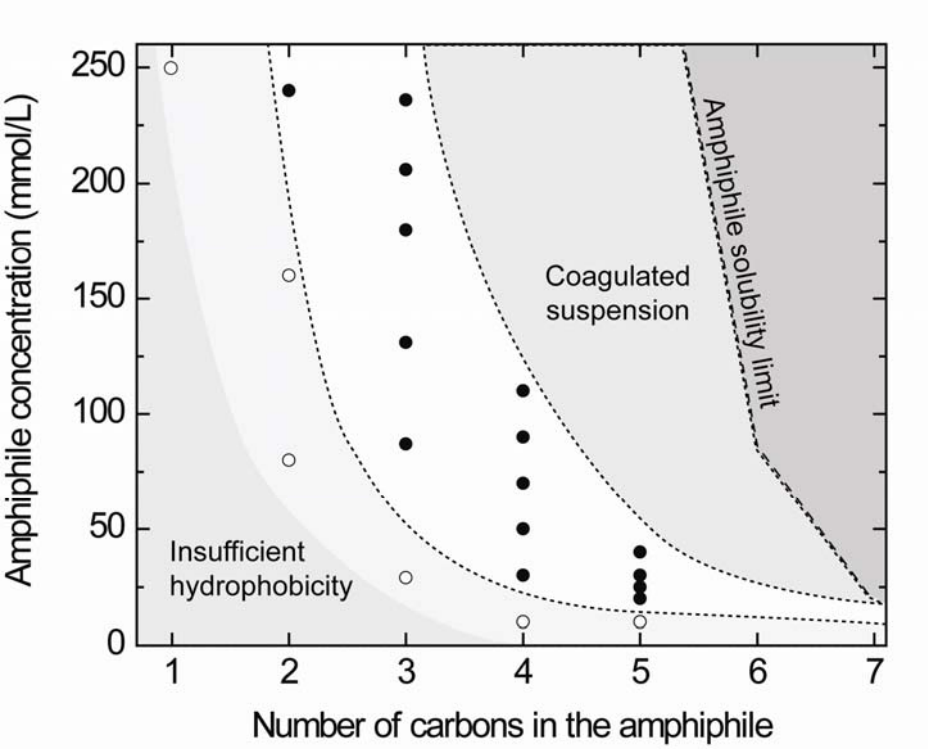

Figure 2.5: Schematic diagram indicating (in white) the conditions required for the preparation of oil-in-water emulsions stabilized with alumina particles modified with short carboxylic acids (72 vol% oil in the emulsion, 35 vol% alumina in the suspension). Full symbols refer to emulsions obtained after 3 min of mixing, whereas open symbols indicate compositions that require mixing times longer than 3 min for complete emulsification.

The first requirement for emulsification is that the amphiphiles exhibit sufficient hydrophobicity to enable the adsorption of free molecules and modified particles at the oil-water interface. This requisite sets the lower limit of the emulsification map shown in Figure 2.5. Emulsification is not possible at too low initial concentrations of amphiphiles (Figure 2.5). A comparison between the emulsification map depicted in Figure 2.5 and the interfacial tension data (Figure 2.1) reveals that a reduction in interfacial tension of about 6 – 11 mN/m is necessary to achieve complete emulsification under the standard mixing conditions applied in this study (3 min, 350 W household mixer). The decrease in interfacial tension is taken here as an indication of the adsorption of free amphiphiles and modified particles at the interface. Since the amphiphile concentrations needed to reduce the interfacial tension by 6 – 11 mN/m decrease with increasing the amphiphile tail length, longer amphiphiles require lower initial concentrations for complete emulsification (Figure 2.5).

The second condition for emulsification is that the suspension is sufficiently viscous to enable the rupture of droplets under shearing but at the same time sufficiently fluid to allow for the incorporation and homogenization of the dispersed oil phase into the suspension. Such requirement sets the upper limit of the emulsification map shown in Figure 2.5. Amphiphiles with long hydrophobic tail and at high concentrations lead to coagulated suspensions with excessively high viscosity, which hinders the homogenization and rupture of oil droplets by mechanical shearing. The high viscosity results from the lower zeta potential and increased hydrophobic interactions between particles observed under these conditions [54].

By comparing the upper limit of the emulsification map (Figure 2.5) with the zeta potential data obtained in an earlier study for alumina particles in carboxylic acid solutions [54], one can conclude that the emulsification process is hindered when the zeta potential of amphiphile-coated particles decreases from +45 mV to values in the range from +5 to +10 mV. This zeta potential reduction leads to strong particle agglomeration and to a pronounced increase in the suspension viscosity. Such decrease in zeta potential is achieved at lower initial concentrations for the case of longer carboxylic acids, which explains the shape of the upper limit curve in the emulsification map (Figure 2.5).

It is important to note that despite the noticeable reduction in interfacial tension achieved with the free amphiphiles alone (Figure 2.2), emulsification could not be achieved using only free amphiphilic molecules as emulsifiers. This was not possible even at very high amphiphile concentrations in water, when the decrease in interfacial tension is significantly higher than the minimum value of 6 – 11 mN/m. This clearly indicates that the surface-modified particles play a decisive role for the formation and stabilization of the emulsions investigated here.

2.3.3 Effect of suspension composition on emulsion microstructure

The microstructure of emulsions stabilized by in situ modified particles can be varied by changing the composition of the initial colloidal suspension. Here, we illustrate the effect of the amphiphile and particle concentrations in the initial suspension on the microstructure of particle-stabilized emulsions.

The droplet size population of all the investigated emulsions followed a log-normal distribution that can be described by [55]

$$p_d = \frac{A}{\sqrt{2\pi}wd} e^{\frac{-\left[\ln\left(\frac{d}{d_c}\right)\right]^2}{2w^2}} \quad \text{Eq. 2.1}$$

where p_d is the radial probability density function, d is the droplet diameter, d_c is the droplet mean diameter, w is the standard deviation of $ln(d)$, and A is a constant equal to 1 for monomodal distributions. In the case of multimodal distributions, the droplet size population can be described by a sum of distributions of the form of Eq. 2.1 with the constant A varying between 0 and 1.

The effect of particle concentration on the droplet size distribution of oil-in-water emulsions is shown in Figure 2.6 for compositions prepared at a fixed oil to water ratio of 4 (dotted line in Figure 2.3) and containing 0.45 wt% propionic acid relative to alumina (81 – 162 mmol/L in the aqueous phase). Emulsions prepared from suspensions containing 25 vol% particles exhibited a multimodal size distribution with main peaks at droplet sizes of 10, 32, and 57 μm (Figure 2.6). Increasing the particle concentration from 25 up to 35 and 40 vol% led to monomodal droplet size distributions with markedly smaller average droplet sizes and narrower distributions, as shown in Figure 2.6. Average droplet sizes of 12 and 7 μm were obtained for compositions prepared with 35 and 40 vol% particles, respectively.

The influence of the amphiphile concentration on the emulsion microstructure was investigated for compositions containing 35 vol% alumina in the initial suspension (particle to water volume ratio of 0.54) and 72 vol% octane in the final emulsion (oil to water volume ratio of 4). Figure 2.7 shows an example of the effect of the amphiphile concentration on the emulsion droplet size distribution for the case of propionic acid. Propionic acid concentrations varying throughout the entire range required for emulsification were investigated (Figure 2.5). Emulsions prepared at a propionic acid concentration close to the lower limit of the emulsification map (87 mmol/L) exhibited a bimodal distribution with peaks at 16.3 and 30.9 μm (Figure 2.7). An increase of the amphiphile concentration resulted in narrower distributions with average droplet sizes down to values in the range of 7 – 14 μm (Figure 2.7). The slight increase in average droplet size observed at the highest amphiphile concentration might be related to the partition of molecules to the oil phase at this extreme condition. Emulsions prepared with increasing concentrations of butyric and valeric acids exhibited a similar behavior.

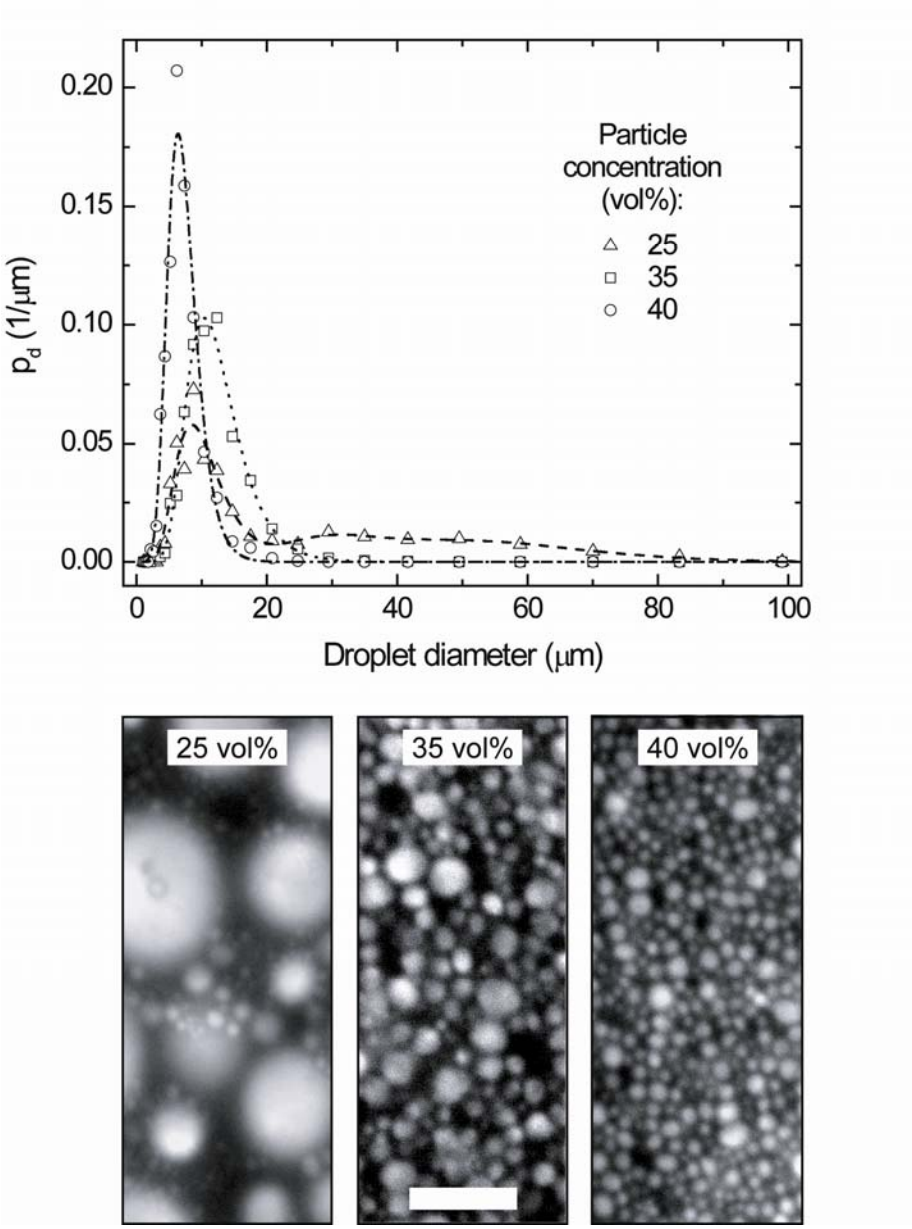

Figure 2.6: Droplet size distributions (top) and optical microscope images (bottom) of oil-in-water emulsions prepared with different particle concentrations in the initial suspension. Emulsions were prepared at a fixed oil to water ratio of 4 (dotted line in Figure 2.3) and with a propionic acid concentration of 0.45 wt% relative to the weight of alumina. The continuous lines correspond to the radial probability density functions used to describe the droplet size distributions. Scale bar: 50 μm.

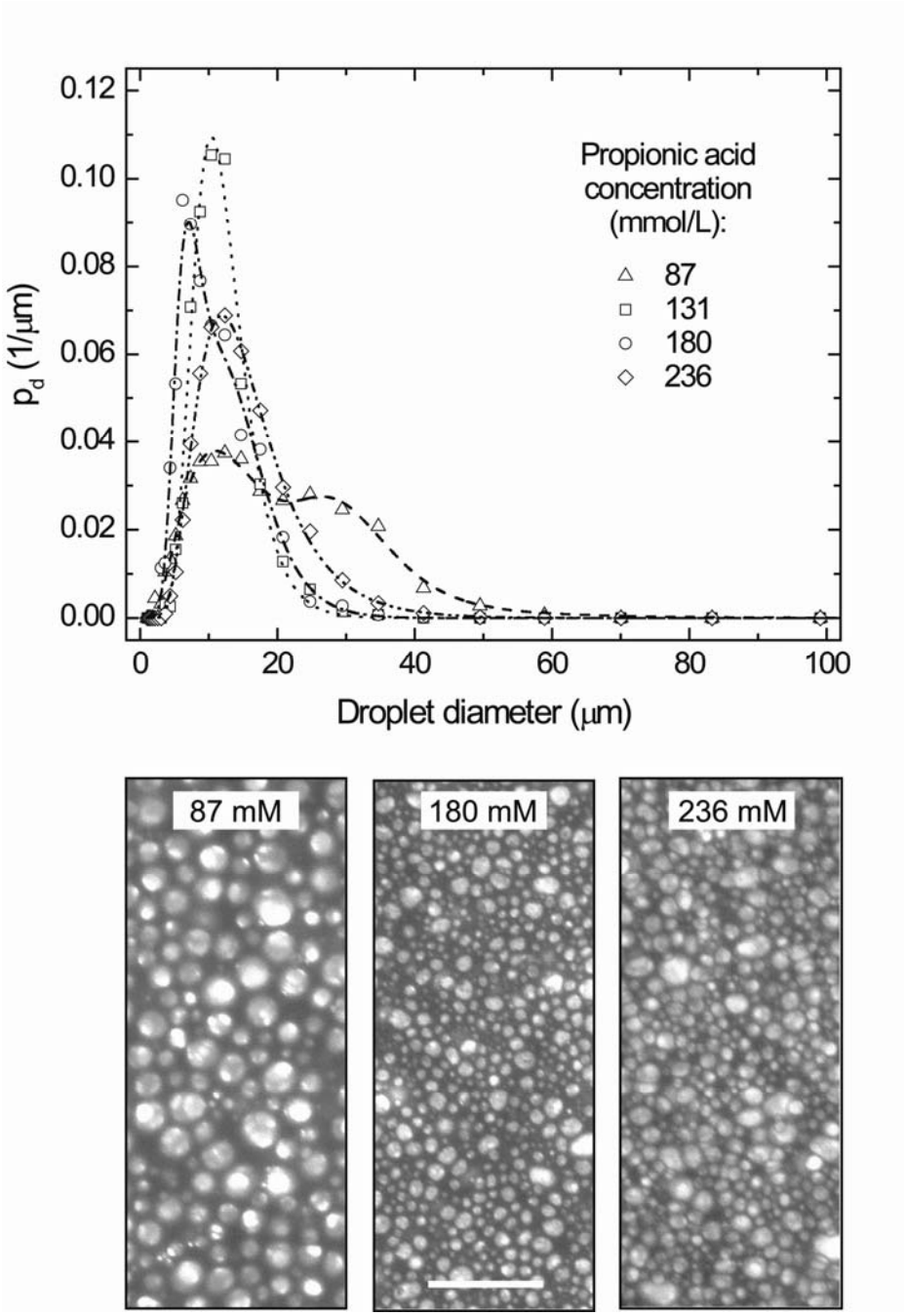

Figure 2.7: Droplet size distributions (top) and optical microscope images (bottom) of oil-in-water emulsions prepared with different concentrations of propionic acid in the initial aqueous suspension. Emulsions were prepared with 72 vol% octane (oil to water volume ratio of 4) and 35 vol% particles in the aqueous phase (particle to water volume ratio of 0.54). The continuous lines correspond to the radial probability density functions used to describe the droplet size distributions. Scale bar: 100 μm.

The dependence of the emulsion droplet size distribution on the suspension composition can be qualitatively explained considering the stresses involved during the rupture of droplets under the shearing process. The rupture of droplets in diluted and concentrated emulsions has been rationalized in terms of a balance between the shearing stresses applied on the droplet ($\tau_{applied}$) and the droplet's resistance to deformation (τ_{resist}) [56-60]. The shear stress applied during emulsification ($\tau_{applied}$) is equal to $\eta_c\dot{\gamma}$, where $\dot{\gamma}$ is the applied shear rate and η_c is the viscosity of the continuous fluid (in this case the concentrated emulsion itself). On the other hand, the droplet's resistance to deformation (τ_{resist}) is proportional to the Laplace pressure σ/d, where σ is the interfacial tension (Figure 1) and d is the droplet size. Assuming that droplet rupture occurs when the stress applied during shearing is comparable to the droplet's resistance to deformation ($\eta_c\dot{\gamma} \approx \sigma/d$), one can expect the final droplet size d to be proportional to $\sigma/\eta_c\dot{\gamma}$. Note that for sake of simplicity we do not consider the critical capillary number in this analysis [61, 62].

On the basis of the relation $d \sim \sigma/\eta_c\dot{\gamma}$, the smaller average droplet sizes of emulsions containing higher particle concentrations (Figure 2.6) can be attributed to the higher viscosity (η_c) of emulsions prepared from suspensions with increased solids content. The influence of the amphiphile concentration on the emulsion droplet size distribution (Figure 2.7) can also be explained considering the relation $d \sim \sigma/\eta_c\dot{\gamma}$. Higher amphiphile contents in the initial suspension decrease the oil-water interfacial tension (Figure 2.1) and is also expected to increase the emulsion viscosity due to a stronger screening of the electrical charges on the particle surface [54]. As a result, the increase of the propionic acid concentration above 87 mmol/L leads to smaller average droplet sizes (Figure 2.7).

2.3.4 Emulsion stability

Emulsions prepared at intermediate amphiphile concentrations (full symbols) in the emulsification area of Figure 2.5 displayed remarkable stability against coalescence, Ostwald ripening, and creaming, as indicated in Figure 2.8 for compositions prepared from 35 vol% alumina suspensions containing propionic acid. No significant change was observed in the droplet size distribution of the emulsions within a time period of more than 2 years after emulsification (Figure 2.8). Dilution of the as-prepared mixture

with up to 1 vol% water also led to very stable fluid emulsions (Figure 2.4.b) which resist coalescence and coarsening for more than 4 days after dilution.

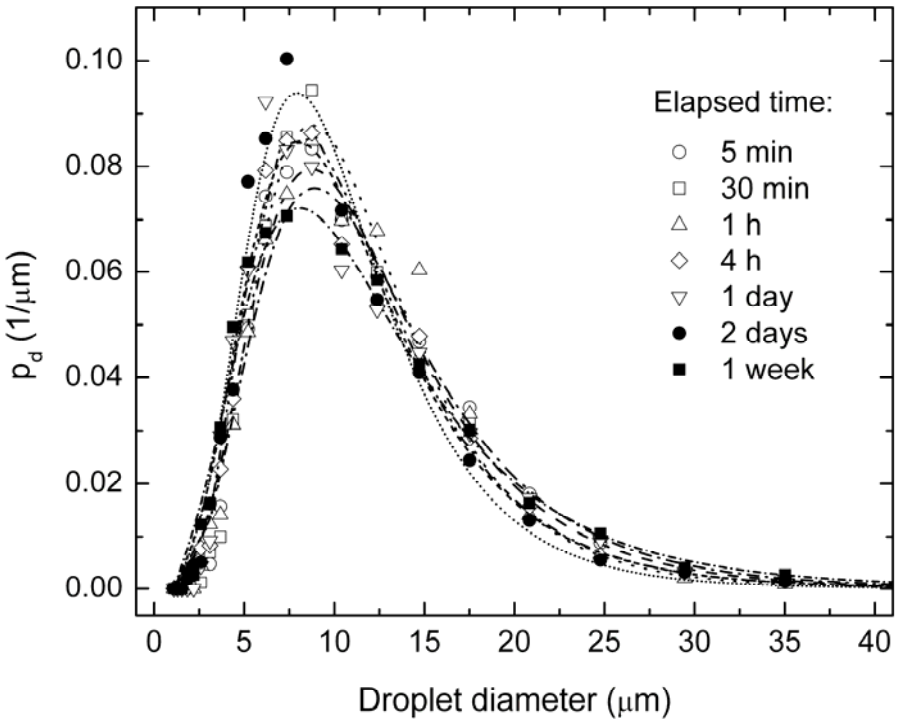

Figure 2.8: Droplet size distribution of oil-in-water emulsions (72 vol% octane) stabilized by alumina particles as a function of time after emulsification. The emulsions were prepared by mixing octane with 35 vol% alumina suspensions containing an initial propionic acid concentration of 180 mmol/L at pH 4.75.

The high stability of the emulsions prepared here can be attributed to the strong attachment of the modified colloidal particles at the oil-water interface. As mentioned earlier, the energy required to remove a colloidal particle from an oil-water interface can amount to thousands of kT [6, 7]. This leads to an irreversible adsorption of particles at the oil-water interface. Particles irreversibly adsorbed at the interface can impede the rupture of the thin film in between neighbour droplets [9, 10, 16] and can halt the expected shrinkage of droplets due to Ostwald ripening. As a result, no droplet coarsening and coalescence takes place within the emulsion for long periods of time (Figure 2.8). The formation of a particle network throughout the continuous phase is also expected to markedly enhance the stability of air-water and oil-water mixtures [63, 64].

2.3.5 Versatility of the method

The in situ surface modification of colloidal particles is a versatile approach for the preparation of oil-in-water emulsions, since the surface hydrophobization can be accomplished on particles of different chemical compositions by just changing the anchoring group of the amphiphilic molecule [52]. Using this approach, we were able to prepare stable oil-in-water emulsions using different metal oxide colloidal particles adsorbed at the oil-water interface (Table 2.1).

Table 2.1: Conditions required for the preparation of particle stabilized oil-in-water emulsions with a wide range of metal oxide powders.

Metal Oxide	**Particle Diameter (d_{50}) (nm)**	**pH**	**Suspension Solids Content (vol%)**	**Amphiphile**	**Amphiphile Content (mmol/L)**	**Oil Content (vol%)**
α-Al_2O_3	200	4.75	35	propionic acid	131	70-80
α-Al_2O_3	200	9.9	35	propyl gallate	100	72.2
δ-Al_2O_3	65	4.75	20	butyric acid	85	81.9
δ-Al_2O_3	65	9.9	20	propyl gallate	70	81.9
SiO_2	80	10.4	35	hexyl amine	60	72.2
Fe_3O_4	40	9.9	10	octyl gallate	44	79.4

In addition to surface hydrophobization of alumina particles at acidic pH conditions upon adsorption of short carboxylic acids in water, alumina particles can be rendered hydrophobic at basic pH conditions by adsorbing short alkyl gallates on the particle surface. The adsorption of short alkyl gallates occurs through ligand-exchange reactions between the amphiphile and the alumina surface [65].

Similarly, magnetic iron oxide particles can be surface hydrophobized in water upon adsorption of octyl gallate onto the particle surface at pH 9.9 (Table 2.1). For silica particles, surface hydrophobization can be achieved through the electrostatic adsorption of alkyl amine molecules initially added to the aqueous phase at pH ~ 10.

The selection of other anchoring groups on the amphiphilic molecules [52] should allow for the preparation of stable emulsions with a large variety of other metal oxide particles, imparting great versatility to the approach herein described.

2.4 Conclusions

Oil-in-water emulsions can be efficiently stabilized by colloidal particles after in situ modification of the particle surface with short amphiphilic molecules. Surface modification with short amphiphiles rendered the particles partially hydrophobic, favoring their adsorption at the oil-water interface. Octane-in-water emulsions containing alumina particles and carboxylic acids as amphiphiles were stabilized for long periods of time using this new approach. Short carboxylic acids containing between two and five carbons were shown to be appropriate surface modifiers, by adsorbing onto the particle surface through electrostatic interactions, leaving the hydrophobic moiety exposed to the aqueous medium. The high solubility and high critical micelle concentration of these molecules in water allows for the in situ modification of a high concentration of submicrometer and nanoparticles for emulsion stabilization. Complete emulsification is achieved at amphiphile concentrations sufficiently high to impart hydrophobicity on the particle surface but low enough to avoid agglomeration of particles in the initial suspension. The microstructure of the particle-stabilized emulsions can be changed by adjusting the composition of the initial aqueous suspension. The effects of the particle and amphiphile concentrations on the emulsion droplet size distribution were qualitatively explained taking into account the stresses involved during the process of droplet rupture under shearing. The method described here can be applied for the stabilization of emulsions with a large variety of metal oxide particles. This versatile approach should thus allow for the preparation of stable emulsions of interest in a number of important applications, including materials manufacturing, food, cosmetics, and pharmaceutical products.

2.5 Acknowledgment

We are very thankful to Ben Seeber (ETH Zurich) for synthesizing the fluorescent silica particles, to Lorenz Bonderer (ETH Zurich) for performing the confocal microscopy experiments, to Dr. Oleg Lukin (ETH Zurich) for fruitful discussions about partitioning,

and to Christina Pecnik, Joëlle Hofstetter, and Jérôme Zemp for their assistance in the experimental work.

2.6 References

1. Becher, P., *Emulsions: Theory and Practice*. 3rd ed. 2001, Washington, D.C., American Chemical Society. 513.

2. Myers, D., *Surfaces, Interfaces and Colloids: Principles and Applications*. 1991, Weinheim, VCH Publishers.

3. Ramsden, W., *Separation of solids in the surface-layers of solutions and suspensions (Observations on surface-membranes, bubbles, emulsions, and mechanical coagulation). Preliminary account*. Proc. Roy. Soc. London, 1903, 72, 156-164.

4. Pickering, S. U., *Emulsions*. J. Chem. Soc., 1907, 91, 2001-2021.

5. Levine, S., Bowen, B. D., Partridge, S. J., *Stabilization of emulsions by fine particles I. Partitioning of particles between continuous phase and oil/water interface*. Colloids Surf., 1989, 38(2), 325-343.

6. Binks, B. P., *Particles as surfactants--similarities and differences*. Curr. Opin. Colloid Interface Sci., 2002, 7(1-2), 21-41.

7. Aveyard, R., Binks, B. P., Clint, J. H., *Emulsions stabilised solely by colloidal particles*. Adv. Colloid Interface Sci., 2003, 100-102, 503-546.

8. Pieranski, P., *Two-dimensional interfacial colloidal crystals*. Phys. Rev. Lett., 1980, 45(7), 569-572.

9. Denkov, N. D., Ivanov, I. B., Kralchevsky, P. A., Wasan, D. T., *A possible mechanism of stabilization of emulsions by solid particles*. J. Colloid Interface Sci., 1992, 150(2), 589-593.

10. Kaptay, G., *On the equation of the maximum capillary pressure induced by solid particles to stabilize emulsions and foams and on the emulsion stability diagrams*. Colloids Surf. A, 2006, 282, 387-401.

11. Tambe, D. E., Sharma, M. M., *Factors controlling the stability of colloid-stabilized emulsions: I. An experimental investigation*. J. Colloid Interface Sci., 1993, 157(1), 244-253.

12. Tambe, D. E., Sharma, M. M., *The effect of colloidal particles on fluid-fluid interfacial properties and emulsion stability*. Adv. Colloid Interface Sci., 1994, 52, 1-63.

13. Ashby, N. P., Binks, B. P., *Pickering emulsions stabilised by Laponite clay particles*. Phys. Chem. Chem. Phys., 2000, 2, 5640-5646.

14. Arditty, S., Whitby, C. P., Binks, B. P., Schmitt, V., Leal-Calderon, F., *Some general features of limited coalescence in solid-stabilized emulsions*. Eur. Phys. J. E, 2003, 11, 273-281.

15. Alargova, R. G., Warhadpande, D. S., Paunov, V. N., Velev, O. D., *Foam superstabilization by polymer microrods*. Langmuir, 2004, 20, 10371-10374.

16. Horozov, T. S., Binks, B., *Particle-stabilized emulsions: A bilayer or a bridging monolayer?* Angew. Chem. Int. Ed., 2006, 45, 773-776.

17. Velev, O. D., Furusawa, K., Nagayama, K., *Assembly of latex particles by using emulsion droplets as templates. 1. Microstructured hollow spheres*. Langmuir, 1996, 12(10), 2374-2384.

18. Dinsmore, A. D., Hsu, M. F., Nikolaides, M. G., Marquez, M., Bausch, A. R., Weitz, D. A., *Colloidosomes: Selectively permeable capsules composed of colloidal particles.* Science, 2002, 298, 1006-1009.

19. Noble, P. F., Cayre, O. J., Alargova, R. G., Velev, O. D., Paunov, V. N., *Fabrication of "Hairy" colloidosomes with shells of polymeric microrods.* J. Am. Chem. Soc., 2004, 126, 8092-8093.

20. Duan, H., Wang, D., Sobal, N. S., Giersig, M., Kurth, D. G., Möhlwald, H., *Magnetic colloidosomes derived from nanoparticle interfacial self-assembly.* Nano Lett., 2005, 5(5), 949-952.

21. Binks, B., Horozov, T. S., Eds., *Colloidal particles at liquid interfaces*. 2006, Cambridge University Press: Cambridge, U. K.

22. Binks, B. P., *Macroporous silica from solid stabilized emulsion templates.* Adv. Mater., 2002, 14(24), 1824-1827.

23. Shah, P. S., Sigman Jr., M. B., Stowell, C. A., Lim, K. T., Johnston, K. P., Korgel, B. A., *Single-step self-organization of ordered macroporous nanocrystal thin films.* Adv. Mater., 2003, 15(12), 971-974.

24. Arditty, S., Schmitt, V., Giermanska-Kahn, J., Leal Calderon, F., *Materials based on solid-stabilized emulsions.* J. Colloid Interface Sci., 2004, 275(2), 659-664.

25. Studart, A. R., Gonzenbach, U. T., Tervoort, E., Gauckler, L. J., *Processing routes to macroporous ceramics: A review.* J. Am. Ceram. Soc., 2006, 89(6), 1771-1789.

26. Schulman, J. H., Leja, J., *Control of contact angles at the oil-water-solid interfaces: Emulsions stabilized by solid particles ($BaSO_4$).* Trans. Far. Soc., 1954, 50(1), 598-605.

27. Tsugita, A., Takemoto, S., Mori, K., Yoneya, T., Otani, Y., *Studies on o/w emulsions stabilized with insoluble montmorillonite-organic complexes.* J. Colloid Interface Sci., 1983, 95(2), 551-560.

28. Gelot, A., Friesen, W., Hamza, H. A., *Emulsification of oil and water in the presence of finely divided solids and surface-active agents.* Colloids Surf., 1984, 12, 271-303.

29. Hassander, H., Johansson, B., Törnell, B., *The mechanism of emulsion stabilization by small silica (Ludox) particles.* Colloids Surf., 1989, 40, 93-105.

30. Binks, B. P., Desforges, A., Duff, D. G., *Synergistic stabilization of emulsions by a mixture of surface-active nanoparticles and surfactant.* Langmuir, 2007, 23(3), 1098-1106.

31. Binks, B. P., Rodrigues, J. A., *Enhanced stabilization of emulsions due to surfactant-induced nanoparticle flocculation.* Langmuir, 2007, 23(14), 7436-7439.

32. Binks, B. P., Rodrigues, J. A., Frith, W. J., *Synergistic interaction in emulsions stabilized by a mixture of silica nanoparticles and cationic surfactant.* Langmuir, 2007, 23(7), 3626-3636.

33. Binks, B. P., Lumsdon, S. O., *Effects of oil type and aqueous phase composition on oil-water mixtures containing particles of intermediate hydrophobicity.* Phys. Chem. Chem. Phys., 2000, 2(13), 2959-2968.

34. Binks, B. P., Lumsdon, S. O., *Transitional phase inversion of solid-stabilized emulsions using particle mixtures.* Langmuir, 2000, 16(8), 3748-3756.

35. Binks, B. P., Lumsdon, S. O., *Influence of particle wettability on the type and stability of surfactant-free emulsions.* Langmuir, 2000, 16(23), 8622-8631.

36. Binks, B. P., Lumsdon, S. O., *Catastrophic phase inversion of water-in-oil emulsions stabilized by hydrophobic silica.* Langmuir, 2000, 16(6), 2539-2547.

37. Binks, B. P., Kirkland, M., *Interfacial structure of solid-stabilised emulsions studied by scanning electron microscopy.* Phys. Chem. Chem. Phys., 2002, 4(15), 3727-3733.

38. Horozov, T. S., Aveyard, R., Clint, J. H., Binks, B. P., *Order-disorder transition in monolayers of modified monodisperse silica particles at the octane-water interface*. Langmuir, 2003, 19, 2822-2829.

39. Vignati, E., Piazza, R., Lockhart, T. P., *Pickering emulsions: Interfacial tension, colloidal layer morphology, and trapped-particle motion*. Langmuir, 2003, 19, 6650-6656.

40. Tarimala, S., Dai, L. L., *Structure of microparticles in solid-stabilized emulsions*. Langmuir, 2004, 20, 3492-3494.

41. Binks, B. P., Philip, J., Rodrigues, J. A., *Inversion of silica-stabilized emulsions induced by particle concentration*. Langmuir, 2005, 21(8), 3296-3302.

42. Xu, Q. Y., Nakajima, M., Binks, B. P., *Preparation of particle-stabilized oil-in-water emulsions with the microchannel emulsification method*. Colloids Surf. A, 2005, 262(1-3), 94-100.

43. Binks, B. P., Lumsdon, S. O., *Pickering emulsions stabilized by monodisperse latex particles: Effects of particle size*. Langmuir, 2001, 17(15), 4540-4547.

44. Stancik, E. J., Kouhkan, M., Fuller, G. G., *Coalescence of particle-laden fluid interfaces*. Langmuir, 2004, 20, 90-94.

45. Hsu, M. F., Nikolaides, M. G., Dinsmore, A. D., Bausch, A. R., Gordon, V. D., Chen, X., Hutchinson, J. W., Weitz, D. A., Marquez, M., *Self-assembled shells composed of colloidal particles: Fabrication and characterization*. Langmuir, 2005, 21, 2963-2970.

46. Subramaniam, A. B., Abkarian, M., Stone, H. A., *Controlled assembly of jammed colloidal shells on fluid droplets*. Nat. Mater., 2005, 4, 553-556.

47. Golemanov, K., Tcholakova, S., Kralchevsky, P. A., Ananthapadmanabhan, K. P., Lips, A., *Latex-particle stabilized emulsions of anti-Bancroft type*. Langmuir, 2006, 22, 4968-4977.

48. Midmore, B. R., *Effect of aqueous phase composition on the properties of a silica-stabilized w/o emulsion*. J. Colloid Interface Sci., 1999, 213(2), 352-359.

49. Binks, B. P., Whitby, C. P., *Silica particle-stabilized emulsions of silicone oil and water: Aspects of emulsification*. Langmuir, 2004, 20, 1130-1137.

50. Studart, A. R., Gonzenbach, U. T., Akartuna, I., Tervoort, E., Gauckler, L. J., *Materials from foams and emulsions stabilized by colloidal particles*. J. Mater. Chem., 2007, 17(31), 3283-3289.

51. Gonzenbach, U. T., Studart, A. R., Tervoort, E., Gauckler, L. J., *Ultrastable particle-stabilized foams*. Angew. Chem. Int. Ed., 2006, 45(21), 3526-3530.

52. Gonzenbach, U. T., Studart, A. R., Tervoort, E., Gauckler, L. J., *Stabilization of foams with inorganic colloidal particles*. Langmuir, 2006, 22(26), 10983-10988.

53. Mason, T. G., Bibette, J., Weitz, D. A., *Yielding and flow of monodisperse emulsions*. J. Colloid Interface Sci., 1996, 179(2), 439-448.

54. Gonzenbach, U. T., Studart, A. R., Tervoort, E., Gauckler, L. J., *Macroporous ceramics from particle-stabilized wet foams*. J. Am. Ceram. Soc., 2007, 90(1), 16-22.

55. Helstrom, C. W., *Probability and Stochastic Processes for Engineers*. 1984, New York, Macmillan Publishing Company.

56. Aronson, M. P., *The role of free surfactant in destabilizing oil-in-water emulsions*. Langmuir, 1989, 5, 494-501.

57. Mason, T. G.,Bibette, J., *Shear rupturing of droplets in complex fluids*. Langmuir, 1997, 13(17), 4600-4613.

58. Welch, C. F., Rose, G. D., Malotky, D., Eckersley, S. T., *Rheology of high internal phase emulsions*. Langmuir, 2006, 22(4), 1544-1550.

59. Taylor, G. I., *The viscosity of a fluid containing small drops of another fluid*. Proc. Roy. Soc. London A, 1932, 138, 41-48.

60. Taylor, G. I., *The formation of emulsions in definable fields of flow*. Proc. Roy. Soc. London A, 1934, 146(A858), 0501-0523.

61. Janssen, J. M. H., Meijer, H. E. H., *Droplet breakup mechanisms-Stepwise equilibrium versus transient dispersion*. J. Rheol., 1993, 37(4), 597-608.

62. Gonzenbach, U. T., Studart, A. R., Tervoort, E., Gauckler, L. J., *Tailoring the microstructure of particle-stabilized wet foams*. Langmuir, 2007, 23(3), 1025-1032.

63. Du, Z., Bilbao-Montoya, M. P., Binks, B. P., Dickinson, E., Ettelaie, R., Murray, B. S., *Outstanding stability of particle-stabilized bubbles*. Langmuir, 2003, 19(8), 3106-3108.

64. Dickinson, E., Ettelaie, R., Kostakis, T., Murray, B. S., *Factors controlling the formation and stability of air bubbles stabilized by partially hydrophobic silica nanoparticles*. Langmuir, 2004, 20(20), 8517-8525.

65. Hidber, P. C., Graule, T. J., Gauckler, L. J., *Influence of the dispersant structure on properties of electrostatically stabilized aqueous alumina suspensions*. J. Eur. Ceram. Soc., 1997, 17, 239-249.

3 Simple and Double Emulsions Stabilized by Colloidal Particles and Short Amphiphiles*

Abstract

The preparation of simple and double emulsions stabilized by colloidal particles often requires grafting of chemical species on the particle surface prior to emulsification. This might involve tedious, inefficient chemical procedures and has limited the chemical compositions of colloidal particles used as stabilizers. We report a simple and general approach for the stabilization of water-in-oil and oil-in-water-in-oil emulsions using oxide particles that are in situ modified with short amphiphilic molecules. This versatile method should add new possibilities for the design and preparation of materials, food, cosmetic, and pharmaceutical products using emulsion technologies.

* *I. Akartuna, A. R. Studart, E. Tervoort, L. J. Gauckler, to be submitted.*

3.1 Introduction

Single and double emulsions find important applications in pharmaceutics, oil recovery, food, cosmetics and have been recently exploited to fabricate unique materials and structures [1-3]. While emulsification is traditionally achieved using surface active molecules, solid particles that are only partially wetted by the immiscible liquids have long been shown to efficiently stabilize emulsions and foams [4-6]. The stabilization of emulsions using particles relies on their strong adsorption at the liquid-liquid interface. The fact that particles can adsorb irreversibly at the interface enables the preparation of emulsions with extremely high stability against coalescence and Ostwald ripening [7-10], which is a major advantage in comparison to surfactant-stabilized systems.

The adsorption of colloidal particles to liquid-liquid interfaces can be achieved by adjusting their wettability in the liquid media or, in other words, their contact angle θ at the liquid interface. In general, particles with contact angles lower than 90° tend to stabilize oil-in-water emulsions, whereas particles exhibiting contact angles higher than 90° yield water-in-oil emulsions [11]. Wettability and contact angle can be tuned by tailoring the particle surface chemistry. Several approaches have been applied to modify the surface chemistry of particles to induce their adsorption at liquid interfaces [9, 12-37]. We have recently shown that amphiphiles with unusually short length can be used to modify the surface of a wide variety of initially hydrophilic particles and thus render remarkably stable oil-in-water emulsions [2, 38]. Here we show that this approach can be generalized to enable the stabilization of water-in-oil emulsions and oil-in-water-in-oil double emulsions using the same combinations of short amphiphiles and hydrophilic colloidal particles.

3.2 Materials and methods

3.2.1 Materials

The metal oxide particles used in the experiments were: (1) α-Al_2O_3 powder (Ceralox HPA-0.5, 99.99% Al_2O_3, Sasol North America Inc., Tucson, AZ, USA) with average particle diameter, d_{50}, of 200 nm, specific surface area of 10 m^2/g and density of 3.98 g/cm^3; (2) Al_2O_3 powder consisting of a mixture of 70% δ- and 30% γ-phase

(Nanophase Technologies Co., Romeoville, IL, USA) with d_{50} of 65 nm, specific surface area of 38 m^2/g and density of 3.6 g/cm^3; and (3) Fe_3O_4 powder (> 98% Fe_3O_4, Nanostructured & Amorphous Materials, Inc., Houston, TX, USA) with d_{50} of 20-30 nm, specific surface area of 60 m^2/g and density of 4.95 g/cm^3. The particle size of the investigated powders was characterized by scanning electron microscopy (SEM; LEO 1530, LEO, Oberkochen, Germany) and X-ray disc centrifuge sedigraph (XDC; Brookhaven Instruments Corp., Holtsville, NY, USA). Specific surface area was determined using a Brunauer-Emmett-Teller (BET) gas-adsorption apparatus (Nova 1000, Quantachrome, Odelzhausen, Germany). The isoelectric points (IEP) of the particles were measured using the electroacoustic colloidal vibration technique (DT-1200, Dispersion Technology, Inc., Mount Kisco, NY, USA). Isoelectric points at pHs 9, 9.2 and 8 were obtained for the α-Al_2O_3, δ-Al_2O_3, and Fe_3O_4 powders, respectively.

Octane (97% pure, boiling temperature T_b = 125 °C, Acros Organics, Belgium) was used as received for the preparation of emulsions. The short amphiphilic molecules used for particle modification were valeric acid (> 99% pure, Sigma-Aldrich Chemie GmbH, Germany) and octyl gallate (> 99% pure, Fluka AG, Buchs, Switzerland). Double deionized water with an electrical resistance of 18 MΩ cm was used in the experiments (Nanopure water system, Barnstead, USA). 2 M hydrochloric acid (HCl) and 1 M sodium hydroxide (NaOH) solutions (Titrisol, Fluka AG, Buchs, Switzerland) were used for pH adjustments.

3.2.2 Preparation of suspensions

Aqueous colloidal suspensions with 58 vol% α-alumina, 30 vol% δ-alumina, and 10 vol% iron oxide were prepared by adding the powders to deionized water. During addition of the α-alumina powder, the pH was maintained at values below 5 by adding small aliquots of 2 N HCl solution. In the case of the δ-alumina powder, a pH of approximately 5 was obtained without addition of acidic solutions. For iron oxide particles, 10 vol% suspensions were prepared by adding particles to 44 mmol/L octyl gallate aqueous solutions at pH 9.9. The pH adjustment was done by adding 1 N NaOH and/or 2 N HCl dropwise.

De-agglomeration of the colloidal particles was performed by ball-milling the suspensions in polyethylene bottles for 22 h using alumina milling balls (10 mm diameter) for α-alumina suspensions and zirconia balls (5, 10 and 20 mm diameter) for

δ-alumina and iron oxide suspensions with a ball/powder weight ratio of 2.5. Following ball-milling, the pH of the aqueous α-alumina, δ-alumina, and iron oxide suspensions was ~5.5, 5.5, and 10.2, respectively. The ball-milled aqueous suspensions were transferred to a glass beaker prior to amphiphile addition. The short amphiphiles were dissolved in water and the resulting aqueous solution was added dropwise to the suspension under magnetic stirring. In case of iron oxide particles, stirring was performed mechanically. The pH of the suspensions was subsequently adjusted to 4.75 and 9.9 for particles modified with short carboxylic acids and alkyl gallates, respectively, by adding 1 – 4 N NaOH and/or 2 N HCl dropwise. The desired solids content of the final aqueous suspensions was achieved by dilution with additional water.

In the case of non-aqueous suspensions, slurries with 10 vol% α-alumina, δ-alumina, and iron oxide were prepared by adding the powders directly into octane containing the desired amount of amphiphile, followed by ball-milling as described above.

3.2.3 Preparation and characterization of emulsions

Different types of emulsions were prepared depending on the initial amphiphile concentration and on the liquid in which the particles are originally dispersed and surface modified (oil or water). Oil-in-water emulsions were prepared by initially adding alumina and iron oxide particles together with low concentrations of valeric acid and octyl gallate, respectively, into water. Water-in-oil emulsions were formed by first adding particles and high concentrations of the same amphiphiles into octane. Emulsification was then performed by vigorously stirring the above suspensions with excess of the dispersed phase for 3 min using a household mixer at full power (Multimix 350 W, Braun, Spain), unless mentioned otherwise. Emulsification could not be achieved using only free amphiphilic molecules or unmodified particles as emulsifiers. This was not possible even after adding very high amphiphile concentrations into the liquid phases. It is important to note that the particle concentration indicated throughout this study refers to the solids content in the initial suspension and is not based on the emulsion's total volume, whereas the volume fraction of the dispersed phase refers to the concentration with respect to the total emulsion volume (water + particles + oil).

To obtain double emulsions, an oil-in-water simple emulsion was first prepared with 67.7 vol% octane and 10 vol% iron oxide particles partially hydrophobized with 44 mmol/L octyl gallate at pH 9.9. This emulsion was then diluted three times with the continuous aqueous phase to achieve a final particle volume fraction of 1 vol%. This diluted emulsion was finally re-emulsified through careful mixing with a suspension containing 1 vol% iron oxide particles and 5 mmol/L octyl gallate in octane for 3 min.

The droplet size distributions of emulsions were determined by evaluating a set of at least five optical microscope images for each composition using the linear intercept method (software Lince®, TU Darmstadt, Germany). Geometric mean droplet sizes (d_{50}) and 68% confidence intervals were obtained by fitting log-normal distributions to the experimental data, as described elsewhere [38]. Rheological measurements were performed at 25 °C using a stress-controlled rheometer (Bohlin-Rheometer CS-50, Bohlin, England) with profiled parallel-plate geometry (25 mm diameter plates). Experiments were carried out with a mechanically-set gap of 1000 µm. Stress-ramp oscillatory measurements were conducted at a constant frequency of 1 Hz by gradually increasing the maximum applied stress from 10 to 1000 Pa.

3.3 Results and discussion

Previously reported oil-in-water emulsions are typically prepared through the addition of short amphiphiles that increase the surface hydrophobicity, while still keeping the particles mostly hydrophilic ($\theta < 90°$). This is exemplified in Figure 3.1 for the case of α- and δ-Al_2O_3 particles modified with valeric acid at concentrations in the initial aqueous suspension in the range of 10-50 and 20-70 mmol/L, respectively. Emulsions are prepared by first dispersing the hydrophilic particles and the short amphiphiles in an aqueous solution at pH 4.75, followed by the addition and vigorous mixing of octane using a household hand mixer. Hydrophobic sites on the particle surface are provided by the short hydrocarbon chains of the adsorbed amphiphilic molecules, whereas the hydrophilic sites are given by the hydroxyl groups originally present on the oxide surface. Protonation of these surface hydroxyl groups at the acidic conditions used for emulsification helps to keep the particle surface predominantly hydrophilic. The electric double layer resulting from such protonation also leads to

repulsive interactions between particles in the aqueous phase, allowing for the dispersion of up to about 40 vol% of particles in the initial suspension.

An increase in the valeric acid concentration above 50-70 mmol/L leads to strong agglomeration of particles in the aqueous suspension due to their increased hydrophobicity. This hinders the stabilization of oil-in-water emulsions at high amphiphile concentrations. However, we found that the addition of such high concentration of amphiphiles and particles to the oil phase rather than to water results in the formation of very stable water-in-oil emulsions, suggesting that the initially hydrophilic particles become predominantly hydrophobic ($\theta > 90°$) above this critical amphiphile concentration, c*. In this case, the density of hydrophobic sites rendered by the amphiphile hydrocarbon tail presumably surpasses the density of hydroxyl groups on the particle surface, as schematically shown in Figure 3.1. Moreover, the low dielectric constant of octane inhibits protonation of the hydroxyl groups further reducing the hydrophilicity of the particle surface. The reduced surface protonation in the oil phase was confirmed by zeta potential measurements. Alumina particles modified with 27.5 mmol/L of valeric acid in octane exhibit a zeta potential of only –7 mV, as opposed to the value of 22 mV obtained for the same amphiphile-coated particles in water. The low density of electrical charges and the absence of a thick steric layer on the particle surface also reduce the maximum concentration of particles that can be initially dispersed in the oil phase.

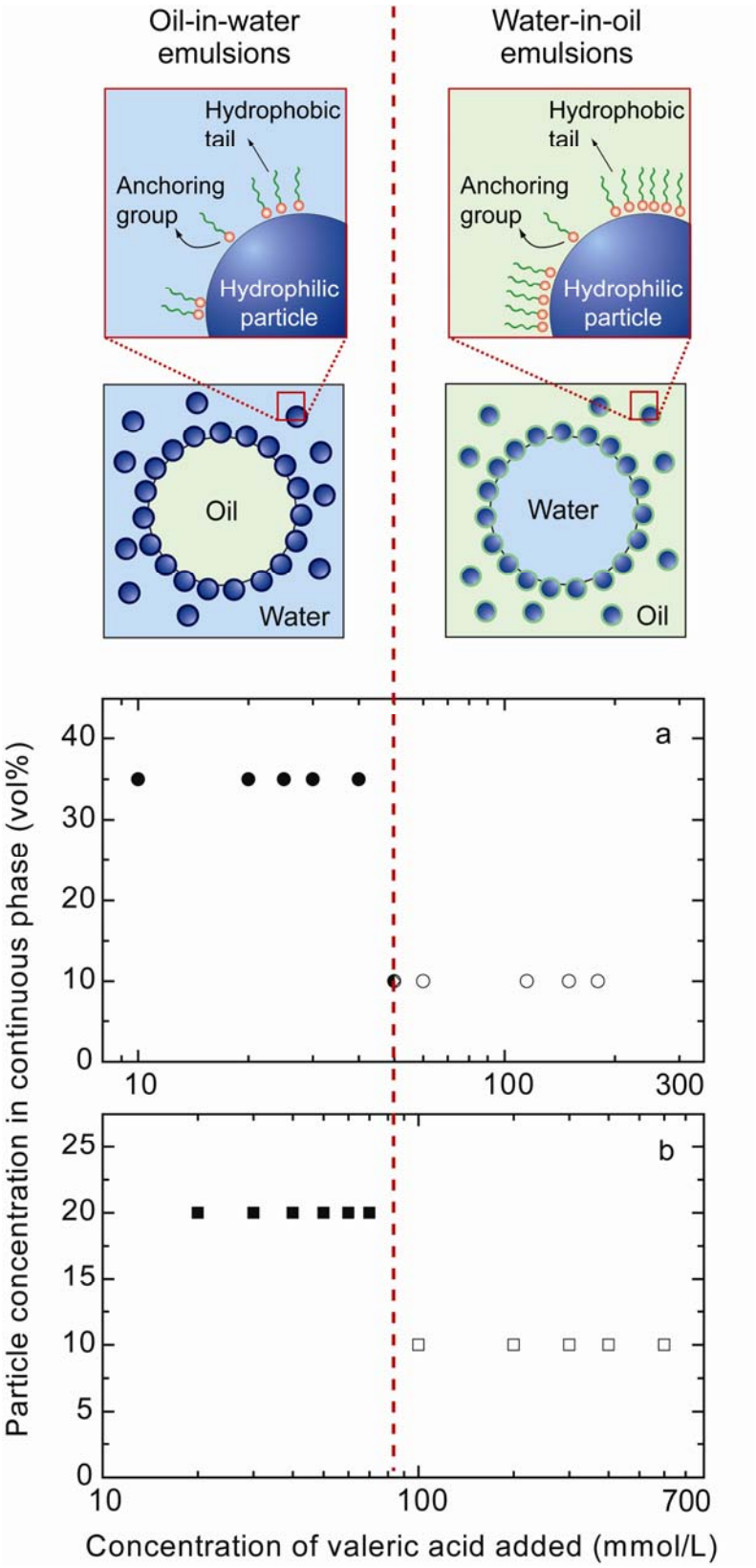

Figure 3.1: Schematic diagram showing the concentration of valeric acid needed for the preparation of oil-in-water (full symbols) and water-in-oil (open symbols) emulsions at different concentrations of (a) α-Al_2O_3 and (b) δ-Al_2O_3 particles.

Using α-Al_2O_3 particles and an intermediate valeric acid concentration of 50 mmol/L, it was possible to stabilize both oil-in-water and water-in-oil emulsions depending only on the liquid phase where the amphiphiles and particles were initially present. Oil-in-water emulsions were obtained when particles and amphiphiles were initially added to the aqueous phase, whereas water-in-oil emulsions were prepared if particles and amphiphiles were initially present in the oil phase. Even though most emulsions were prepared by adding an excess of the dispersed phase into the particle-containing continuous liquid, the critical amphiphile concentration, c* did not depend on the relative volume ratio of water and oil.

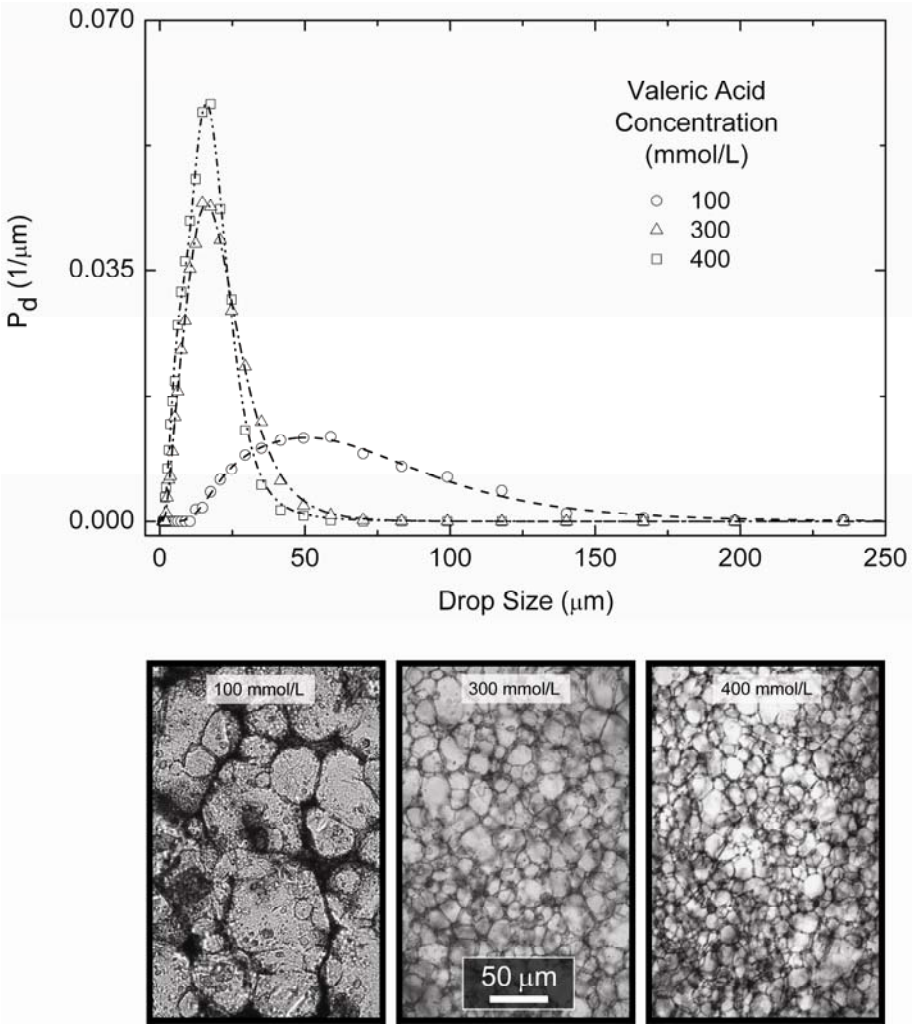

Figure 3.2: Droplet size distributions (top) and optical microscope images (bottom) of water-in-oil emulsions prepared with δ-Al_2O_3 particles and different concentrations of valeric acid. Emulsions were prepared by mixing 83.6 vol% water with suspensions of 10 vol% alumina in octane.

The excess of dispersed phase added during emulsification led to compressed emulsions with volume fractions of droplets in a range from 70 to 84%. Due to the high concentration of distorted droplets, the emulsions showed viscoelastic behavior with a finite yield stress in the order of 0.5 to 1.0 kPa (see Figure 11.5 in Appendix). Emulsions containing high concentrations of dispersed droplets were also remarkably stable against coalescence, Ostwald ripening, and creaming. No significant change was observed in the emulsion droplet size distribution within a time period of more than two years after emulsification. This remarkable stability can be attributed to the strong adsorption of particles at the oil-water interface [7, 10] and to the formation of an attractive particle network throughout the highly concentrated continuous phase [38].

In general, emulsions exhibited log-normal droplet size distributions with mean diameters varying from 7.6 to 91 μm depending on the amphiphile initial concentration, as exemplified in Figure 3.2 for water-in-oil emulsions containing 10 vol% δ-Al_2O_3 particles. The initial amphiphile concentration had a minor effect on the mean droplet size of oil-in-water emulsions containing α-Al_2O_3 and δ-Al_2O_3 particles (Figure 3.3), in agreement with previous data reported for this system [38]. In contrast, water-in-oil emulsions containing α-Al_2O_3 and δ-Al_2O_3 exhibited a three- and six-fold decrease in the mean droplet size as the amphiphile concentration was increased above 60 and 100 mmol/L, respectively (Figure 3.3). These results differ from trends observed for particle-stabilized emulsions in the absence of amphiphiles, where the smallest droplet sizes were achieved with particles of intermediate rather than high hydrophobicity [16]. It is important to note that the valeric acid molecules used here as short amphiphiles exhibit a molecular structure with a large hydrophilic head group and a small hydrocarbon tail that favors their adsorption onto oil rather than water droplets [9]. Therefore, the water-in-oil emulsions prepared with valeric acid and alumina particles are expected to be stabilized solely by the in situ surface modified particles.

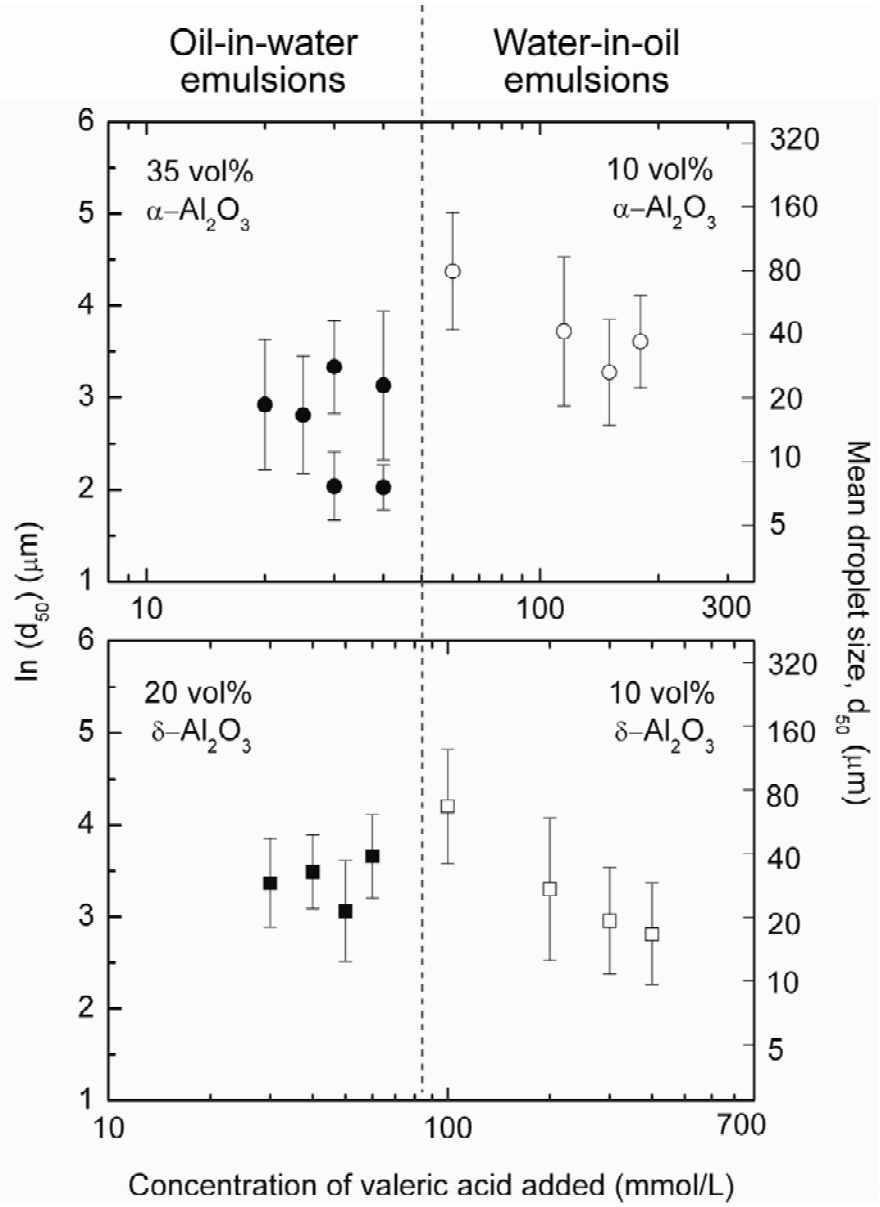

Figure 3.3: Mean droplet size of oil-in-water (full symbols) and water-in-oil (open symbols) emulsions at different concentrations of α-Al_2O_3 and δ-Al_2O_3 as a function of the valeric acid concentration.

The approach used here for the preparation of particle-stabilized emulsions was also extended to other types of amphiphiles and colloidal particles. Oil-in-water and water-in-oil emulsions were prepared using for example 10 vol% iron oxide particles after in situ surface modification with octyl gallate (Figure 3.4). Oil-in-water emulsions were obtained by initially adding the particles and 44 mmol/L octyl gallate to water at pH 9.9 and afterwards mixing the resulting suspension with 79.4 vol% octane. Water-in-oil emulsions were prepared by initially dispersing the particles and 55 mmol/L octyl gallate in octane followed my mixing of this suspension with 78 vol% water.

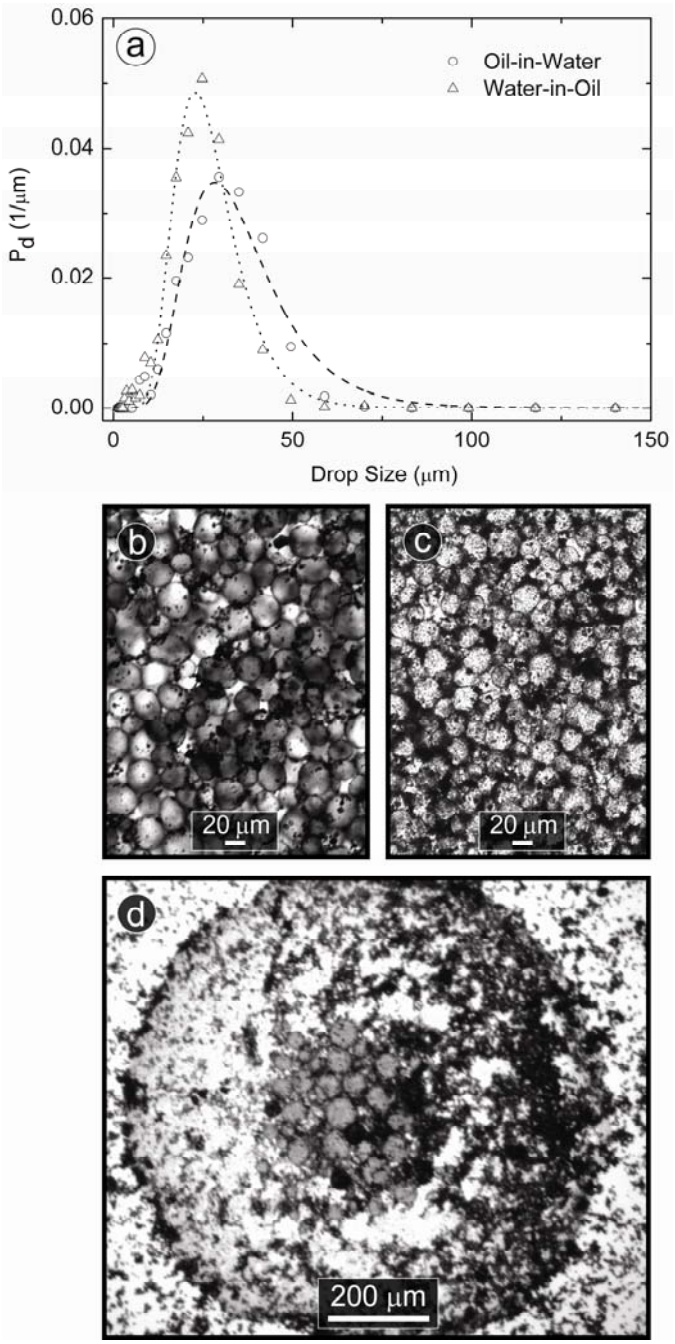

Figure 3.4: (a) Droplet size distributions and optical microscope images of (b) oil-in-water and (c) water-in-oil emulsions prepared with iron oxide particles and different concentrations of octyl gallate. The continuous lines in (a) correspond to the log-normal distribution functions used to describe the droplet size distributions. The optical microscope image in (d) shows an oil-in-water-in-oil double emulsion prepared with 1 vol% iron oxide particles and intermediate concentrations of octyl gallate.

The possibility to obtain both oil-in-water and water-in-oil emulsions at similar amphiphile concentrations also enabled the preparation of particle-stabilized double

emulsions. Oil-in-water-in-oil emulsions for example were obtained through the addition and careful mixing of octane containing 1 vol% iron oxide particles and 5 mmol/L octyl gallate with a previously prepared oil-in-water emulsion containing 22.7 vol% octane, 1 vol% iron oxide particles, and 4 mmol/L octyl gallate (Figure 3.4). The volume fraction of oil-containing water droplets in the final double emulsion was 60%. Such double emulsions contained water droplets with size ranging from 100 to 650 µm and oil droplets with average sizes between 20 and 50 µm. In contrast to surfactant-stabilized systems, particle transfer from inner to outer interfaces and vice versa is impeded in this case due to the irreversible adsorption of particles, which significantly increases the stability of the double emulsions. The fact that double emulsions with colloidal particles of various chemical compositions can be produced using properly selected amphiphiles [38, 39] adds numerous other possibilities for the design of particle-coated shells for encapsulation purposes, since most of the available methods are restricted to silica particles containing chemically grafted surface modifiers.

The various types of emulsions that can be formed using different combinations of colloidal particles and short amphiphiles makes this approach a very general method for the preparation of simple and multiple particle-stabilized emulsions. Such great versatility should be of major advantage for the manufacture of new materials, food, cosmetics, and pharmaceutical products.

3.4 Acknowledgment

We are thankful to Jérôme Zemp, Joëlle Hofstetter, Pierrick Prétat, and Felix Schuler for their assistance in the experimental work.

3.5 References

1. Utada, A. S., Lorenceau, E., Link, D. R., Kaplan, P. D., Stone, H. A., Weitz, D. A., *Monodisperse double emulsions generated from a microcapillary device.* Science, 2005, 308(5721), 537-541.

2. Akartuna, I., Studart, A. R., Tervoort, E., Gauckler, L. J., *Macroporous ceramics from particle-stabilized emulsions.* Adv. Mater., 2008, 20(24), 4714-4718.

3. Studart, A. R., Gonzenbach, U. T., Akartuna, I., Tervoort, E., Gauckler, L. J., *Materials from foams and emulsions stabilized by colloidal particles.* J. Mater. Chem., 2007, 17(31), 3283-3289.

4. Levine, S., Bowen, B. D., Partridge, S. J., *Stabilization of emulsions by fine particles I. Partitioning of particles between continuous phase and oil/water interface.* Colloids Surf., 1989, 38(2), 325-343.

5. Pickering, S. U., *Emulsions.* J. Chem. Soc., 1907, 91, 2001-2021.

6. Ramsden, W., *Separation of solids in the surface-layers of solutions and suspensions (Observations on surface-membranes, bubbles, emulsions, and mechanical coagulation). Preliminary account.* Proc. Roy. Soc. London, 1903, 72, 156-164.

7. Pieranski, P., *Two-dimensional interfacial colloidal crystals.* Phys. Rev. Lett., 1980, 45(7), 569-572.

8. Binks, B., Horozov, T. S., Eds., *Colloidal particles at liquid interfaces*. 2006, Cambridge University Press: Cambridge, U. K.

9. Aveyard, R., Binks, B. P., Clint, J. H., *Emulsions stabilised solely by colloidal particles.* Adv. Colloid Interface Sci., 2003, 100-102, 503-546.

10. Binks, B. P., *Particles as surfactants--similarities and differences.* Curr. Opin. Colloid Interface Sci., 2002, 7(1-2), 21-41.

11. Kaptay, G., *On the equation of the maximum capillary pressure induced by solid particles to stabilize emulsions and foams and on the emulsion stability diagrams.* Colloids Surf. A, 2006, 282, 387-401.

12. Vignati, E., Piazza, R., Lockhart, T. P., *Pickering emulsions: Interfacial tension, colloidal layer morphology, and trapped-particle motion.* Langmuir, 2003, 19, 6650-6656.

13. Horozov, T. S., Binks, B., *Particle-stabilized emulsions: A bilayer or a bridging monolayer?* Angew. Chem. Int. Ed., 2006, 45, 773-776.

14. Binks, B. P., Lumsdon, S. O., *Effects of oil type and aqueous phase composition on oil-water mixtures containing particles of intermediate hydrophobicity.* Phys. Chem. Chem. Phys., 2000, 2(13), 2959-2968.

15. Binks, B. P., Lumsdon, S. O., *Transitional phase inversion of solid-stabilized emulsions using particle mixtures.* Langmuir, 2000, 16(8), 3748-3756.

16. Binks, B. P., Lumsdon, S. O., *Influence of particle wettability on the type and stability of surfactant-free emulsions.* Langmuir, 2000, 16(23), 8622-8631.

17. Binks, B. P., Lumsdon, S. O., *Catastrophic phase inversion of water-in-oil emulsions stabilized by hydrophobic silica.* Langmuir, 2000, 16(6), 2539-2547.

18. Binks, B. P., Kirkland, M., *Interfacial structure of solid-stabilised emulsions studied by scanning electron microscopy.* Phys. Chem. Chem. Phys., 2002, 4(15), 3727-3733.

19. Horozov, T. S., Aveyard, R., Clint, J. H., Binks, B. P., *Order-disorder transition in monolayers of modified monodisperse silica particles at the octane-water interface.* Langmuir, 2003, 19, 2822-2829.

20. Tarimala, S., Dai, L. L., *Structure of microparticles in solid-stabilized emulsions.* Langmuir, 2004, 20, 3492-3494.

21. Binks, B. P., Philip, J., Rodrigues, J. A., *Inversion of silica-stabilized emulsions induced by particle concentration.* Langmuir, 2005, 21(8), 3296-3302.

22. Xu, Q. Y., Nakajima, M., Binks, B. P., *Preparation of particle-stabilized oil-in-water emulsions with the microchannel emulsification method.* Colloids Surf. A, 2005, 262(1-3), 94-100.

23. Tambe, D. E., Sharma, M. M., *Factors controlling the stability of colloid-stabilized emulsions: I. An experimental investigation.* J. Colloid Interface Sci., 1993, 157(1), 244-253.

24. Velev, O. D., Furusawa, K., Nagayama, K., *Assembly of latex particles by using emulsion droplets as templates. 1. Microstructured hollow spheres.* Langmuir, 1996, 12(10), 2374-2384.

25. Schulman, J. H., Leja, J., *Control of contact angles at the oil-water-solid interfaces: Emulsions stabilized by solid particles ($BaSO_4$)*. Trans. Far. Soc., 1954, 50(1), 598-605.

26. Tsugita, A., Takemoto, S., Mori, K., Yoneya, T., Otani, Y., *Studies on o/w emulsions stabilized with insoluble montmorillonite-organic complexes*. J. Colloid Interface Sci., 1983, 95(2), 551-560.

27. Gelot, A., Friesen, W., Hamza, H. A., *Emulsification of oil and water in the presence of finely divided solids and surface-active agents*. Colloids Surf., 1984, 12, 271-303.

28. Hassander, H., Johansson, B., Törnell, B., *The mechanism of emulsion stabilization by small silica (Ludox) particles*. Colloids Surf., 1989, 40, 93-105.

29. Binks, B. P., Desforges, A., Duff, D. G., *Synergistic stabilization of emulsions by a mixture of surface-active nanoparticles and surfactant*. Langmuir, 2007, 23(3), 1098-1106.

30. Binks, B. P., Rodrigues, J. A., *Enhanced stabilization of emulsions due to surfactant-induced nanoparticle flocculation*. Langmuir, 2007, 23(14), 7436-7439.

31. Binks, B. P., Rodrigues, J. A., Frith, W. J., *Synergistic interaction in emulsions stabilized by a mixture of silica nanoparticles and cationic surfactant*. Langmuir, 2007, 23(7), 3626-3636.

32. Noble, P. F., Cayre, O. J., Alargova, R. G., Velev, O. D., Paunov, V. N., *Fabrication of "hairy" colloidosomes with shells of polymeric microrods*. J. Am. Chem. Soc., 2004, 126, 8092-8093.

33. Binks, B. P., Lumsdon, S. O., *Pickering emulsions stabilized by monodisperse latex particles: Effects of particle size*. Langmuir, 2001, 17(15), 4540-4547.

34. Stancik, E. J., Kouhkan, M., Fuller, G. G., *Coalescence of particle-laden fluid interfaces*. Langmuir, 2004, 20, 90-94.

35. Hsu, M. F., Nikolaides, M. G., Dinsmore, A. D., Bausch, A. R., Gordon, V. D., Chen, X., Hutchinson, J. W., Weitz, D. A., Marquez, M., *Self-assembled shells composed of colloidal particles: Fabrication and characterization*. Langmuir, 2005, 21, 2963-2970.

36. Subramaniam, A. B., Abkarian, M., Stone, H. A., *Controlled assembly of jammed colloidal shells on fluid droplets*. Nat. Mater., 2005, 4, 553-556.

37. Golemanov, K., Tcholakova, S., Kralchevsky, P. A., Ananthapadmanabhan, K. P., Lips, A., *Latex-particle stabilized emulsions of anti-Bancroft type*. Langmuir, 2006, 22, 4968-4977.

38. Akartuna, I., Studart, A. R., Tervoort, E., Gonzenbach, U. T., Gauckler, L. J., *Stabilization of oil-in-water emulsions by colloidal particles modified with short amphiphiles*. Langmuir, 2008, 24(14), 7161-7168.

39. Gonzenbach, U. T., Studart, A. R., Tervoort, E., Gauckler, L. J., *Stabilization of foams with inorganic colloidal particles*. Langmuir, 2006, 22(26), 10983-10988.

4 Macroporous Ceramics from Particle-Stabilized Emulsions*

Abstract

The fabrication of porous materials from emulsion templates often requires inconvenient and elaborated sol-gel chemical reactions. The use of particles for the stabilization of emulsions eliminates the need of chemical reactions to obtain porous materials, but has been mainly restricted to a few chemical compositions. We report a versatile and simple approach to produce macroporous ceramics from emulsions stabilized with particles of various chemical compositions. The long-term stability of the particle-stabilized emulsions allows the evaporation of the liquid phases without collapsing the structure, rendering unique porous ceramics after sintering at high temperatures without any chemical reaction. The viscoelastic nature of the wet emulsions enables their processing into porous structures using conventional shaping technologies. The versatility of the method is expected to bring many advantages in areas ranging from sustainable and clean energy systems to tissue engineering and biomedical devices.

* *I. Akartuna, A. R. Studart, E. Tervoort, and L. J. Gauckler, Adv. Mater., 2008, 20, 1-5.*

4.1 Introduction

Macroporous ceramics with controlled microstructure and chemical composition are required in an increasing number of applications [1]. Methods that enable tuning of the porosity, pore morphology, and size distribution of these porous structures are of particular interest for the fabrication of chemical sensors, filtration membranes for molten metals and hot gases, bioreactors, catalyst carriers, electrodes for batteries and solid oxide fuel cells, insulators, and scaffolds for bone replacement and tissue engineering [1-4].

The use of emulsions as templates for the production of porous materials is a versatile method that allows for the deliberate design of the porous structure [5]. The emulsion templating method involves the preparation of emulsions with inorganic precursors or particles in the continuous phase and subsequent removal of the dispersed droplets by drying and heat treatment.

Gelation of the continuous phase or the formation of a rigid shell around the liquid droplets is required to avoid collapse of the emulsion structure during liquid removal. Therefore, emulsion templating has been often applied in combination with a sol-gel process. Macroporous silica [6-8], titania [6, 7, 9] and zirconia [6, 7] were produced by gelling and drying a surfactant-stabilized emulsion consisting of monodisperse oil droplets dispersed in a formamide sol with alkoxide precursors. Gelation occurs via condensation of the hydrolyzed alkoxide in the liquid surrounding the droplets. Subsequent heat treatment of such emulsions resulted in ordered materials with porosities up to 90% and pore sizes ranging from 50 nm to 10 μm [6, 7, 9]. In another approach, metal alkoxide molecules initially added to polydisperse oil droplets were used to gel the oil-formamide interface and thus render porous titania structures with a broad pore size distribution [10]. Recently, Sen et al. mixed silica precursors with a surfactant-stabilized oil-in-water emulsion to form disordered macroporous silica with pore sizes ranging from a few hundred nanometers to a few micrometers after creaming of oil droplets [11, 12]. Furthermore, Carn et al. prepared porous monoliths of silica with hierarchical pore structure from a mixture of a silica precursor and a surfactant-stabilized concentrated oil-in-water emulsion [13, 14]. The monoliths exhibited pore sizes ranging from 0.5 to 100 μm with porosities up to 92%.

In addition to sol-gel transitions, colloidal particles adsorbed at liquid interfaces have also been used to stabilize emulsions in the wet state and produce macroporous ceramics after drying and sintering. Macroporous silica structures with average pore sizes in the range from 5 to 50 μm were prepared by drying emulsions stabilized by silica particles of controlled wettability [15, 16]. Porous alumina with pore sizes in the range of 20 to 250 μm and porosities up to 66% has also been produced by the electrophoretic deposition of alumina-loaded oil-in-water emulsions, with subsequent removal of the oil phase by drying and heat treatment [17].

While considerable progress has been made on the fabrication of porous materials via emulsion templating, currently available methods still have important limitations. Emulsions consolidated by sol-gel processes require a strict control over the reaction chemistry, and may become challenging for chemical compositions other than those for which sol-gel transitions have been well documented. The use of particles to stabilize the emulsion droplets does not require chemical reactions, but on the other hand has been mostly limited to particles whose surface wettability can be tailored through prior chemical treatments, e.g., the silanization of SiO_2 and TiO_2. Hence, the fabrication of porous materials using an emulsion templating approach that would not need chemical reactions and that could be easily extended to a wide variety of chemical compositions would be highly desirable.

Here we describe a versatile and simple approach to produce solid macroporous ceramics from emulsions stabilized with particles of various chemical compositions. Stabilization with particles hinders extensive droplet coalescence during solvent extraction, allowing for drying and sintering of the emulsions directly into macroporous materials in the absence of any chemical reaction.

4.2 Materials and methods

4.2.1 Materials

α-Al_2O_3 powder (Ceralox HPA-0.5, 99.99% Al_2O_3) with average particle diameter, d_{50}, of 200 nm, specific surface area of 10 m^2/g, and density of 3.98 g/cm^3 was purchased from Sasol North America Inc. (Tucson, AZ, USA). The SiO_2 powder (grade Snowtex ZL) was acquired from Nissan Chemical (Houston, TX, USA) and exhibited d_{50} of 80 nm, specific surface area of 25 m^2/g, and density of 2.1 g/cm^3. Fe_3O_4 powder (>98%

Fe_3O_4) with d_{50} of 20-30 nm, specific surface area of 60 m^2/g, and density of 4.95 g/cm^3 was supplied by Nanostructured & Amorphous Materials, Inc. (Houston, TX; USA). Octane (97% pure, Boiling temperature T_b = 125 °C) was purchased from Acros Organics (Belgium) and used as received. The short amphiphilic molecules used for particle modification were propionic acid (> 99%, Sigma-Aldrich Chemie GmbH, Germany), hexyl amine, and octyl gallate (> 98%, and > 99% pure, respectively, Fluka AG, Buchs, Switzerland). Double deionized water with an electrical resistance of 18 MΩcm was used in the experiments (Nanopure water system, Barnstead, USA).

4.2.2 Methods

Prior to emulsification, colloidal suspensions of particles were prepared by adding powders to the continuous liquid phase under steady mixing. The concentration of particles in the suspension was 10 and 35 vol% for the iron oxide and silica particles, respectively. For alumina particles, suspensions were prepared with 15 and 35 vol% powder. It is important to note that the particle concentration indicated throughout this study refers to the solids content in the initial aqueous suspension, and is not based on the emulsion total volume. In the case of aqueous suspensions of alumina and silica particles, in situ surface hydrophobization of initially hydrophilic particles was performed by de-agglomerating the powder for 22 h in a ball-mill, followed by a gradual addition of aqueous solutions containing the short amphiphiles (Table 4.1). For non-aqueous suspensions of iron oxide, a mixture containing octane, powder, and short amphiphiles was ball-milled for 22 h. Ball-milling was carried out at a ball/powder ratio of 2.5, using 10 mm alumina balls for the alumina suspensions, and 5, 10 and, 20 mm zirconia balls for the silica and iron oxide suspensions. 2 M HCl or 1 M NaOH solutions were used for pH adjustments. After the preparation of suspensions, emulsification was performed by vigorously stirring the suspension and the dispersed phase for 3 min using a household mixer at full power (Multimix 350 W, Braun, Spain). Droplet size distributions were determined by evaluating a set of at least five optical microscope images for each composition, using the linear intercept method (software Lince, TU Darmstadt, Germany). Average droplet sizes and 68% confidence intervals were obtained by fitting log-normal distributions to the experimental data. Rheology measurements were performed at 25 °C using a stress-controlled rheometer (Bohlin-Rheometer CS-50, Bohlin, England) with profiled parallel-plate geometry (25 mm plate diameter). Experiments were carried out with a mechanically set gap of 1000 μm.

Oscillatory measurements were conducted at a constant frequency of 1 Hz by gradually increasing the maximum applied stress from 10 to 1000 Pa. Steady-state experiments were carried out by progressively increasing the applied stress from 200 to 1000 Pa. All emulsions were placed into plastic cylindrical beakers (350 cm^3, 13 cm height, and 6 cm diameter) after emulsification, and then left to dry in air for 2 days in the case of oil-in-water emulsions, and 1 week for water-in-oil emulsions to allow evaporation of oil and water. Following drying, alumina and silica samples were sintered in air for 2 h at 1600 °C, while iron oxide samples were sintered under vacuum for 2 h at 1100 °C. The porous ceramics obtained after sintering were investigated by scanning electron microscopy (SEM, LEO 1530). SEM samples were prepared by Pt sputtering for 55 s at 60 mA. Pore size distributions of sintered ceramics were determined by evaluating a set of at least five SEM images for each composition, using the linear intercept method. Log-normal distributions were used to describe the experimental data and to obtain average droplet sizes and 68% confidence intervals.

4.3 Results and discussion

Emulsions were stabilized by adsorbing surface modified inorganic particles at the oil-water interface. Surface modification was achieved through the in situ adsorption of short amphiphilic molecules on the surface of initially hydrophilic particles. In order to modify colloidal particles of different surface chemistry we chose short amphiphiles with a head group that shows high affinity towards the particle surface. On the basis of our earlier work [18, 19], short carboxylic acids, alkyl amines, and alkyl gallates were used for the in situ modification of alumina, silica, and iron oxide particles, respectively (Table 4.1).

Table 4.1: Conditions required for the preparation of particle-stabilized emulsions with a wide range of metal oxide powders. The amount of the dispersed phase was calculated with respect to the emulsion total volume (water + particles + oil).

Metal Oxide	Particle Diameter (d_{50}) (nm)	pH	Suspension Solids Content (vol%)	Amphiphile	Amphiphile Content (mmol/L)	Oil/Water Content (vol%)
α-Al_2O_3	200	4.75	35	Propionic acid	131	72
α-Al_2O_3	200	4.75	15	Propionic acid	43	71
SiO_2	80	10.4	35	Hexyl amine	60	72
Fe_3O_4	40	-	10	Octyl gallate	55	78

Different types of emulsions were formed depending on in which of the immiscible liquids (oil or water) the particles were initially dispersed and surface modified. Oil-in-water emulsions, for example, were obtained by dispersing alumina and silica particles in water and rendering them slightly hydrophobic via surface modification in the aqueous phase. Surface modification was promoted in this case by the electrostatic attraction of alkyl amine and carboxylic acid molecules onto the oppositely charged silica and alumina particles, respectively, at pH values in the vicinity of the pK_a values of the short amphiphiles [20]. The initial hydrophilic nature of the colloidal particles enables the preparation of homogeneous dispersions of highly concentrated suspensions prior to surface modification. In this case, the main advantage of using short amphiphiles is their high solubility and high critical micelle concentration in the continuous phase. This allows for the surface modification of high concentrations of particles of wide size range in the absence of competing micelle formation.

Water-in-oil emulsions were also produced by dispersing iron oxide particles in octane prior to emulsification. To achieve good dispersion in the oil phase the initially hydrophilic iron oxide particles were hydrophobized through the surface adsorption of alkyl gallates. Surface modification does not render the particles completely

hydrophobic, enabling the stabilization of water-in-oil emulsions through the adsorption of slightly hydrophilic particles at the oil-water interface.

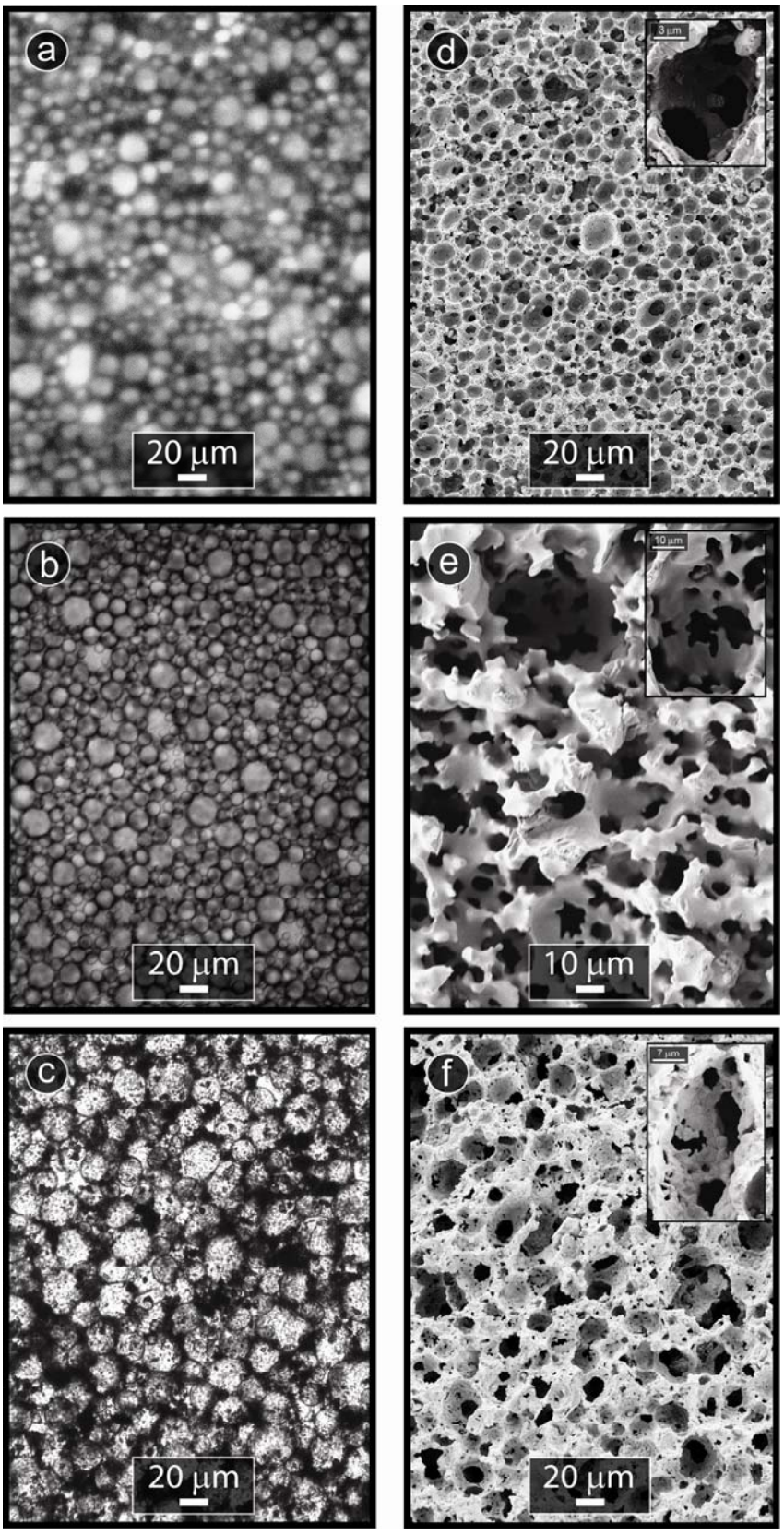

Figure 4.1: Microstructures of emulsions and sintered porous ceramics prepared with various inorganic particles hydrophobized by different short chain amphiphiles. a) Oil-in-water emulsion with 72 vol% octane and 35 vol% alumina particles hydrophobized with 131 mmol/L propionic acid at pH 4.75; b) Oil-in-water emulsion with 72 vol% octane and 35 vol% silica particles hydrophobized with 60 mmol/L hexyl amine at pH 10.4; c) Water-in-oil emulsion with 78 vol% water and 10 vol% magnetite particles hydrophobized with 55 mmol/L octyl gallate; d) Porous alumina obtained after sintering the emulsion in (a) at 1600 °C; e) Porous silica obtained after sintering the emulsion in (b) at 1600 °C; f) Porous iron oxide obtained after sintering the emulsion in (c) at 1100 °C. The emulsions shown in (b) and (c) were diluted 3x with the continuous phase in order to facilitate the observation of droplets. The porous structures (e) and (f) were obtained from concentrated non-diluted emulsions. The insets in (d-f) show the interconnecting windows formed in the pore walls after sintering.

Particle-stabilized emulsions were formed by mechanical shearing a mixture containing the dispersed phase and concentrated suspensions of alumina, silica and iron oxide particles modified with short amphiphiles. The adsorption of surface modified particles onto the freshly created oil-water interface led to formation of stable droplets dispersed throughout the suspension, as shown in Figure 4.1. The amount of the dispersed phase in the final emulsion varied from 72 to 78 vol% (Table 4.1). Emulsions stabilized by alumina, silica, and iron oxide particles exhibited relatively broad droplet size distributions with average sizes of 11, 13, and 25 μm, and 68% confidence intervals of 8-15, 9-19, and 19-34 μm, respectively (Figure 4.2.a). The microstructure of the emulsions could be further tailored by varying the amount of particles in the initial suspension. Decreasing for example the alumina concentration in the initial suspension from 35 to 15 vol%, led to a multimodal distribution of larger droplets with average mean sizes of 16, 30, and 80 μm, and 68% confidence intervals of 11-24, 27-33, and 54-119 μm, respectively. Such increase in droplet size results from the lower viscosity of the continuous suspension, which decreases the shearing stresses applied on the droplets during emulsification [18].

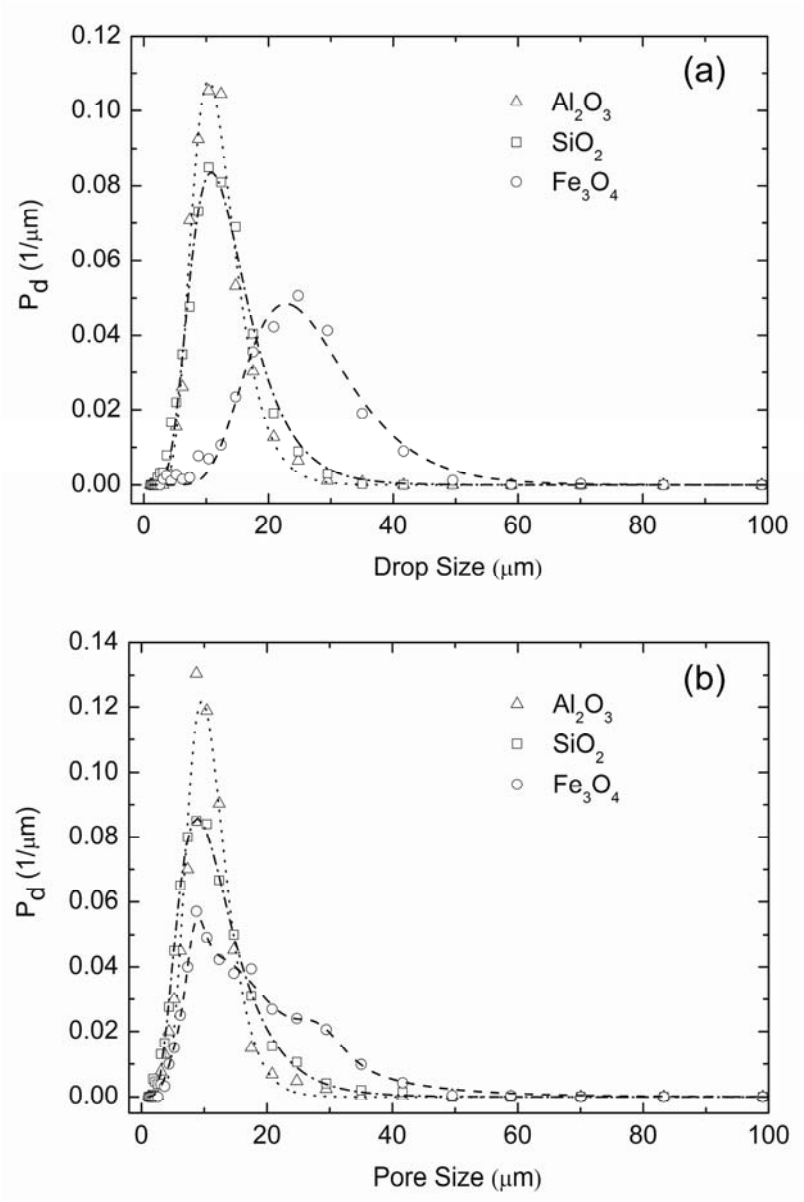

Figure 4.2: (a) Droplet- and (b) pore size distributions of particle-stabilized emulsions and sintered porous ceramics prepared with various inorganic particles hydrophobized using different short chain amphiphiles. The compositions of the emulsions and porous ceramics are described in Figure 4.1. The continuous lines correspond to the radial probability density functions, used to describe the droplet size distributions.

The as-prepared particle-stabilized emulsions showed viscoelastic behavior with a noticeable yield stress, as exemplified in Figure 4.3 for alumina-stabilized emulsions probed under oscillatory shear. Under steady-state conditions, the viscoelastic character led to a typical shear-thinning behavior with a marked decrease in apparent viscosity as the shear rate is increased (Figure 4.3, inset). The extent of shear-thinning

and the magnitude of the yield stress could be easily tuned by simply diluting the as-prepared emulsion with the continuous phase. The liquid-like behavior at stresses higher than the yield stress enables the injection or the deposition of the emulsions into molds or onto substrates using conventional technologies such as injection molding, extrusion, robocasting, ink-jet printing, screen-printing, and spin-coating. The elastic behavior obtained when the stresses are ceased after deposition allows for the emulsion to keep its shape without requiring any further gelation or strengthening reaction. Oil-in-water emulsions containing 35 vol% alumina particles, for instance, were extruded (Figure 4.3.b) and injection molded into various shapes without need of further strengthening of the material prior to the de-molding step.

The emulsions also exhibited remarkable stability against extensive coalescence, Ostwald ripening, and creaming. No significant change was observed in the emulsion droplet size distribution within a time period of more than two years after emulsification. This remarkable stability can be attributed to the strong adsorption of particles at the oil-water interface [21, 22]. The irreversibly adsorbed particles hinder the rupture of the thin liquid film between the droplets, and act as a barrier against the shrinkage of droplets expected from Ostwald ripening. The formation of an attractive particle network throughout the highly concentrated continuous phase is also expected to enhance the emulsion stability.

Following emulsification, the wet emulsions stabilized by different particles were dried in air to remove water and oil. The relatively high vapor pressure of octane and water (1.47 and 2.34 kPa, respectively, at 20 °C) allowed for evaporation of the emulsion droplets at room temperature. The dried samples were finally sintered at 1100 °C (iron oxide) and 1600 °C (alumina and silica) for 2 h to obtain porous inorganic structures.

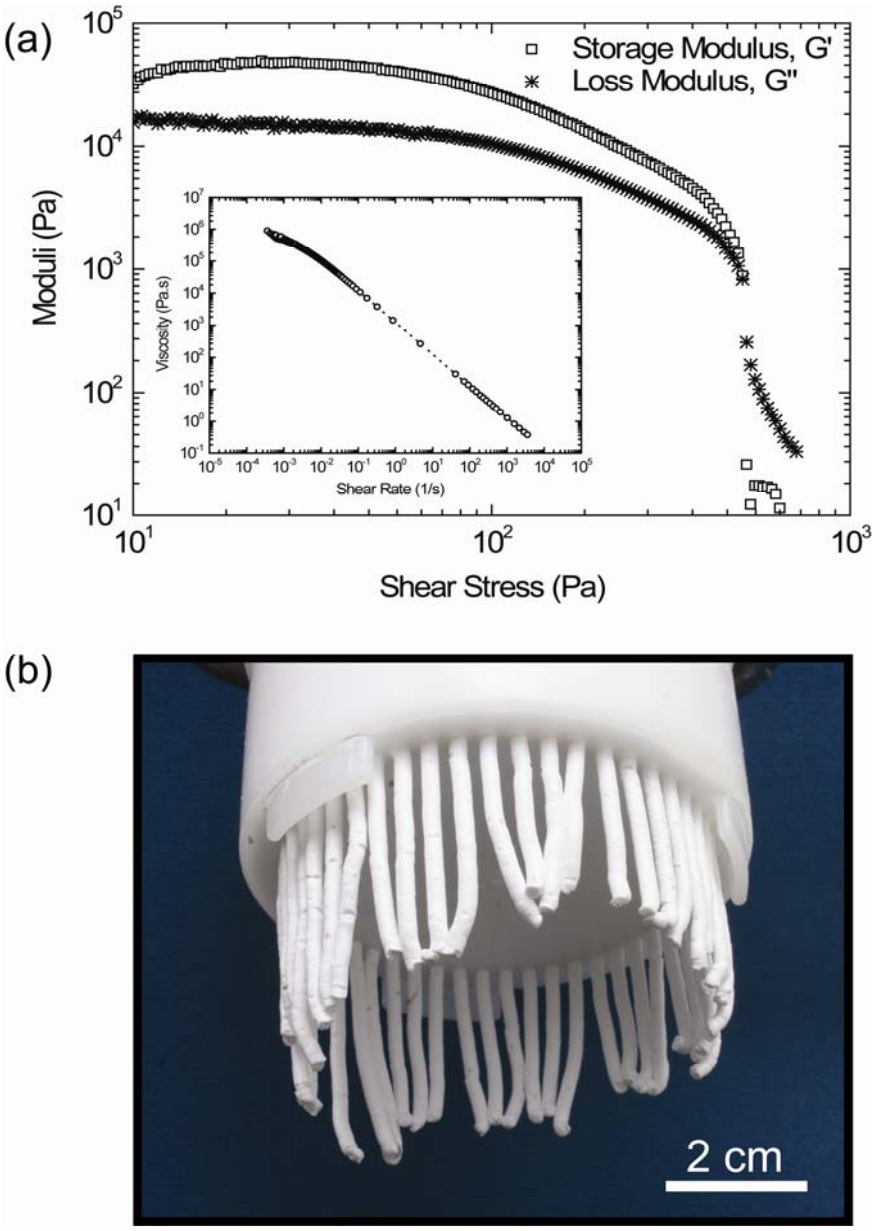

Figure 4.3: (a) Storage (G', □) and loss (G", ∗) moduli as functions of applied shear stress for an octane-in-water emulsion containing 35 vol% alumina particles, 131 mmol/L propionic acid, and 72 vol% octane. Inset: Apparent viscosity (○) of the same emulsion as a function of applied shear rate. (b) Image of the same oil-in-water emulsion extruded through the holes of a cylindrical plastic tool.

Macroporous ceramics fabricated from emulsions stabilized by different inorganic particles are shown in Figure 4.1. Sintering of emulsions containing alumina, silica, and iron oxide particles yielded porous structures exhibiting *quasi*-spherical interconnected pores with sizes close to the droplet sizes of the initial emulsions, namely of 10, 11, and 29 μm, with 68% confidence intervals of 7-13, 7-18, and 26-32 μm,

respectively (Figure 4.2). The iron oxide structure in particular showed a considerable amount of smaller pores with peak sizes at 9 and 17 μm (68% confidence intervals of 8-10 and 9-31 μm, respectively), which correspond mainly to open windows in the lamella walls separating larger pores. The total porosity of the sintered samples was equivalent to the amount of the dispersed phase added into the initial emulsion: 72% for the alumina and silica samples, and 78% for the iron oxide structure. The porosity and pore size obtained after sintering (Figure 4.2.a and b) confirms that the particle-stabilized emulsions used as initial templates are sufficiently strong to withstand the high capillary stresses developed during drying without distortion of its internal structure (Figure 4.4). This adds great flexibility to the process, since it enables one to tailor the porosity and pore size of the final inorganic structure by changing the oil content and droplet size of the initial emulsion.

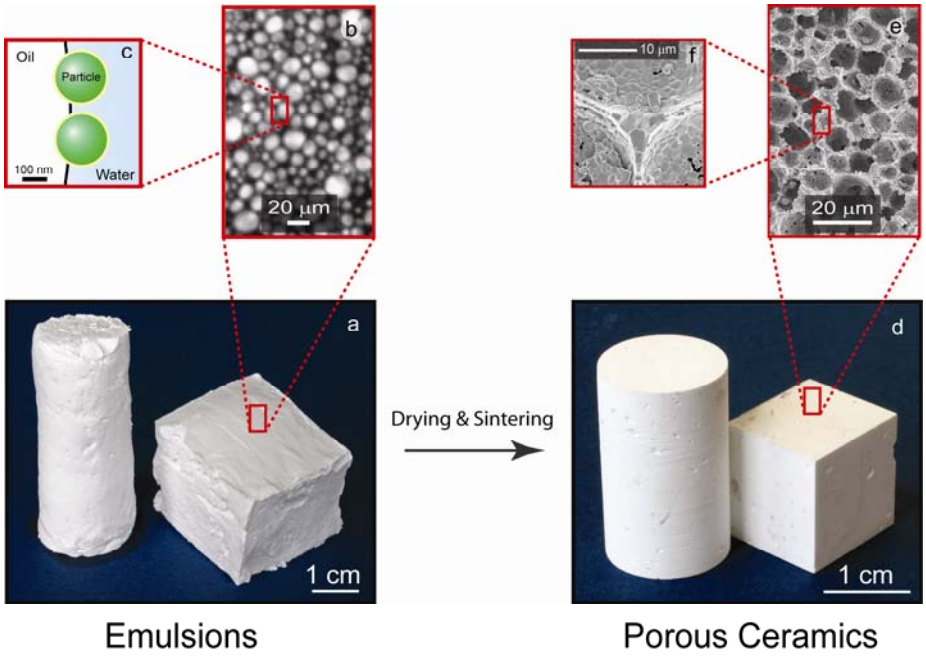

Figure 4.4: Macroporous ceramics obtained from particle-stabilized emulsions. Highly stable emulsions of different shapes (a) containing 10-20 μm droplets (b) are formed through the adsorption of submicrometer-sized colloidal particles at the oil-water interface (c). The attachment of particles at the oil-water interface is achieved through the in situ adsorption of short amphiphilic molecules on the surface of initially hydrophilic particles. Drying and sintering of these emulsions lead to mechanically robust porous ceramics (d) with interconnected 10-15 μm pores (e) and dense, crack free struts (f).

The densification of particles in the continuous phase and at the droplet interface during sintering led to the formation of dense struts and cell walls that are only a few particles thick (Figure 4.4.f). The linear shrinkage of the porous samples during sintering was about 12%. Interestingly, the sintered macroporous materials showed different degrees of pore interconnectivity, with the silica structure exhibiting the most interconnected pores, followed by the iron oxide and alumina samples (Figure 4.1.d-f insets). Interconnected pores might result from the partial coalescence of droplets before or during the drying process (see Figure 11.6 in Appendix). Partial coalescence presumably leads to the formation of an open window between touching droplets without changing the overall droplet size distribution [23]. Liquid formation during sintering is expected to enlarge open pores and smooth the pore walls, which was evident in the case of the silica structures (Figure 4.1.e). The distinct sintering behavior of the investigated particles and possible variations in the stability of the wet emulsions might explain the different pore connectivity observed in the final porous structures (Figure 4.1.d-f). The pore size and pore connectivity of the porous structures could be also tuned by varying the amount of particles in the initial suspension. A decrease in the amount of alumina particles from 35 to 15 vol%, for example, resulted in larger pores (> 50 μm) with interconnected windows in the range of 10-20 μm.

Macroporous ceramics produced from alumina-stabilized emulsions also exhibited remarkable mechanical strength. Compressive strengths as high as 13 MPa were obtained from sintered porous alumina at a porosity of 72%. Such high strength values can be attributed to the flawless and dense struts obtained in the sintered particle-stabilized emulsions.

4.4 Conclusions

The general and versatile emulsion templating process described here allows for the fabrication of macroporous ceramics of various shapes and chemical compositions in a very straightforward manner. Using short amphiphiles that can efficiently hydrophobize oxide particles with isoelectric points varying from 2 up to about 10, we developed a universal toolbox for the preparation of particle-stabilized emulsions and porous ceramics with a wide range of chemical compositions. The long-term stability and the viscoelastic behavior of the particle-stabilized emulsions enable their processing into porous structures using conventional shaping technologies.

Macroporous ceramics prepared by this approach can be used as low-weight structural components, porous media for chemical and biological separation, thermal and electrical insulating materials, catalyst supports, refractory filters for gases, and scaffolds for tissue engineering and medical implants.

4.5 Acknowledgment

We thank Ciba Specialty Chemicals (Switzerland) for funding this study and to Lars Fleig, Christina Pecnik, and Joëlle Hofstetter for their assistance in the experimental work.

4.6 References

1. Scheffler, M., Colombo, P., *Cellular Ceramics: Structure, Manufacturing, Properties and Applications*. 2005, Weinheim, Wiley - VCH.

2. Ishizaki, K., Komarneni, S., Nanko, M., *Porous Materials: Process Technology and Applications*. 1998, Dordrecht, Kluwer Academic Publishers.

3. Saggio-Woyansky, J., Scott, C. E., Minnear, W. P., *Processing of porous ceramics.* Am. Ceram. Soc. Bull., 1992, 71(11), 1674-1682.

4. Colombo, P., *Conventional and novel processing methods for cellular ceramics.* Philos. Trans. Roy. Soc. A, 2006, 364, 109-124.

5. Studart, A. R., Gonzenbach, U. T., Tervoort, E., Gauckler, L. J., *Processing routes to macroporous ceramics: A review.* J. Am. Ceram. Soc., 2006, 89(6), 1771-1789.

6. Imhof, A., Pine, D. J., *Ordered macroporous materials by emulsion templating.* Nature, 1997, 389(6654), 948-951.

7. Imhof, A., Pine, D. J., *Uniform macroporous ceramics and plastics by emulsion templating.* Adv. Mater., 1998, 10(9), 697-700.

8. Yi, G.-R., Yang, S.-M., *Microstructures of porous silica prepared in aqueous and nonaqueous emulsion templates.* Chem. Mater., 1999, 11(9), 2322-2325.

9. Manoharan, V. N., Imhof, A., Thorne, J. D., Pine, D. J., *Photonic crystals from emulsion templates.* Adv. Mater., 2001, 13(6), 447-450.

10. Imhof, A., Pine, D. J., *Preparation of titania foams.* Adv. Mater., 1999, 11(4), 311-314.

11. Sen, T., Tiddy, G. J. T., Casci, J. L., Anderson, K. R., *Macro-cellular silica foams: Synthesis during the natural creaming process of an oil-in-water emulsion.* Chem. Commun., 2003, 2182-2183.

12. Sen, T., Tiddy, G. J. T., Casci, J. L., Anderson, M. W., *Meso-cellular silica foams, macro-cellular silica foams and mesoporous solids: A study of emulsion mediated synthesis.* Microporous Mesoporous Mater., 2005, 78, 255-263.

13. Carn, F., Colin, A., Achard, M.-F., Deleuze, H., Sellier, E., Birot, M., Backov, R., *Inorganic monoliths hierarchically textured via concentrated direct emulsion and micellar templates.* J. Mater. Chem., 2004, 14(9), 1370-1376.

14. Carn, F., Colin, A., Schmitt, V., Leal Calderon, F., Backov, R., *Soft matter, sol-gel process and external magnetic field to design macrocellular silica scaffolds.* Colloids Surf., A, 2005, 263, 341-346.

15. Binks, B. P., *Macroporous silica from solid stabilized emulsion templates.* Adv. Mater., 2002, 14(24), 1824-1827.

16. Arditty, S., Schmitt, V., Giermanska-Kahn, J., Leal Calderon, F., *Materials based on solid-stabilized emulsions.* J. Colloid Interface Sci., 2004, 275(2), 659-664.

17. Neirinck, B., Fransaer, J., Van der Biest, O., Vleugels, J., *Production of porous materials through consolidation of pickering emulsions.* Adv. Eng. Mater., 2007, 9(1-2), 57-59.

18. Akartuna, I., Studart, A. R., Tervoort, E., Gonzenbach, U. T., Gauckler, L. J., *Stabilization of oil-in-water emulsions by colloidal particles modified with short amphiphiles.* Langmuir, 2008, 24(14), 7161-7168.

19. Studart, A. R., Amstad, E., Antoni, M., Gauckler, L. J., *Rheology of concentrated suspensions containing weakly attractive alumina nanoparticles.* J. Am. Ceram. Soc., 2006, 89(8), 2418-2425.

20. Hidber, P. C., Graule, T. J., Gauckler, L. J., *Influence of the dispersant structure on properties of electrostatically stabilized aqueous alumina suspensions.* J. Eur. Ceram. Soc., 1997, 17, 239-249.

21. Pieranski, P., *Two-dimensional interfacial colloidal crystals.* Phys. Rev. Lett., 1980, 45(7), 569-572.

22. Binks, B. P., *Particles as surfactants-Similarities and differences.* Curr. Opin. Colloid Interface Sci., 2002, 7(1-2), 21-41.

23. Studart, A. R., Shum, H. C., Weitz, D. A., *Arrested coalescence of particle-coated droplets into nonspherical supracolloidal structures*. J. Phys. Chem. B, 2008, 113 (12), 3914-3919.

5 Hierarchical Porous Ceramics from Particle-Stabilized Emulsions and Foams*

Abstract

We present a simple approach to produce macroporous alumina with tailored microstructure and porosity using particle-stabilized emulsions and foams. The approach is based on the stabilization of oil-water and air-water interface through the adsorption of in situ hydrophobized colloidal alumina particles. Variation of the volume fraction of oil in the original emulsions allows for the introduction of air bubbles into the particle-stabilized emulsion system. Sintering of the particle-oil-water-air systems gives rise to porous structures exhibiting pore sizes ranging from single to multimodal pore populations at length scales differing by one order of magnitude. Tailoring the pore structure in different length scales enables the fabrication of porous ceramics with porosities up to 96% and compressive strengths up to 13 MPa.

---

* *I. Akartuna, A. R. Studart, E. Tervoort, and L. J. Gauckler, to be submitted.*

5.1 Introduction

Macroporous ceramics are becoming increasingly important in many applications and technological processes. Precise control over the composition and microstructure of the porous ceramics would allow tailoring the properties of porous ceramics for specific applications.

Hierarchical porous ceramics have attracted particular interest in a wide range of applications including filtration, catalysis, separation, fuel cell electrodes, insulators, and scaffolds for bone replacement and tissue engineering [1, 2]. Porous ceramics with a hierarchical pore size distribution can offer improved mass transport and functionality compared with homogenously structured ceramics.

Cellular structures available in nature have also become inspiring for the fabrication of many hierarchical macrocellular ceramics due to their hierarchically built architecture. Hierarchical inorganic materials with pores in the micro-meso [3-6], meso-macro [7-12], micro-macro [13-15] and micro-meso-macro [16-20] range have been prepared by combining various template-assisted assembly methods at multiple length scales. In addition to these hierarchical inorganic structures obtained in multiple length scales, many efforts have been made to produce macroporous ceramics with controlled hierarchical pore size distribution within a single length scale. For instance, certain wood types have been used as biotemplates for the preparation of hierarchical macroporous ceramics, particularly for the potential applications as high-temperature-resistant gas filters, catalyst carriers, heat exchangers, and thermal insulation devices, due to their open-cell and hierarchical pore morphology, which might be difficult to produce by conventional processing methods [21]. Macroporous ceramics of SiC [22-25], SiSiC [26], and Al_2O_3 [27, 28] have been produced by infiltration of pyrolyzed wood preforms with gaseous or liquid metals, and subsequent sintering at high temperatures. Alternatively, sintering of liquid sol infiltrated charcoal or dried wood structures resulted in hierarchical macroporous structures of SiC [29], SiO_2 [30], Al_2O_3 [31], TiO_2 [32], Fe_2O_3 [33], MnO_2 [34], YSZ [35]. These wood-derived cellular structures exhibited pore sizes between 5-300 μm with porosities ranging from 63 to 94%.

In addition to biomorphic cellular ceramics templated from wood, the polymer replica approach was used for mimicking the graded hierarchical pore structure of bone. Hierarchical macroporous hydroxyapatite/tri-calcium phosphate (HA/TCP) bioceramics with 0.5-3 mm open pores were produced by impregnation of an assembly

of porous polymer foams of different pore sizes with a ceramic slurry [36]. Similarly, multiple partial impregnation of cellulose sponges with HA slurries resulted in hierarchical ceramics with pore sizes between 0.5-2 mm [37]. To obtain graded hierarchical structures, polymer foams were also compression molded into different shapes that have position-dependent porosity [38]. Infiltration of the graded foams with ceramic slurry, followed by pyrolysis of the polymer and sintering of the ceramic, produced ceramic components with pore sizes and porosities ranging from 100-400 µm and 50 to 3%, respectively.

Recently, macroporous structures exhibiting a hierarchical pore size distribution have also been produced by the use of water or volatile oils as sacrificial phase in emulsions. Macroporous materials of TiO_2 were produced by incorporation of a third phase such as water into the surfactant stabilized non-aqueous emulsions with 50 vol% oil; following consolidation of the continuous phase through sol-gel process [39]. Subsequent heat treatment of such emulsions resulted in macroporous materials of 96% porosity, having small pores ranging from 1-5 µm in between the larger pores (>40 µm). Similarly, consolidation of surfactant stabilized 70% aqueous emulsions with sol-gel transitions at acidic conditions led to fabrication of macroporous SiO_2 with hierarchical pore structures [40]. The monoliths had pore sizes ranging from 1 to 100 µm with a porosity of 92%.

In spite of a variety of hierarchical porous structures, the aforementioned templating methods still have some drawbacks. In the case of polymer and wood replica methods, the order and degree of the hierarchical pore structure and porosity is mainly template dependant. During the infiltration steps of the wood templation, some of the hierarchical pore structure of the original wood template might not be retained as a result of the closing of the pores. Furthermore, several time-consuming steps involved during the process might bring additional production costs. For emulsion templating method, preparation of hierarchical pore structures has been so far limited to surfactant-stabilized emulsions consolidated by sol-gel processes that involve multiple chemical reactions and may be restrictive with respect to the materials used. Hence, a simple and versatile approach to fabricate large-scale hierarchical macroporous ceramics with controlled porosity and pore size distribution is still required.

Recently, we described a new approach to fabricate porous inorganic materials of silica [41], iron oxide [41] and alumina [41, 42]. Fabrication of macroporous ceramics was

accomplished through the sintering of emulsions and foams stabilized by high concentration of colloidal inorganic particles. The attachment of particles to the oil-water and air-water interface was induced by tuning the wettability of particles upon adsorption of short amphiphilic molecules with various chemistries. In this work, we describe a simple and straightforward method for the fabrication of macroporous alumina with tailored microstructure and porosity using particle-stabilized emulsions, foams, and mixtures thereof. Stabilization of oil-water and air-water interface is achieved by interfacial adsorption of colloidal alumina particles in situ surface modified with a short carboxylic acid molecule. Macroporous alumina with microstructures ranging from homogeneous to hierarchical pore structure was obtained by simply varying the amount of dispersed phase in the wet emulsions. Combination of air bubbles and oil droplets in a single step process enabled production of porous alumina with controlled porosity and mechanical strength upon sintering. To illustrate the main features of this method, macroporous alumina was characterized with respect to porosity, pore size, and mechanical strength.

5.2 Materials and methods

5.2.1 Materials

Experiments were performed using α-Al_2O_3 powder (Ceralox HPA-0.5, 99.99% Al_2O_3, Sasol North America Inc., Tucson, AZ, USA) with average particle diameter, d_{50}, of 200 nm, specific surface area of 10 m^2/g and density of 3.98 g/cm^3. Octane (97 % pure, Boiling temperature T_b = 125 °C, Acros Organics, Belgium) was used as received. The short amphiphilic molecule used for particle modification was propionic acid (> 99, Sigma-Aldrich Chemie GmbH, Germany). Double deionized water with an electrical resistance of 18 MΩcm was used in the experiments (Nanopure water system, Barnstead, USA). 2 M hydrochloric acid (HCl) and 1 M sodium hydroxide (NaOH) solutions (Titrisol, Fluka AG, Buchs, Switzerland) were used to adjust the pH.

5.2.2 Fabrication of porous ceramics

Colloidal suspensions with 58 vol% alumina were prepared by adding alumina powder into deionized water. During powder addition, the pH was maintained at values below 5 by adding small aliquots of 2 N HCl solution. In order to de-agglomerate

and homogeneously disperse the colloidal particles in the aqueous phase, suspensions were ball-milled in polyethylene bottles for 22 h using alumina milling balls (10 mm diameter). A ball/powder weight ratio of 2.5 was used. After the ball-milling procedure, the pH of the alumina suspensions was ~5.5. The ball-milled suspension was transferred to a glass beaker prior to addition of surface modifier. 180 mmol/L propionic acid was dissolved in water and the resulting aqueous solution was added dropwise to the suspension under magnetic stirring. The pH of the alumina suspensions was subsequently adjusted to 4.75 by adding 1 N NaOH and/or 2 N HCl dropwise. Finally, additional water was added to adjust the solids content of the suspensions to 35 vol%.

Emulsification was performed by vigorously stirring the suspension and octane for 3 min in ambient conditions, unless mentioned otherwise, using a household mixer at full power (Kenwood, Schumpf AG, Baar, Switzerland). It is important to note that the amount of the oil phase indicated throughout this study refers to the oil content with respect to the total emulsion volume (water + particles + oil). In the case of particle-stabilized foams, foaming was done by mechanically shearing the suspensions with 35 vol% alumina and 180 mmol/L propionic acid for 3 min.

The as-prepared wet emulsions and foams were hand-shaped into cylindrical parts (diameter of 100 mm, height of 30 mm) and dried in air for 48 h at 25 °C. After drying, the samples underwent a stepwise heat treatment to extract the remaining oil and water within the emulsion. Dried samples were heated for 5 h at 90 °C (with a heating rate of 0.3 °C/min), then for 5 h at 150 °C (with a heating rate of 0.3 °C/min), and finally for 5 h at 300 °C (with a heating rate of 0.5 °C/min). Sintering of the dried emulsions was performed in an electrical furnace (HT 40/16, Nabertherm, Germany) for 2 h at 1600 °C (with a heating rate of 1 °C/min).

5.2.3 Characterization

The cell size distribution of the resulting emulsions and foams was evaluated using an optical microscope in transmission mode (Polyvar MET, Reichert-Jung, Austria) connected to a digital camera (DC 300, Leica, Switzerland). Air bubbles incorporated into the particle-oil-water mixtures during mixing were indentified for the composition containing 35 vol% alumina particles, 180 mmol/L propionic acid, and 30 vol% octane via a scanning confocal microscope (Leica, SP1, Germany) using a 20x, 0.4NA PLAN FLUOTAR objective at an excitation wave length of 488 nm. To distinguish air bubbles

from oil droplets, the oil phase was dyed with Nile red (Invitrogen, Switzerland) prior to emulsification.

The cell size of the wet emulsions and sintered structures was measured with the linear intercept method using the software Lince (TU Darmstadt, Germany). Log-normal distributions were used to describe the experimental data and to obtain average cell sizes, and 68% confidence intervals. The porosity of the sintered samples was determined by geometrical and Archimedes methods. The geometrical method is based on the determination of the porosity from the relative density of a ceramic sample, which is the ratio between the calculated geometrical density of the sample and the theoretical density of the material. The Archimedes method was performed according to the ASTM norm C20 [43]. Compressive strength measurements were performed with a universal testing machine (Instron 8562, model A1477-1003, Norwood, USA). Sintered emulsions were ground on both sides to provide homogeneous sample loading during compression. Cylindrical samples with diameters of 10 mm and 15 mm, and lengths of 25 mm were prepared by drilling the sintered emulsions with a diamond core drill. Cylindrical samples were then crushed under a compression speed of 0.5 mm/min. The porous ceramics obtained after sintering were investigated by scanning electron microscope (SEM, LEO 1530). Samples were prepared by Pt sputtering for 55 s at 60 mA.

5.3 Results and discussion

5.3.1 Microstructure of wet particle-stabilized systems

The basic requirement for the fabrication of porous ceramics from emulsions and foams is the stabilization of oil-water and air-water interface by high concentration of colloidal alumina particles that were in situ surface hydrophobized through the adsorption of propionic acid in the continuous water phase.

Incorporation of a second phase, oil and/or air during mechanical shearing of suspension of hydrophobized alumina particles yielded dispersions ranging from particle stabilized emulsions to foams (Figure 5.1). All compositions were prepared with suspensions containing 35 vol% alumina particles (at a fixed particle to water volume ratio of 0.54) and 180 mmol/L propionic acid at pH 4.75. The maximum volume fraction of oil that could be incorporated in the final dispersions was 72 vol%. Oil contents beyond this value led to formation of emulsions with a phase-separated layer of oil on

the top (Figure 5.1). Dispersions having 72 vol% oil in the final emulsion resulted in highly stable oil-in-water emulsions stabilized by alumina particles [44] (Figure 5.2.a). Since partially hydrophobized particles could also adsorb at the air-water interface and stabilize air bubbles incorporated into the system during shearing, dispersions containing both air bubbles and oil droplets in various proportions were obtained when the oil volume fraction in the emulsion was varied between 0 and 72 vol%, as illustrated in Figure 5.2. To identify the air bubbles incorporated to the particle-stabilized emulsions upon mixing, a fluorescent dye was added to the oil phase in a system containing 30 vol% octane prior to mixing. As demonstrated in the fluorescence confocal image in Figure 5.3, the oil droplets which contained the fluorescent dye appear green, while the air bubbles due to the absence of the dye are detected as red cells. In the absence of oil, mechanical shearing of 35 vol% alumina suspensions led to formation of particle-stabilized foams (Figure 5.2.e), which was in agreement with the previously reported study [42].

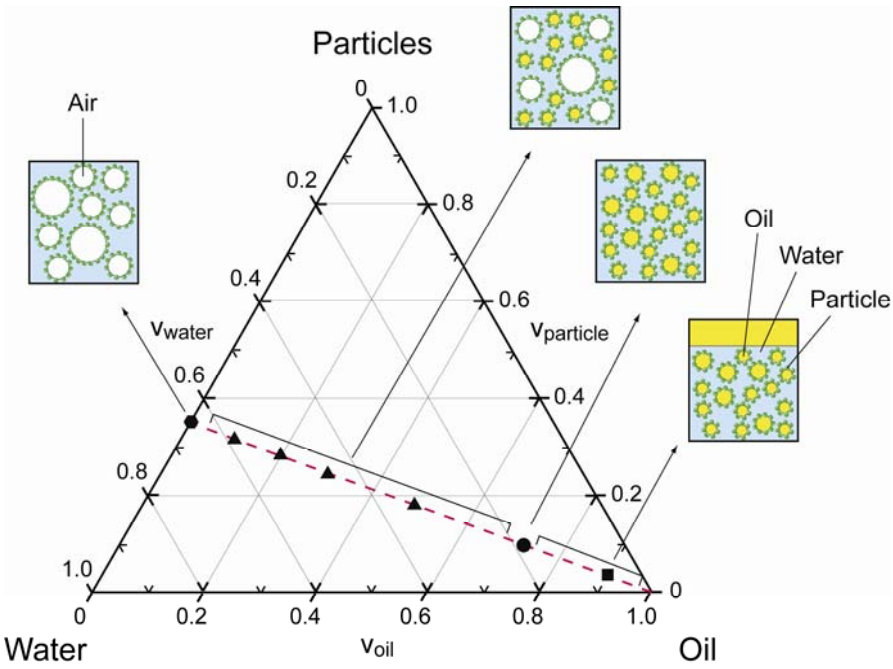

Figure 5.1: Compositional diagram indicating the particle-oil-water formulations evaluated in this study and the resulting microstructures of the mixtures obtained. The volume fractions of water, oil, and particles are indicated by v_{water}, v_{oil} and $v_{particles}$, respectively. The dashed line indicates the compositions prepared at a constant particle concentration of 35 vol% in the suspension, which corresponds to a particle to water volume ratio of 0.54.

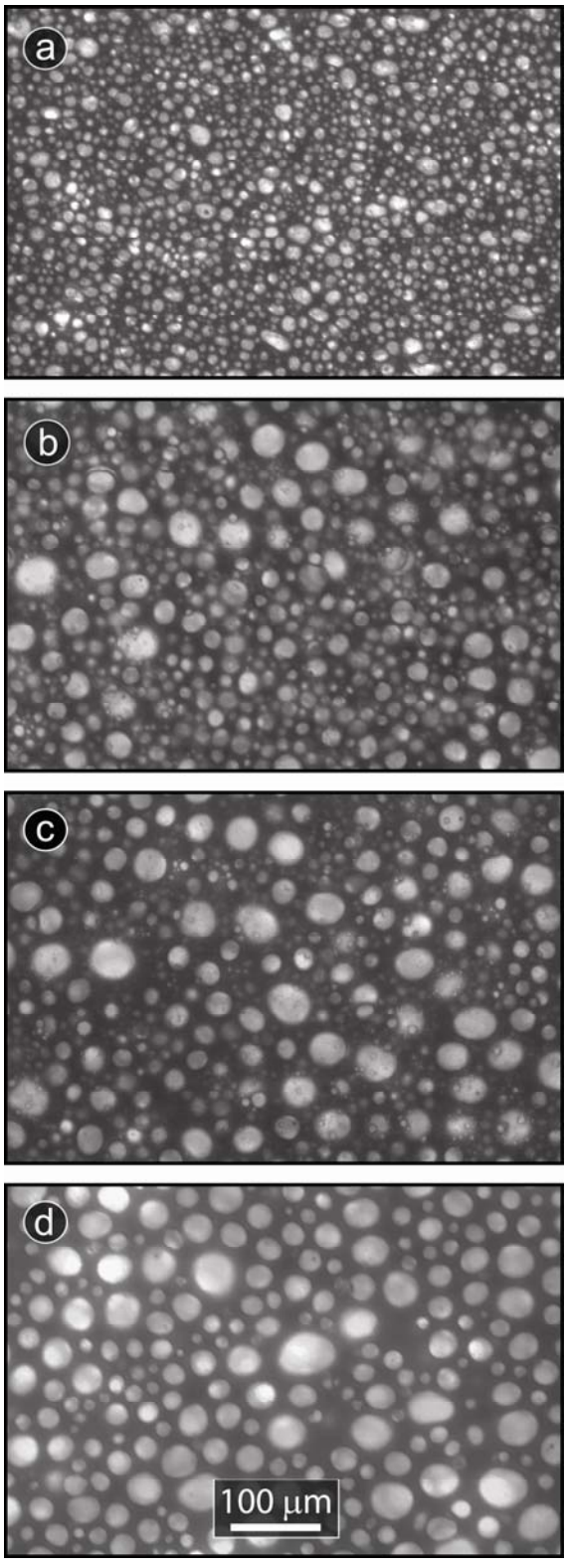

Figure 5.2: Optical microscope images of wet particle-oil-water mixtures prepared with different oil concentrations. Compositions were prepared with mixing aqueous suspensions containing 35 vol% particles (particle to water volume ratio of 0.54) and 180 mmol/L propionic acid at pH 4.75 with a) 72 vol% octane; b) 50 vol% octane; c) 30 vol% octane; and d) in the absence of oil, foam.

The effect of oil content on the average cell size of particle-oil-water mixtures was determined from the evaluation of wet microstructures shown in Figure 5.2. In the case of oil volume fractions of 72 vol%, the oil-in-water emulsions stabilized by in-situ hydrophobized alumina particles exhibited an average droplet size of 11.7 μm [41, 44]. Decreasing the volume fraction of oil in the particle-oil-water mixture led to cell sizes between 11-40 μm for 50 vol% octane, and 12-70 μm for 30 vol% octane (Figure 5.2). In the absence of oil, the particle-stabilized wet foams exhibited an average bubble size of 35 μm.

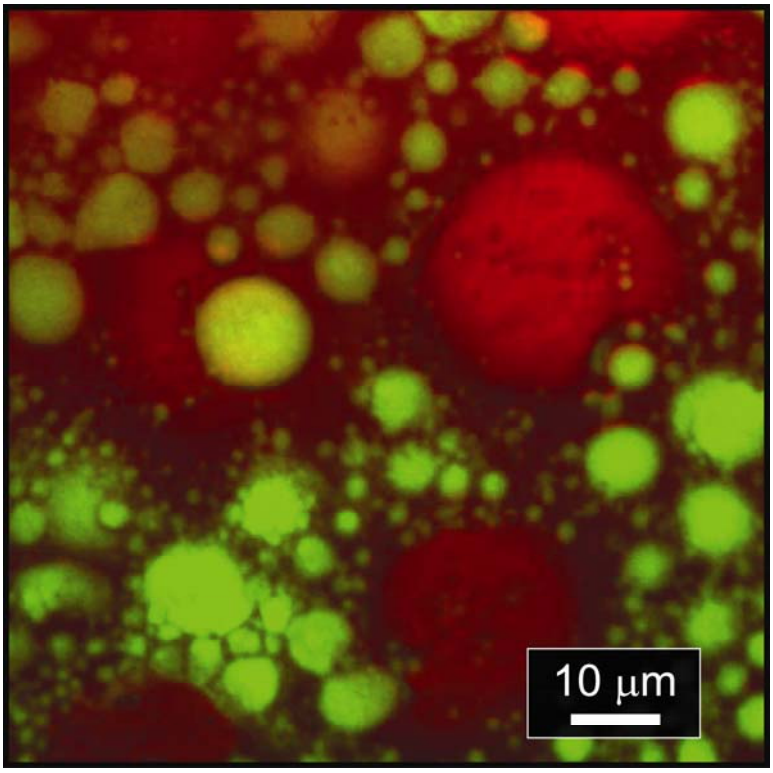

Figure 5.3: Confocal scanning microscope image of a wet particle-oil-water-air mixture prepared by mixing 30 vol% octane with 35 vol% alumina suspensions (particle to water volume ratio of 0.54) containing 180 mmol/L propionic acid at pH 4.75. The image clearly shows alumina-stabilized oil droplets (green cells) and air bubbles (red cells) incorporated to the system at low oil contents upon mixing.

The presence of the bigger cell sizes observed at low oil contents is mainly due to the introduction of air bubbles into the particle-oil-water system. At low oil contents where oil droplets are loosely packed, partially hydrophobized particles also adsorb at the air-water interface during shearing, thereby stabilizing air bubbles introduced into the emulsion. The resulting system is therefore comprised of a mixture of particle

stabilized emulsion droplets and foam bubbles. Due to the relatively higher surface tension of the air-water interface with respect to the oil-water interface, air bubbles exhibit much bigger cell sizes than oil droplets. As the amount oil decreases and more air bubbles are introduced into the mixture, the system resembles more to the pure foam microstructure, exhibiting higher fraction of bigger cells and lower fractions of smaller cells.

5.3.2 Microstructure of porous ceramics

Sintering of the alumina-stabilized emulsions, foams, and mixtures thereof containing different amount of oil resulted in porous ceramics with various microstructures (Figure 5.4). Porous ceramics obtained from particle-stabilized emulsions with 72 vol% oil yielded interconnected pores with an average pore size of 11.5 μm, which was equivalent to the average droplet size of the wet emulsions. Decreasing the amount of oil to 50 vol% within the particle-stabilized emulsions led to average pore sizes in the range of 13-500 μm. At oil content of 30 vol%, sintering of particle-stabilized oil-water-air mixtures yielded pore sizes between 16-1219.7 μm. In the absence of oil, the macroporous ceramics obtained from sintered particle-stabilized wet foams led to pores within the range of 40-4000 μm.

Comparison of the average cell sizes of the particle-stabilized oil-water-air mixtures and foams before and after sintering shows that the cell sizes of the samples increase upon drying and sintering. This increase in the average cell size of the sintered porous ceramics is mainly due to the instability of wet air bubbles during drying and sintering. As previously shown [42], wet foams stabilized by colloidal alumina particles in situ modified with 180 mmol/L propionic acid are not stable against bubble growth and drainage. Wet foams exhibit bubble growth already within one hour after mixing. Compared to these wet foams, wet emulsions stabilized by alumina particles in situ modified with 180 mmol/L propionic acid display long-term stability against coalescence, Ostwald ripening, and creaming [44]. No significant change is observed in the emulsion droplet size distribution within a time period of more than two years after emulsification. Hence, porous ceramics produced from sintered particle-stabilized emulsions (72 vol% oil) exhibit pores with sizes close to the droplet sizes of the initial emulsions, while sintered particle-stabilized foams yield porous structures with much bigger pore sizes than the bubble size of the initial wet foams. In the case of particle-

oil-water-air mixtures (e.g., 30 vol% oil), drying and sintering result in assembly of small pores (~11 μm) close to the droplet size of the initial emulsions, and bigger pores (> 30 μm) that were retained after the growth of the foam bubbles.

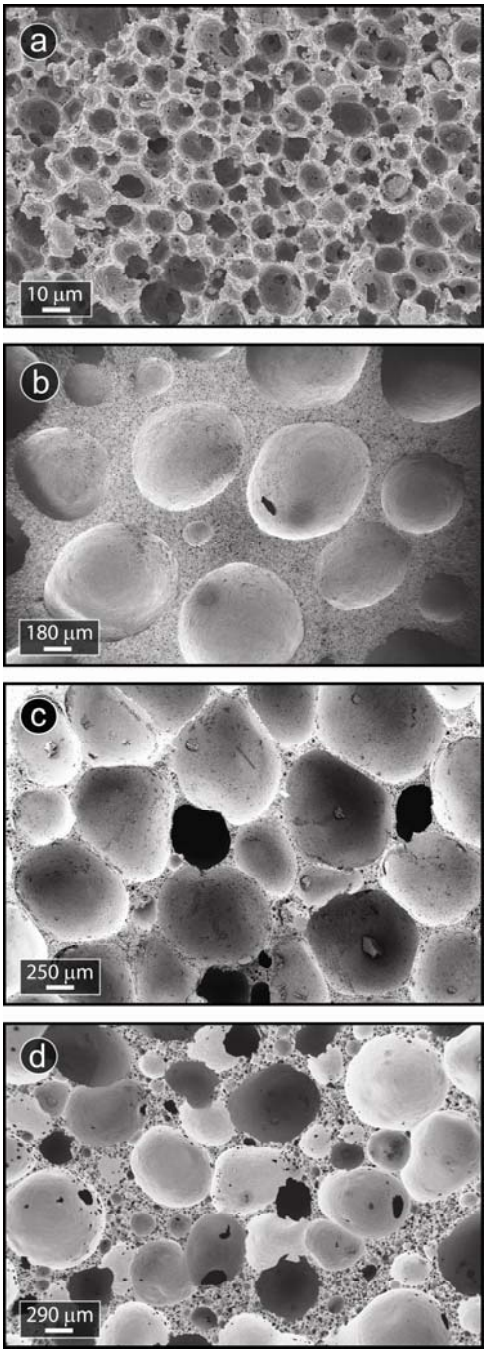

Figure 5.4: Microstructures of sintered particle-oil-water mixtures prepared with different oil concentrations. Compositions were prepared with mixing aqueous suspensions containing 35 vol% particles (particle to water volume ratio of 0.54) and 180 mmol/L propionic acid at pH 4.75 with a) 72 vol% octane; b) 50 vol% octane; c) 30 vol% octane; and d) in the absence of oil, foam.

The change of the average pore sizes from single to multiple size pores in sintered ceramics with decreasing oil content is attributed to the formation of big pores that originate from the particle-stabilized air bubbles in the matrix of smaller pores which are left after the extraction of the oil droplets. As the amount of air within the particle-stabilized oil-water-air mixtures increases, the size of the pores in the sintered samples increases. Interestingly, increasing the amount of oil within the particle stabilized mixtures leads to more homogeneous pore distributions and a decrease in the average sizes of the pores retained from the air bubbles. This decrease in the size of the big pores retained from air bubbles might be related to the enhanced stability of air bubbles due the presence of oil droplets. Similar to the surfactant-stabilized foamed emulsions [45, 46], in which both oil droplets and air bubbles are stabilized with surfactants, the stability of the foams can be increased as the emulsion droplets accumulating within the plateau borders of the draining foam increase the viscosity of the draining liquid, thereby increasing the resistance to the flow of liquid, and inhibiting the foam drainage.

Figure 5.5 shows the microstructures of macroporous alumina obtained after drying and sintering of particle-oil-water-air mixtures containing 30 vol% oil. The incorporation of a third phase such as air into the wet emulsions allows fabrication of macroporous ceramics with hierarchical pore structure with pores at size scales differing by one order of magnitude. The hierarchy in the pore structure is defined by the assembly of 3-10 µm small pores in between 500-1200 µm big pores. The big pores originate as a result of the coalescence of air bubbles during drying, while smaller pores are retained from the oil droplets. Stabilization of air bubbles and oil droplets by a dense layer of modified particles promotes the formation of closed cell porous ceramics. Unlike porous ceramics produced with 72 vol% oil, the hierarchical porous ceramics exhibit porous struts comprising of 3-10 µm pores. As the continuous water phase starts to evaporate during drying, the oil droplets most probably reside among the coarser air bubbles, leaving behind porous struts in the final porous structure upon sintering. As a result of such a rearrangement, the assembly of oil droplets and air bubbles enable the production of pore structure in multiple size scales.

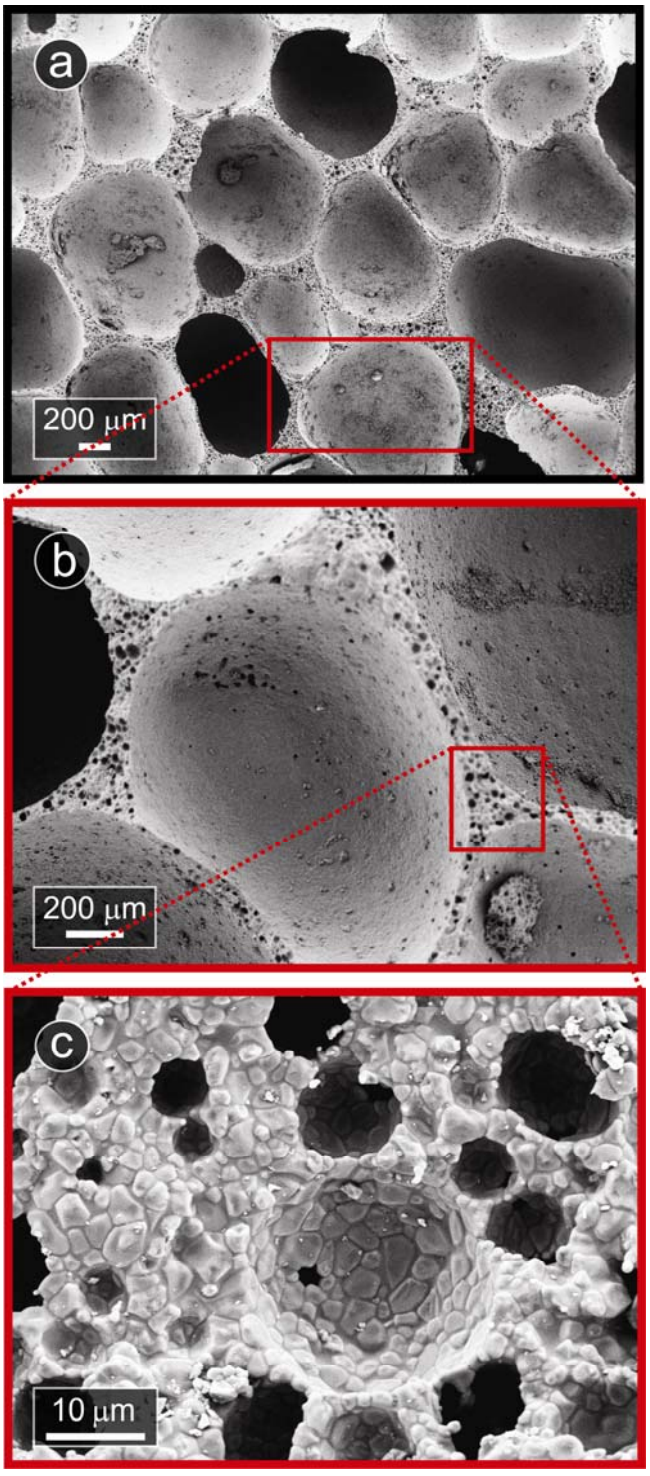

Figure 5.5: Scanning electron microscope images of sintered particle-oil-water mixtures prepared by mixing aqueous suspensions of 35 vol% alumina particles and 180 mmol/L propionic acid pH 4.75 with 30 vol% octane. Hierarchical features of the sintered particle-stabilized mixtures obtained as a result of a decrease in the amount of oil involve (a) bulk macroporous ceramics, (b) with pore sizes within the range of 500-800 µm, and (c) porous struts exhibiting pore sizes of 3-10 µm.

Macroporous ceramics fabricated from alumina-stabilized emulsions and emulsion-foam mixtures are shown in Figure 5.6. The incorporation of air as the third phase into the particle-stabilized emulsions allowed for tailoring the porosity of the final porous ceramics. The sintering of alumina-stabilized oil-water-air mixtures yielded macroporous ceramics with porosities up to 95%. In the case of porous ceramics obtained from particle-stabilized emulsions, the total porosity of 72% was equivalent to the amount of the oil added into the initial emulsions. Porous ceramics produced from alumina-stabilized oil-water-air mixtures exhibited 85% and 90% porosity for mixtures prepared with 50 vol% and 30 vol% octane, respectively. These porosity levels imply that higher porosities can be achieved even at low oil contents upon incorporation of air bubbles into the wet emulsions. In the absence of oil, sintering of particle stabilized foams led to porosities as high as 96%.

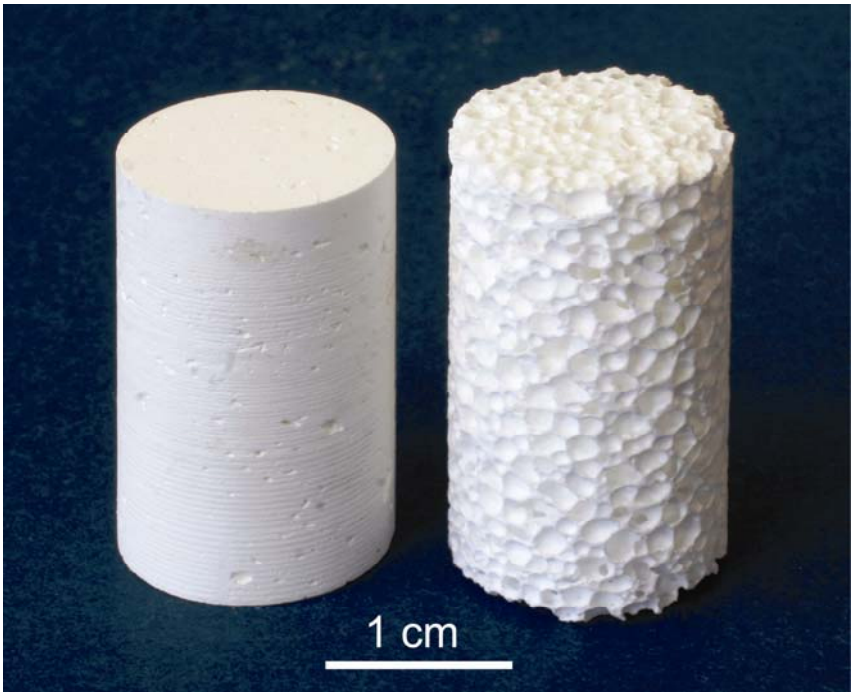

Figure 5.6: Macroporous ceramics obtained after sintering of particle-oil-water mixtures. The samples are prepared with 35 vol% alumina particles, 180 mmol/L propionic acid, and a) 72 vol% octane; b) 50 vol% octane.

Macroporous alumina fabricated from particle-stabilized emulsions exhibited compression strength of 13 MPa at 72% porosity. Such remarkably high mechanical strengths are achieved as a result of the dense cell walls and struts obtained from sintered particle-stabilized emulsions. In contrast to porous ceramics obtained from

particle-stabilized emulsions, macroporous ceramics produced from particle-oil-water-air mixtures exhibit compressive strengths of 1.5 and 1 MPa at 85% and 90% porosity, respectively. In the case of porous ceramics produced from particle stabilized foams, the compression strength data could not be obtained at the same conditions as the porous samples with 50 vol% and 30 vol% oil due to the structural weakness of these samples. The decrease in the mechanical strength of the porous ceramics with an increase in porosity is mainly attributed to the formation of porous struts and big pores with windows following drying and sintering of particle-oil-water mixtures.

5.4 Conclusions

Macroporous alumina with a variety of microstructures was produced by using particle-stabilized emulsions and foams. Stabilization of the oil-water and air-water interface by colloidal inorganic particles in situ surface modified thorough the adsorption of a short amphiphilic molecule allowed for tailoring the microstructure and porosity of the porous components in a single step process. Changing the oil content in the initial emulsions led to formation of porous ceramics ranging from homogeneous to hierarchical pore structures. Such a variation in the pore structure was attained upon incorporation of air bubbles into the matrix of oil droplets during mechanical shearing of the particle-oil-water mixtures in ambient conditions. Sintering of crack-free dried mixtures gave rise to macroporous structures with pore distributions at length scales differing by one order of magnitude. Different populations of pores were achieved due to the differences in the interfacial tensions of the oil-water and air-water interface, and in the stability of oil droplets and air bubbles. Tuning the microstructure of the porous ceramics allowed for achieving porosities within the range of 72%–96% and mechanical strength levels between 1-13 MPa. Macroporous ceramics prepared by this approach may be used in several applications, as low-weight structural components, porous media for chemical and biological separation, thermal and electrical insulating materials, catalyst supports, refractory filters for molten metals, and scaffolds for tissue engineering and medical implants.

5.5 Acknowledgment

The authors would like to thank Ciba Specialty Chemicals (Switzerland) for funding this project and Dr. Gabor Csucs (ETH Zurich) for performing the confocal microscopy experiments.

5.6 References

1. Ishizaki, K., Komarneni, S., Nanko, M., *Porous Materials: Process Technology and Applications*. 1998, Dordrecht, Kluwer Academic Publishers.

2. Scheffler, M., Colombo, P., *Cellular Ceramics: Structure, Manufacturing, Properties and Applications*. 2005, Weinheim, Wiley - VCH.

3. Wang, H., Wang, Z., Huang, L., Mitra, A., Holmberg, B., Yan, Y., *High-surface-area zeolitic silica with mesoporosity*. J. Mater. Chem., 2001, 11(9), 2307-2310.

4. Soler-Illia, G. J. d. A., Sanchez, C., Lebeau, B., Patarin, J., *Chemical strategies to design textured materials: From microporous and mesoporous oxides to nanonetworks and hierarchical structures*. Chem. Rev., 2002, 102(11), 4093-4138.

5. Liu, Y., Pinnavaia, T. J., *Assembly of hydrothermally stable aluminosilicate foams and large-pore hexagonal mesostructures from zeolite seeds under strongly acidic conditions*. Chem. Mater., 2002, 14(1), 3-5.

6. Carr, C. S., Kaskel, S., Shantz, D. F., *Self-assembly of colloidal zeolite precursors into extended hierarchically ordered solids*. Chem. Mater., 2004, 16, 3139-3146.

7. Yang, P., Deng, T., Zhao, D., Feng, P., Pine, D., Chmelka, B. F., Whitesides, G. M., Stucky, G. D., *Hierarchically ordered oxides*. Science, 1998, 282(5397), 2244-2246.

8. Holland, B. T., Blanford, C. F., Do, T., Stein, A., *Synthesis of highly ordered, three-dimensional, macroporous structures of amorphous or crystalline inorganic oxides, phosphates, and hybrid composites*. Chem. Mater., 1999, 11, 795-805.

9. Lebeau, B., Fowler, C. E., Mann, S., Farcet, C., Charleux, B., Sanchez, C., *Synthesis of hierarchically ordered dye-functionalised mesoporous silica with macroporous architecture by dual templating*. J. Mater. Chem., 2000, 10(9), 2105-2108.

10. Yuan, Z. Y.,Su, B. L., *Insights into hierarchically meso-macroporous structured materials*. J. Mater. Chem., 2006, 16(7), 663-677.

11. Costacurta, S., Biasetto, L., Pippel, E., Woltersdorf, J., Colombo, P., *Hierarchical porosity components by infiltration of a ceramic foam*. J. Am. Ceram. Soc., 2007, 90(7), 2172-2177.

12. Yun, H.-s., Kim, S.-e., Hyeon, Y.-t., *Design and preparation of bioactive glasses with hierarchical pore networks*. Chem. Commun., 2007, 2139-2141.

13. Holland, B. T., Abrams, L., Stein, A., *Dual templating of macroporous silicates with zeolitic microporous frameworks*. J. Am. Chem. Soc., 1999, 121, 4308-4309.

14. Anderson, M. W., Holmes, S. M., Hanif, N., Cundy, C. S., *Hierarchical pore structures through diatom zeolitization*. Angew. Chem. Int. Ed. , 2000, 39(15), 2707-2710.

15. Lee, Y.-J., Lee, J. S., Park, Y. S., Yoon, K. B., *Synthesis of large monolithic zeolite foams with variable macropore architectures*. Adv. Mater., 2001, 13(16), 1259-1263.

16. Rhodes, K. H., Davis, S. A., Caruso, F., Zhang, B., Mann, S., *Hierarchical assembly of zeolite nanoparticles into ordered macroporous monoliths using core-shell building blocks.* Chem. Mater., 2000, 12(10), 2832-2834.

17. Sen, T., Tiddy, G. J. T., Casci, J. L., Anderson, M. T., *One-pot synthesis of hierarchically ordered porous-silica materials with three orders of length scale.* Angew. Chem. Int. Ed., 2003, 42, 4649-4653.

18. Valtchev, V. P., Smaihi, M., Faust, A. C., Vidal, L., *Equisetum arvense templating of zeolite beta macrostructures with hierarchical porosity.* Chem. Mater., 2004, 16(7), 1350-1355.

19. Carn, F., Achard, M. F., Babot, O., Deleuze, H., Reculusa, S., Backov, R., *Syntheses and characterization of highly mesoporous crystalline TiO_2 macrocellular foams.* J. Mater. Chem., 2005, 15(35-36), 3887-3895.

20. Vantomme, A., Léonard, A., Yuan, Z.-Y., Su, B.-L., *Self-formation of hierarchical micro-meso-macroporous structures: Generation of the new concept "hierarchical catalysis".* Colloids Surf. A, 2007, 300, 70-78.

21. Sieber, H., Hoffman, C., Kaindl, A., Greil, P., *Biomorphic cellular ceramics.* Adv. Eng. Mater., 2000, 2(3), 105-109.

22. Vogli, E., Mukerji, J., Hoffman, C., Kladny, R., Sieber, H., Greil, P., *Conversion of oak to cellular silicon carbide ceramic by gas-phase reaction with silicon monoxide.* J. Am. Ceram. Soc., 2001, 84(6), 1236-1240.

23. Esposito, L., Sciti, D., Piancastelli, A., Bellosi, A., *Microstructure and properties of porous β-SiC templated from soft woods.* J. Eur. Ceram. Soc., 2004, 24, 533-540.

24. Herzog, A., Klingner, R., Vogt, U., Graule, T., *Wood-derived porous SiC ceramics by sol infiltration and carbothermal reduction.* J. Am. Ceram. Soc., 2004, 87(5), 784–793.

25. Qian, J., Wang, J., Jin, Z., *Preparation of biomorphic SiC ceramic by carbothermal reduction of oak wood charcoal.* Mater. Sci. Eng., A, 2004, 371(1-2), 229-235.

26. Zollfrank, C., Travitzky, N., Sieber, H., Selchert, T., Greil, P., *Biomorphous SiSiC/Al-Si ceramic composites manufactured by squeeze casting: Microstructure and mechanical properties.* Adv. Eng. Mater., 2005, 7(8), 743-746.

27. Rambo, C. R., Sieber, H., *Novel synthetic route to biomorphic Al_2O_3 ceramics.* Adv. Mater., 2005, 17(8), 1088-1091.

28. Rambo, C. R., Andrade, T., Fey, T., Sieber, H., Martinelli, A. E., Greil, P., *Microcellular Al_2O_3 ceramics from wood for filter applications.* J. Am. Ceram. Soc., 2008, 91(3), 852-859.

29. Ota, T., Takahashi, M., Hibi, T., Ozawa, M., Suzuki, S., Hikichi, Y., Suzuki, H., *Biomimetic process for producing SiC "wood".* J. Am. Ceram. Soc., 1995, 78(12), 3409-3411.

30. Shin, Y., Liu, J., Chang, J. H., Nie, Z., Exarhos, G. J., *Hierarchically ordered ceramics through surfactant-templated sol-gel mineralization of biological cellular structures.* Adv. Mater., 2001, 13(10), 728-732.

31. Cao, J., Rambo, C. R., Sieber, H., *Preparation of porous Al_2O_3-ceramics by biotemplating of wood.* J. Porous Mater., 2004, 11(163-172).

32. Cao, J., Rusina, O., Sieber, H., *Processing of porous TiO_2-ceramics from biological preforms.* Ceram. Int., 2004, 30, 1971-1974.

33. Liu, Z., Fan, T., Zhang, W., Zhang, D., *The synthesis of hierarchical porous iron oxide with wood templates.* Microporous Mesoporous Mater., 2005, 85, 82–88.

34. Li, X., Fan, T., Liu, Z., Ding, J., Guo, Q., Zhang, D., *Synthesis and hierarchical pore structure of biomorphic manganese oxide derived from woods*. J. Eur. Ceram. Soc., 2006, 26, 3657-3664.

35. Rambo, C. R., Cao, J., Sieber, H., *Preparation and properties of highly porous, biomorphic YSZ ceramics*. Mater. Chem. Phys., 2004, 87, 345–352.

36. Hsu, Y. H., Turner, I. G., Miles, A. W., *Fabrication of porous bioceramics with porosity gradients similar to the biomodal structure of cortical and cancellous bone*. J. Mater. Sci.: Mater. Med., 2007, 18, 2251-2256.

37. Tampieri, A., Celotti, G., Sprio, S., Delcogliano, A., Franzese, S., *Porosity-graded hydroxyapatite ceramics to replace natural bone*. Biomaterials, 2001, 22, 1365-1370.

38. Cichocki Jr, F. R., Trumble, K. P., Rödel, J., *Tailored porosity gradients via colloidal infiltration of compression-molded sponges*. J. Am. Ceram. Soc., 1998, 6(1661-1664).

39. Imhof, A.,Pine, D. J., *Preparation of titania foams*. Adv. Mater., 1999, 11(4), 311-314.

40. Carn, F., Colin, A., Achard, M.-F., Deleuze, H., Sellier, E., Birot, M., Backov, R., *Inorganic monoliths hierarchically textured via concentrated direct emulsion and micellar templates*. J. Mater. Chem., 2004, 14(9), 1370-1376.

41. Akartuna, I., Studart, A. R., Tervoort, E., Gauckler, L. J., *Macroporous ceramics from particle-stabilized emulsions*. Adv. Mater., 2008, 20(24), 4714-4718.

42. Gonzenbach, U. T., Studart, A. R., Tervoort, E., Gauckler, L. J., *Macroporous ceramics from particle-stabilized wet foams*. J. Am. Ceram. Soc., 2007, 90(1), 16-22.

43. ASTM, *Standard test methods for apparent porosity, water absorption, apparent specific gravity, and bulk density of burned refractory brick and shapes by boiling water*, ASTM International: West Conshohocken, United States.

44. Akartuna, I., Studart, A. R., Tervoort, E., Gonzenbach, U. T., Gauckler, L. J., *Stabilization of oil-in-water emulsions by colloidal particles modified with short amphiphiles*. Langmuir, 2008, 24(14), 7161-7168.

45. Koczo, K., Lobo, L. A., Wasan, D. T., *Effect of oil on foam stability: Aqueous foams stabilized by emulsions*. J. Colloid and Interface Science, 1992, 150(2), 492-506.

46. Turner, D., Dlugogorski, B., Palmer, T., *Factors affecting the stability of foamed concentrated emulsions*. Colloids Surf., A, 1999, 150(1-3), 171-184.

6 Macroporous Polymers from Particle-Stabilized Emulsions*

Abstract

Macroporous polymers are attractive materials due to their low density, low cost, recyclability, and tunable mechanical and functional properties. Here, we report a new approach to prepare macroporous polymers from emulsions stabilized with colloidal polymeric particles in the absence of chemical reactions. Stable water-in-oil emulsions were prepared using Poly(vinylidiene difluoride) (PVDF), poly(tetrafluoroethylene) (PTFE), and poly(etheretherketone) (PEEK) as stabilizing polymeric particles in emulsions. The partial wetting of the polymeric particles by the two immiscible liquids drives particles at the water-oil interface during emulsification, leading to extremely stable water-in-oil emulsions. The particle-stabilized emulsions were processed into highly porous solid polymer components upon drying and sintering. The high stability of emulsions also allows for the preparation of hollow polymeric microcapsules. We describe the conditions required for the adsorption of particles at the liquid-liquid interface, we show the rheological behavior of the polymer-loaded wet emulsions, and we discuss the effect of the emulsions' initial compositions on the final sintered porous structures. This new approach for the fabrication of macroporous PVDF, PTFE, and PEEK polymers is particularly suited for the preparation of porous materials from

* *I. Akartuna, E. Tervoort, J. C. H. Wong, A. R. Studart, J. L. Gauckler, Polymer, 2009, 50, 3645-3651.*

intractable polymers but can also be easily applied to a variety of other polymeric particles.

6.1 Introduction

Porous polymers find numerous applications as, for example, mechanical dampers, supports for catalysis, thermal, acoustic and electrical insulators, piezoelectric electrets, furnishing and construction materials, scaffolds for tissue engineering, and encapsulants for drug delivery [1-5]. The main processing methods used for the preparation of macroporous polymers are foaming of a polymer melt or solution through the incorporation of a gaseous phase [6, 7], fibre bonding [8, 9], phase separation [10], or sacrificial templating using ice crystals [11, 12], emulsion droplets [13, 14], wax [15], and salt particles [16] as fugitive phase.

The sacrificial template method enables tuning of the porosity, pore size distribution, and pore morphology of the final material by adjusting the amount, size, and shape of the fugitive phase. The use of volatile emulsion droplets as templates to produce porous polymers has been employed for many decades [17-21]. Macroporous polymers with pore sizes in the range of 1-100 μm have been produced by polymerization of the continuous phase of high (or medium) internal phase emulsions (HIPEs/MIPEs), followed by the subsequent removal of the internal phase by drying and heat treatment [13, 22-28]. The preparation of porous polymers from poly(MIPEs/HIPEs) involves the stabilization of the internal droplet phase using conventional surfactants in a monomer solution. The volume fraction of the dispersed phase corresponds to 0.6 and >0.74 for MIPEs and HIPEs, respectively [21, 26, 27, 29]. To increase the stability of the emulsions against collapse during liquid removal, the structure is locked by the polymerization of the continuous monomer phase. In addition to surfactants, the internal droplet phase of HIPEs has also been stabilized by colloidal particles adsorbed at the liquid interfaces, leading to particle-stabilized Pickering emulsions [30-32]. Macroporous polymers with porosities up to 90% and pore sizes in the range of 100-400 μm have been prepared by polymerizing the continuous phase of Pickering-HIPEs stabilized with carbon nanotubes [29], silica [33] and titania nanoparticles [34], and microgel latex particles [35], followed by evaporation of the dispersed phase.

Recently, particle-stabilized emulsions were used to produce porous polymeric structures in the absence of polymerization reactions. Porous membranes with pore

sizes up to 20 μm were formed through phase inversion of a polymeric emulsion stabilized by zeolite nanoparticles [36].

Although emulsions have long been used as templates for the production of highly porous polymers, the technique has been mostly limited to polymers that can be polymerized in situ within the continuous phase or to polymers that are melt-processable. Hence, an emulsion templating approach that would not involve any chemical reactions and that could be easily applied to a wide variety of polymers, including "intractable" polymers that can not be melt-processed would be highly desirable for the fabrication of macroporous polymers. Fluorinated polymers such as poly(vinylidene difluoride) (PVDF) and poly(tetrafluorethylene) (PTFE) are particularly interesting due to their piezoelectric behavior (PVDF) and non-adherent properties combined with high temperature resistance (PTFE).

Powder processing routes are often used for shaping and consolidating intractable polymers such as PTFE. Therefore, a wide variety of intractable polymers are commercially available in powder form. Such polymeric particles can potentially be used to stabilize Pickering emulsions and also be the major constituent of macroporous polymers obtained after removal of the droplet templates. We recently developed a simple powder-based route to produce macroporous ceramics from emulsions stabilized with inorganic particles of various chemical compositions [37]. In that case, the adsorption of initially hydrophilic particles at the oil-water interface was achieved through the in situ adsorption of short amphiphilic molecules on the surface of particles. Here, we extend this powder-based approach for the preparation of macroporous polymers from emulsions stabilized by polymeric particles of different chemical compositions. The method relies on the adsorption of colloidal polymeric particles at the oil-water interface for the formation of stable water-in-oil emulsions that are subsequently used as templates for the preparation of porous polymers. The particles adsorbed at the liquid interface act as a barrier against extensive droplet coalescence, allowing for drying and sintering of the emulsions directly into macroporous polymers in the absence of any chemical reaction.

6.2 Materials and methods

6.2.1 Materials

Poly(vinylidene difluoride) powder (PVDF) with average particle diameter, d_{50}, of 250 nm, specific density of 1.78 g/cm^3 , and melting temperature of 160.5°C was purchased from Polysciences, Inc. (Warrington, PA, USA). Poly(tetrafluoroethylene) powder (PTFE) with d_{50} ~ 300 nm, specific density of 2.15 g/cm^3, and melting temperature of 328.7°C was obtained from Algoflon (Ausimont S.P.A., Italy). Poly(etheretherketone) powder (PEEK, VICOTE^{TM} 707) with d_{50} ~ 16 μm, specific density of 1.3 g/cm^3, and melting temperature of 343°C was acquired from Victrex plc (Rotherham, UK). The melting temperatures reported above were measured by differential scanning calorimetry (DSC). These values are comparable to those reported in the literature for the pure polymers, indicating that the commercial powders are surfactant-free. We also determined the contact angle of water droplets in air deposited on the surface of flat substrates made out of the commercial polymers. The contact angles measured through the water phase were 90°, 114°, and 77° for PVDF, PTFE, and PEEK particles, respectively, which are within the range accepted in literature.

Decane (≥98% pure, boiling temperature T_b = 171-174°C, Fluka Chemie, Switzerland), octane (97% pure, boiling temperature T_b = 125 °C, Acros Organics, Belgium), hexane (96% pure, boiling temperature T_b = 69 °C, Scharlau, Spain), and toluene (99.99% pure, T_b = 110.6°C, Acros Organics, Belgium) were used as received. Diblock copolymer based on styrene and ethylene/propylene, G-1701E was purchased from Kraton Polymers LLC (Houston, TX, USA) and used as received. The interfacial tensions of decane-water, octane-water, hexane-water, and toluene-water interfaces were measured to be 51.8, 51.4, 50.0, and 36 mN/m, respectively (PAT1, Sinterface Technologies, Berlin, Germany). Double deionized water with an electrical resistance of 18 MΩcm was used in all the experiments (Nanopure water system, Barnstead, USA).

6.2.2 Preparation of suspensions

Prior to emulsification, colloidal suspensions of particles were prepared by adding powders to oil under steady stirring in a conventional lab-scale mixer. In the case of hexane, the emulsion was cooled in an ice bath to prevent evaporation of hexane during mixing. The concentration of particles in the suspension varied between

5 and 17 vol% for the PVDF particles and was kept constant at 15 vol% and 26 vol% for the PTFE and PEEK particles, respectively. The detailed compositions of the investigated emulsions are shown in Table 6.1.

Table 6.1: Compositions of the emulsions stabilized by PVDF, PTFE, and PEEK polymeric particles. The amount of the water phase was calculated with respect to the emulsion total volume (water + particles + oil).

Particle	Suspension Solids Content (vol %)	Oil	Water Content (vol%)
PVDF	5-17	Octane	30-65
PTFE	15	Hexane	50
PTFE	15	Octane	50
PTFE	15	Decane	50
PEEK	26	Octane	40

6.2.3 Preparation of emulsions

Emulsification was performed by vigorously stirring mixtures of water and concentrated suspensions of PVDF, PTFE, and PEEK particles in oil for 3 min using a household mixer at full power (Multimix 350 W, Braun, Spain).

6.2.4 Rheology

Rheological tests were performed at 25 °C using a stress-controlled rheometer (Bohlin-Rheometer CS-50, Bohlin, England) with profiled parallel-plate geometry (25 mm plate diameter). Experiments were carried out with a mechanically set gap of 1000 μm. Oscillatory measurements were conducted to determine the storage and loss moduli of the wet emulsions by gradually increasing the maximum applied stress from 10 to 1000 Pa at a constant frequency of 1 Hz. Steady-state experiments were carried out to measure the emulsion apparent viscosity as a function of shear rate by progressively increasing the applied stress from 200 to 1000 Pa.

6.2.5 Drying and sintering

After emulsification, all emulsions were shaped and dried in air at 25°C and ambient pressure for 2 days. Following drying, the PVDF samples were sintered at 177 °C for 4 h, the PTFE samples were sintered at 343 °C for 7 h, and the PEEK samples were sintered at 360°C for 6 h to obtain polymeric macroporous structures.

6.2.6 Microstructural analysis

Optical micrographs were obtained by placing wet emulsion samples between two glass slides in an optical microscope (Polyvar MET, Reichert-Jung, Austria) connected to a camera (DC300, Leica, Switzerland) in transmitting light mode. The porous polymers obtained after sintering were investigated by scanning electron microscopy (SEM, LEO 1530). SEM samples were sputtered with platinum for 55 s at 60 mA. Droplet size distributions of the wet emulsions and pore size distributions of the sintered polymers were determined by evaluating a set of at least five microscope images for each composition using the linear intercept method (software Lince, TU Darmstadt, Germany). Average sizes and 68% confidence intervals were obtained by fitting log-normal distributions to the experimental data. Porosities of the sintered samples were determined from the geometrical dimensions of the samples, their weight and the theoretical density of the materials.

6.2.7 Preparation of polymer capsules

Colloidal capsules were formed by diluting the wet emulsions 500x by volume with the continuous oil phase. Prior to dilution, 0.05 mg/mL diblock copolymer was added to the oil phase to lock the particle layers that form the capsules' walls. Water capsules were harvested from the diluted emulsions by removing the upper oil phase with a pipette after sedimentation of the water droplets. Dry hollow capsules were prepared by depositing several drops of diluted wet capsules onto a clean, aluminum SEM sample holder, followed by drying in air at room temperature for 1 day.

6.3 Results and discussion

Water-in-oil emulsions stabilized by polymeric particles were obtained by dispersing the particles in the oil phase prior to emulsification. The initial hydrophobic

nature of the polymeric particles allowed for the preparation of homogeneous dispersions of high particle concentrations in oil (Table 6.1).

Despite their predominantly hydrophobic nature, we observed that PVDF, PTFE, and PEEK particles readily adsorb at oil-water interfaces when water is mixed with to the initial particle-containing oil suspension. This led to stable particle-coated water droplets dispersed throughout the continuous oil phase, as exemplified in Figure 6.1 for the case of PVDF particles. Such results indicate that the particles are not fully wetted by the oil phase when their surface also exposed to water, which results in a finite contact angle of the water-oil interface on the polymer surface. A finite contact angle in the range of 60-120° (measured through the aqueous phase) is also observed for water-air interfaces on most polymer surfaces [38]. The fact that water can partially wet the surface of polymers in contact with air or alkanes is probably due to the high interfacial tensions of water-alkane and water-air interfaces: 50.0-51.8 and 72.8 mN/m, respectively. According to Young-Laplace's force balance [39], a high interfacial tension of the water-alkane or water-air interfaces tend to hinder complete spreading of the hydrophobic fluid (alkane or air) on the polymer surface. Based on this argument, non-polar liquids of interfacial tension lower than that of alkanes (with respect to water) should wet the polymer surface to a larger extent and should thus make the adsorption of polymeric particles at the oil-water interface less favorable. Indeed, additional experiments using toluene as oil phase resulted in less stable emulsions, suggesting that the lower interfacial tension between toluene and water (36 mN/m) favors wetting on the polymer surface and thus inhibits the adsorption of polymeric particles on the surface of water droplets.

The results obtained here indicate that a high interfacial tension of the water-oil interface is a key requirement for the stabilization of emulsions using polymeric particles, since this should lead to a finite contact angle of the water-oil interface on the polymer surface. Taking the water-air interface as an example of a high-energy interface at which most polymers form a finite contact angle between 60 and 120° [38], one should expect that particle-stabilized emulsions could be in principle obtained with a variety of other polymeric particles, as long as oils with a high interfacial tension with respect to water are used. The type of emulsions would then be determined by the exact contact angle of the water-oil interface on the polymer surface. Oil-in-water emulsions are expected for contact angles lower than 90°, whereas water-in-oil emulsions should result from contact angles larger than 90°. Emulsification would not

be possible only close to a contact angle of 90° where the thin liquid film separating droplets might not be thick enough to prevent droplet coalescence [40].

The microstructure of wet emulsions stabilized by polymeric particles was varied by changing the amount of particles in the initial suspension and the water content in the emulsion (Figure 6.1). For a fixed water content of 65 vol%, an increase in the concentration of PVDF particles from 5 to 17 vol% leads to a decrease in the cell size range of the wet emulsions from 11-266 μm to 16-69 μm, as indicated in the multimodal droplet size distributions shown in Figure 6.1.a. The decrease in the range of droplet sizes with increasing particle concentration results from the higher viscosity of the initial suspension, which induces higher shearing stresses on the droplets during mixing [37, 41].

The influence of water content on the emulsion microstructure was investigated for PVDF-stabilized emulsions at a fixed particle concentration of 17 vol%. No significant change in the droplet size distribution was observed for water concentrations between 30 and 60 vol%. Interestingly, an increase in the water volume fraction from 60 to 65 vol% decreased the droplet size range from 19-121 μm to 16-69 μm, as illustrated in Figure 6.1.b. This reduction in droplet size range is probably due to a pronounced increase in the viscosity of the emulsion when the volume fraction of droplets approaches the condition of random close packing (~ 64 vol% for monodisperse spheres). Water contents higher than 65 vol% resulted in emulsions with a phase-separated layer of water on the top of the mixture.

Emulsions comprising 65 vol% water and 17 vol% PVDF particles exhibited remarkable stability against coalescence, Ostwald ripening, and sedimentation. No significant change was observed in the emulsion droplet size distribution within a time period of more than 1 year after emulsification. This long-term stability can be attributed to the irreversible adsorption of particles at the oil-water interface. Due to the high energies required to remove a particle from the oil-water interface, particles can impede the rupture of the thin liquid film between droplets, as well as inhibit the shrinkage of droplets induced by Ostwald ripening.

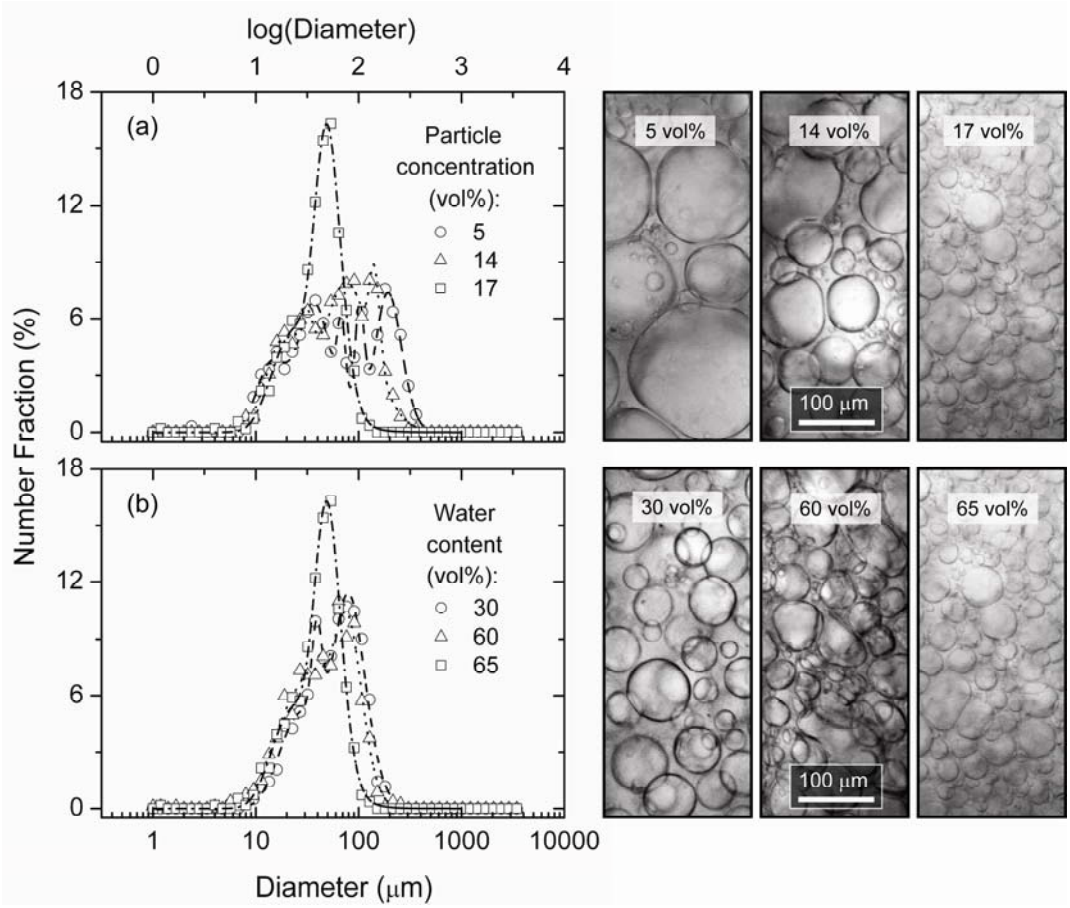

Figure 6.1: Droplet size distributions and optical microscope images of water-in-oil emulsions prepared with (a) different concentrations of PVDF particles at a fixed water content of 65 vol%, (b) different water contents at a fixed particle concentration of 17 vol% in oil.

Similar to PVDF-stabilized emulsions, the adsorption of PTFE and PEEK particles at the oil-water interface resulted in stable particle-stabilized emulsions with water droplets dispersed throughout the continuous oil phase, as demonstrated in Figure 6.2.a, b. Emulsions stabilized by PTFE and PEEK particles exhibited broad droplet size distributions with sizes in the range from 67 to 234 μm and 77 to 203 μm, respectively (Figure 6.2.c).

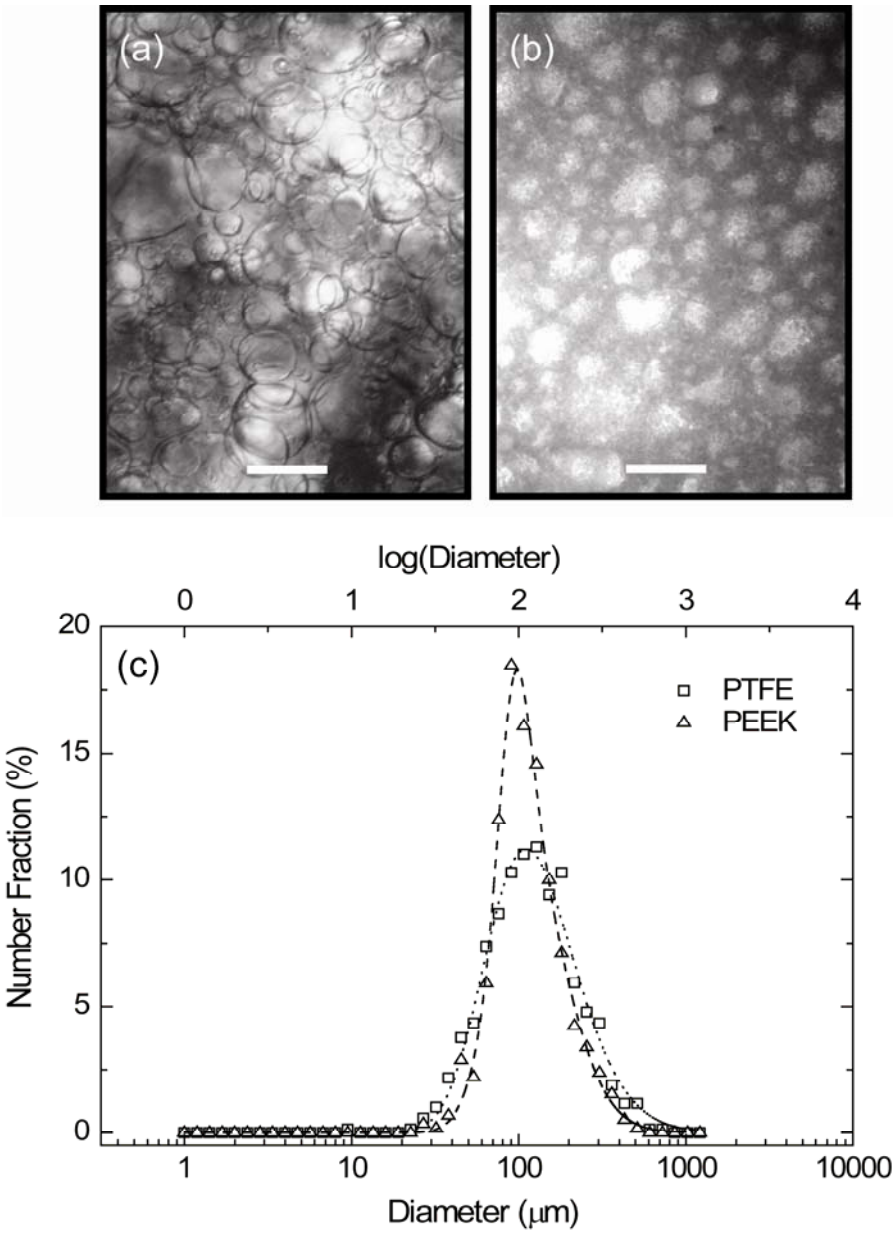

Figure 6.2: (a, b) Optical microscope image and (c) droplet size distribution of water-in-oil emulsion stabilized with PTFE and PEEK particles. The emulsions were prepared by mixing suspensions of (a) 15 vol% PTFE particles in hexane with 50 vol% water, (b) 26 vol% PEEK particles in octane with 40 vol% water. The continuous lines correspond to the radial probability density functions used to describe the droplet size distributions. Scale bar: 200 μm.

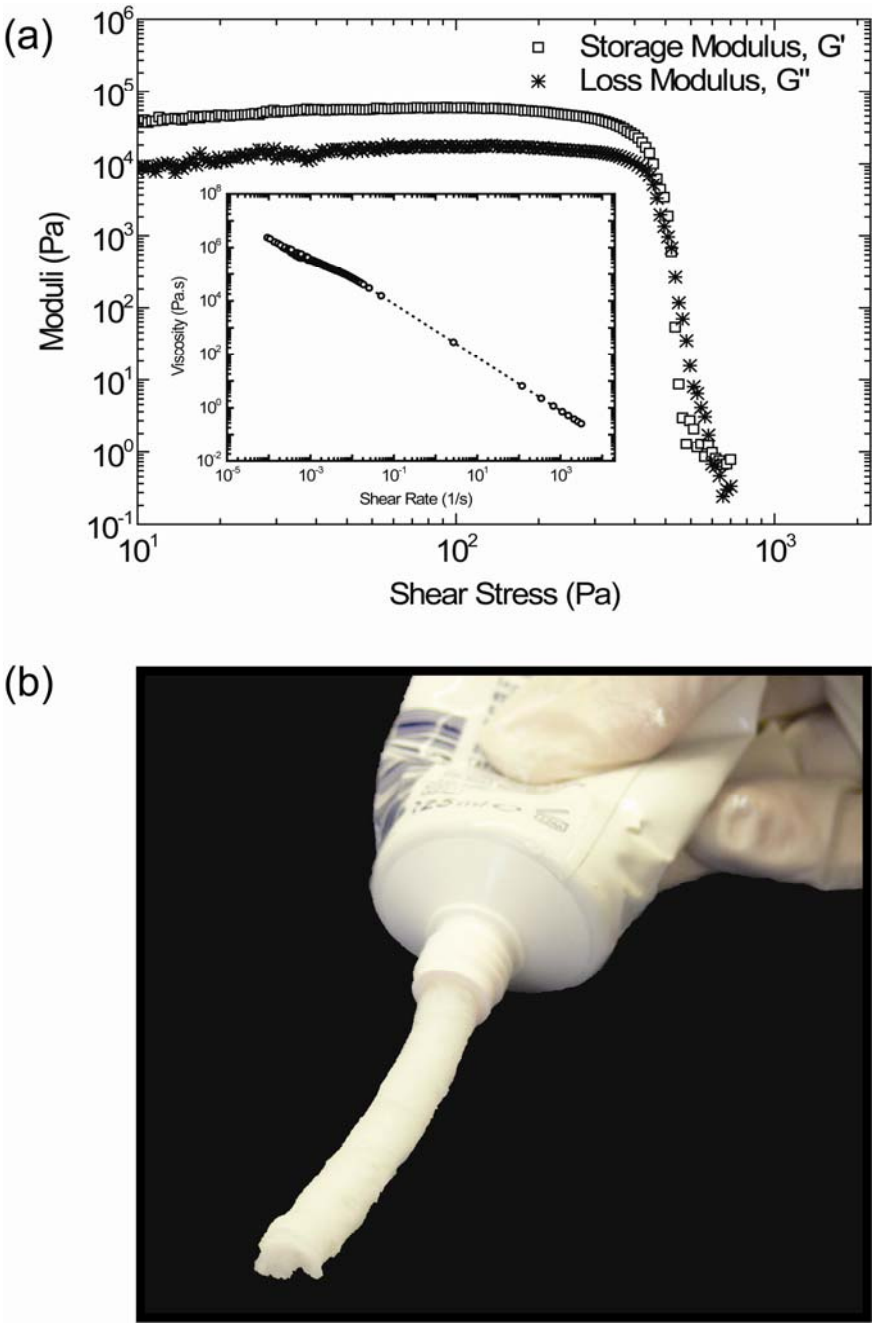

Figure 6.3: (a) Storage (G', □) and loss (G", ∗) moduli as functions of applied shear stress for a water-in-octane emulsion containing 17 vol% PVDF particles and 65 vol% water. Inset: Apparent viscosity (○) of the same emulsion as a function of applied shear rate. (b) Image of the same water-in-oil emulsion extruded through a tube.

As a result of the densely packed water droplets and the high concentration of particles in the continuous phase, the wet emulsions exhibit viscoelastic behavior with a noticeable yield stress, as shown in Figure 6.3 for a PVDF-stabilized emulsion. Under steady-shear conditions, the viscoelastic character led to a typical shear-thinning

behavior with a marked decrease in the apparent viscosity as the shear rate is increased (Figure 6.3, inset). This viscoelastic behavior enables shaping of the emulsions using conventional technologies such as injection molding and extrusion without requiring any further gelation or strengthening reaction. Water-in-oil emulsions containing 17 vol% PVDF particles and 65 vol% water for instance can be extruded without need of further strengthening to keep the shape of the material after the extrusion process (Figure 6.3.b).

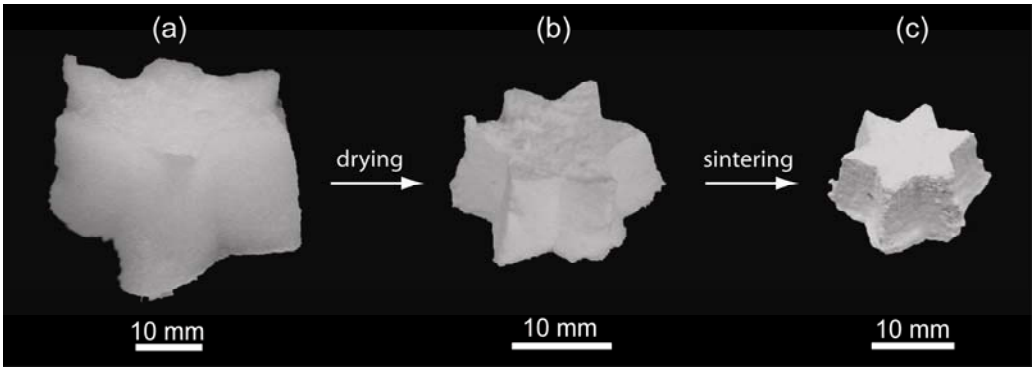

Figure 6.4: Macroporous polymers obtained from PTFE stabilized water-in-hexane emulsions. (a) Highly stable emulsions are formed through the adsorption of submicrometer-sized colloidal particles at the oil-water interface. The long term stability of these emulsions allows for (b) drying and (c) sintering of the shaped materials directly into macroporous polymers without requiring any further gelation or strengthening reaction.

The high stability achieved by the presence of particles adsorbed on the droplet surface and spanning throughout the continuous phase allowed for drying and sintering of the wet emulsions directly into macroporous polymers, as exemplified in Figure 6.4 for a PTFE-stabilized emulsion.

Microstructures of porous polymers fabricated from PVDF, PTFE, and PEEK stabilized emulsions are shown in Figure 6.5. Sintered PVDF structures obtained from emulsions containing 17 vol% PVDF particles and 65 vol% water showed pore sizes in the range from 16 to 100 μm (Figure 6.6). Sintering of emulsions containing 15 vol% PTFE particles and 50 vol% water, and 26 vol% PEEK particles and 40vol% water yielded porous structures with slightly larger pores in the range from 58 to 195 μm, and 80 to 180 μm, respectively (Figure 6.6).

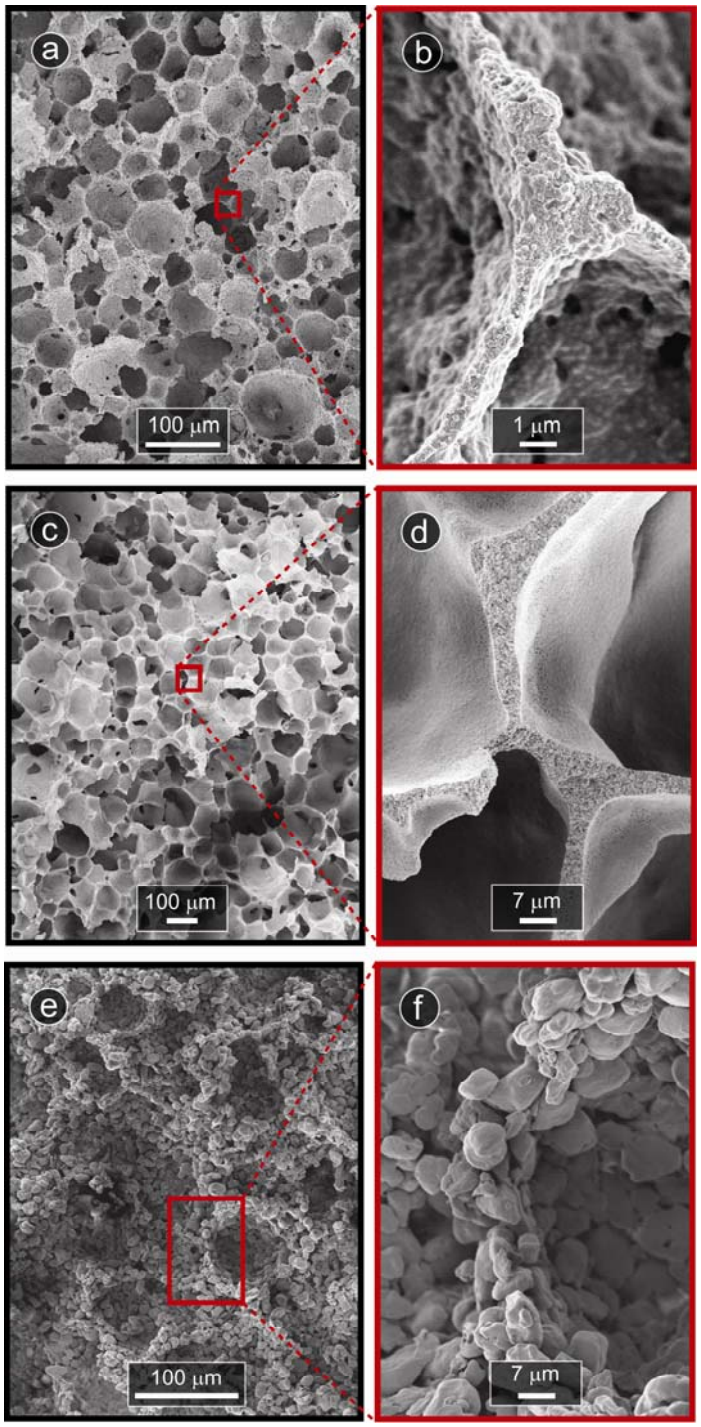

Figure 6.5: Microstructures of sintered porous polymers prepared with PVDF, PTFE, and PEEK particles. (a) Porous PVDF obtained after sintering the water-in-octane emulsion with 65 vol% water and 17 vol% PVDF particles at 177 °C; b) the dense strut of the sintered porous PVDF obtained after sintering; c) porous PTFE obtained after sintering the water-in-hexane emulsion with 50 vol% water and 15 vol% PTFE particles at 343 °C; d) the dense struts and the cell walls of the sintered porous PTFE formed after sintering; e) porous PEEK obtained after sintering the water-in-octane emulsion with 40 vol% water and 26 vol% PEEK particles at 360 °C; f) the cell walls of the sintered porous PEEK.

To avoid the collapse of porous components upon heating, the samples were sintered slightly above the melting temperature within a narrow temperature range. At this temperature range, the viscosity of the polymers is presumably still sufficiently high to avoid the collapse of the structures. Fusion of particles in the continuous phase and at the pore surfaces during sintering led to the formation of dense struts and 1-5 μm thick walls (Figure 6.5.b and d). The porous PVDF and PTFE samples exhibited linear shrinkage of 30% and 13% during drying and sintering, respectively. The total porosity after sintering was 79% for the PVDF structures and 82% for the PTFE samples.

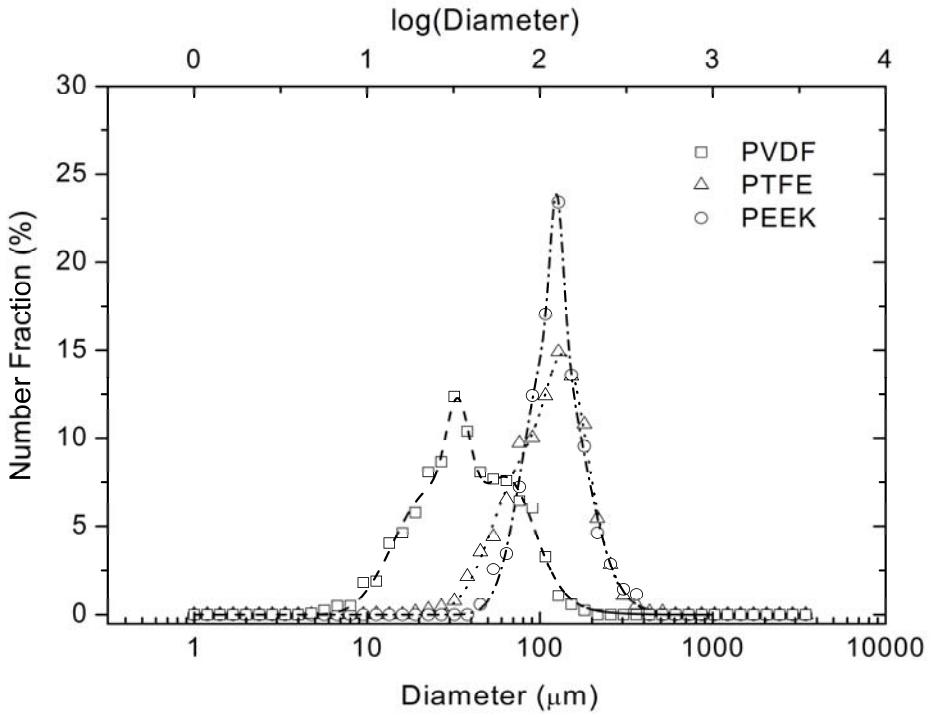

Figure 6.6: Pore size distributions of sintered porous polymers prepared with PVDF, PTFE, and PEEK particles. (□) Porous PVDF obtained after sintering the water-in-octane emulsion with 65 vol% water and 17 vol% PVDF particles at 177 °C; (Δ) porous PTFE obtained after sintering the water-in-hexane emulsion with 50 vol% water and 15 vol% PTFE particles at 343 °C; (○) porous PEEK obtained after sintering the water-in-octane emulsion with 40 vol% and 26 vol% PEEK particles at 360 °C.

In addition to bulk macroporous polymers, the stability of wet emulsions enabled harvesting of semi-permeable particle-coated capsules. Wet capsules comprised of polymeric particles in the outer shell were obtained by diluting the PVDF-stabilized emulsions with the continuous oil phase. Locking the close-packed particle

shells surrounding each water droplet with a diblock copolymer strengthened the particles outer layer and allowed for the production of polymeric hollow capsules upon drying, as shown in Figure 6.7. Colloidal capsules coated with functional polymers such as PVDF, PTFE, and PEEK might be attractive materials for the encapsulation and delivery of active agents in food processing, pharmaceutics, agriculture, and medicine.

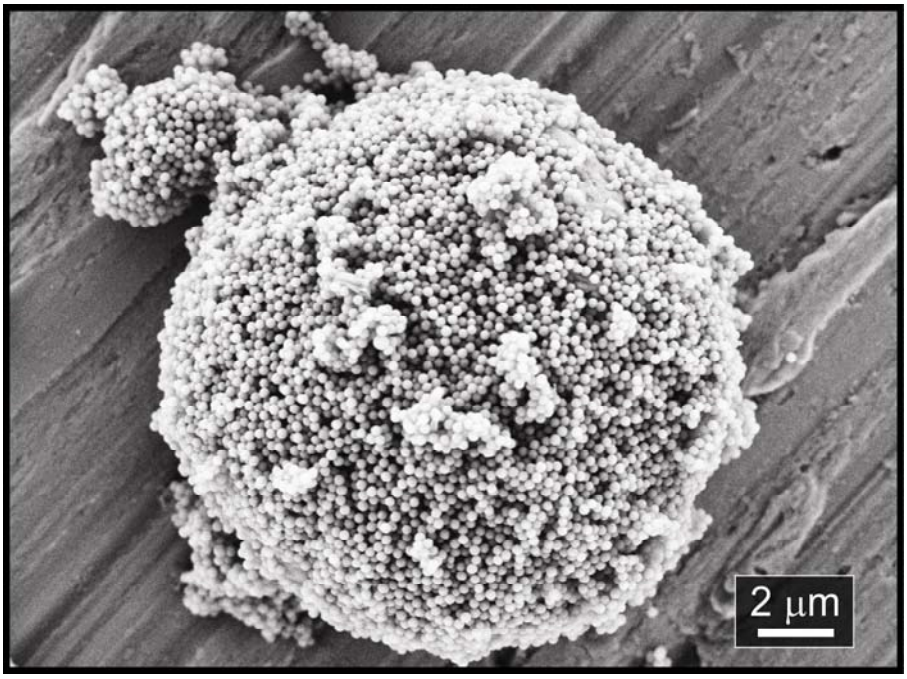

Figure 6.7: SEM image of a dry PVDF capsule obtained after 500x dilution of PVDF stabilized wet emulsion with a continuous oil phase containing 0.05 mg/mL diblock copolymer.

6.4 Conclusions

We described a simple and versatile approach to produce macroporous polymers from emulsions stabilized with polymeric particles of different chemical compositions. The adsorption of colloidal polymeric particles at the oil-water interface allows for the stabilization of water-in-oil emulsions that can be further processed into polymeric macroporous structures in the absence of any chemical reaction. Particle adsorption at the oil-water interface is accomplished by choosing oils that do not completely wet the surface of the polymeric particles. In the case of PVDF, PTFE, and PEEK particles, for instance, this condition is valid when short alkanes exhibiting high interfacial tension with respect to water are used as oil phase. Taking poly(vinylidene difluoride), poly(tetrafluoroethylene), and poly(etheretherketone) particles as examples, we

obtained bulk porous polymers with porosities up to 82% and pore sizes within a range from 16 to 200 μm. The high stability of the wet emulsions allows for harvesting of single hollow microcapsules composed of close-packed shells of polymeric particles. Macroporous polymers prepared by this approach may be used in many applications, as low-weight structural components, mechanical dampers, thermal and electrical insulating materials, piezoelectric electrets, scaffolds for tissue engineering, and encapsulants for drug delivery.

6.5 Acknowledgment

We are very thankful to Michael Müller, Boris Iwanovsky, Fabian Fischer, and Yasmina Ries for their assistance in the experimental work.

6.6 References

1. Gibson, L. J., Ashby, M. F., *Cellular Solids: Structure and properties*. 2nd ed. Solid State Science Series, Clarke, D. R., Suresh, S., Ward, I. M., Editors. 1997, Cambridge: Cambridge University Press.

2. Okoroafor, M. O., Frisch, K. C., *Introduction to Foams and Foam Formation*, in *Handbook of Plastic Foams: Types, properties, manufacture and applications*, Landrock, A. H., Editor. 1995, William Andrew Publishing/Noyes: New Jersey. p. 1-10.

3. Lee, S. T., *Introduction: Polymeric Foams, Mechanisms and Materials*, in *Polymeric Foams: Mechanisms and Materials*, Lee, S. T., Ramesh, N. S., Editors. 2004, CRC Press: Boca Raton.

4. Bauer, S., Gerhard-Multhaupt, R., Sessler, G. M., *Ferroelectrets: Soft electroactive foams for transducers*. Phys. Today, 2004. 57(2): 37-43.

5. Dinsmore, A. D., Hsu, M. F., Nikolaides, M. G., Marquez, M., Bausch, A. R., Weitz, D. A., *Colloidosomes: Selectively permeable capsules composed of colloidal particles*. Science, 2002. 298: 1006-1009.

6. Werner, P., Verdejo, R., Wöllecke, F., Altstädt, V., Sandler, J. K. W., Shaffer, M. S. P., *Carbon nanofibers allow foaming of semicrystalline poly(ether ether ketone)*. Adv. Mater., 2005. 17: 2864-2869.

7. Heng, L., Wang, X., Zhai, J., Sun, Z., Jiang, L., *Fabrication of stable polyaniline foams and their photoelectric conversion behaviors*. Chem. Phys. Chem., 2008. 9: 1559-1563.

8. Mikos, A. G., Bao, Y., Cima, L. G., Ingber, D. E., Vacanti, J. P., Langer, R., *Preparation of poly(glycolic acid) bonded fibre structures for cell attachment and transplantation* J. Biomed. Mater. Res., 1993. 29: 183-189.

9. Lewis, J. L., Johnson, S. L., Oegma, T. R., Jr., *Interfibrillar collagen bonding exists in matrix produced by chondrocytes in culture: evidence by electron microscopy*. Tissue Eng., 2002. 8(6): 989-995.

10. Yang, F., Qu, X., Cui, W. J., Bei, J. Z., Yu, F. Y., Lu, S. B., Wang, S. G., *Manufacturing and morphology structure of polylactide-type microtubules orientation-structured scaffolds*. Biomaterials, 2006. 27(28): 4923-4933.

11. Chen, G. P., Ushida, T., Tateishi, T., *Preparation of poly(L-lactic acid) and poly(DL-lactic-co-glycolic acid) foams by use of ice microparticulates.* Biomaterials, 2001. 22(18): 2563-2567.

12. Zhang, H., Cooper, A. I., *Aligned porous structures by directional freezing.* Adv. Mater., 2007. 19(11): 1529-1533.

13. Imhof, A., Pine, D. J., *Uniform macroporous ceramics and plastics by emulsion templating.* Adv. Mater., 1998. 10(9): 697-700.

14. Zhang, H., Cooper, A. I., *Synthesis and applications of emulsion-templated porous materials.* Soft Matter, 2005. 1: 107-113.

15. Shastri, V. P., Martin, I., Langer, R., *Macroporous polymer foams by hydrocarbon templating.* Proc. Natl. Acad. Sci. U. S. A., 2000. 97(5): 1970-1975.

16. Lee, S. Y., Oh, J. H., Kim, J. C., Kim, Y. H., Kim, S. H., Choi, J. W., *In vivo conjunctival reconstruction using modified PLGA grafts for decreased scar formation and contraction.* Biomaterials, 2003. 24: 5049-5059.

17. Bartl, M. H., v Bonin, W., *About the polymerization in reversed emulsion*. Makromol., 1962. 57: 74-95.

18. Bartl, M. H., v. Bonin, W., *About the polymerization in reversed emulsion II*. Makromol., 1963. 66: 151-156.

19. Lissant, K. J., *The geometry of high-internal-phase-ratio emulsions.* J. Colloid Interface Sci., 1966. 22(5): 462-468.

20. Lissant, K. J., Mayhan, K. G., *A study of medium and high internal phase ratio water/polymer emulsions.* J. Colloid Interface Sci., 1973. 42(1): 201-208.

21. Barby, D., Haq, Z., *Low density porous cross-linked polymeric materials and their preparation*. EP0060138, 1982.

22. Cameron, N. R., Sherrington, D. C., Ando, I., Kurosu, H., *Chemical modification of monolithic poly(styrene-divinylbenzene) PolyHIPE(R) materials.* J. Mater. Chem., 1996. 6(5): 719-726.

23. Cameron, N. R., Sherrington, D. C., *Preparation and glass transition temperatures of elastomeric PolyHIPE materials.* J. Mater. Chem., 1997. 7(11): 2209-2212.

24. Cameron, N. R., Sherrington, D. C., *Synthesis and characterization of poly(aryl ether sulfone) PolyHIPE materials.* Macromolecules, 1997. 30(19): 5860-5869.

25. Butler, R., Davies, C. M., Cooper, A. I., *Emulsion templating using high internal phase supercritical fluid emulsions.* Adv. Mater., 2001. 13(19): 1459-1463.

26. Cameron, N. R., *High internal phase emulsion templating as a route to well-defined porous polymers.* Polymer, 2005. 46(5): 1439-1449.

27. Menner, A., Powell, R., Bismarck, A., *Open porous polymer foams via inverse emulsion polymerization: Should the definition of high internal phase (ratio) emulsions be extended?* Macromolecules, 2006. 39(6): 2034-2035.

28. Haibach, K., Menner, A., Powell, R., Bismarck, A., *Tailoring mechanical properties of highly porous polymer foams: Silica particle reinforced polymer foams via emulsion templating.* Polymer, 2006. 47(13): 4513-4519.

29. Menner, A., Verdejo, R., Shaffer, M., Bismarck, A., *Particle-stabilized surfactant-free medium internal phase emulsions as templates for porous nanocomposite materials: Poly-pickering-foams.* Langmuir, 2007. 23(5): 2398-2403.

30. Pickering, S. U., *Emulsions*. J. Chem. Soc., 1907. 91: 2001-2021.

31. Aveyard, R., Binks, B. P., Clint, J. H., *Emulsions stabilised solely by colloidal particles*. Adv. Colloid Interface Sci., 2003. 100-102: 503-546.

32. Binks, B. P., Lumsdon, S. O., *Pickering emulsions stabilized by monodisperse latex particles: Effects of particle size*. Langmuir, 2001. 17(15): 4540-4547.

33. Ikem, Vivian O., Menner, A., Bismarck, A., *High internal phase emulsions stabilized solely by functionalized silica particles*. Angew. Chem. Int. Ed., 2008. 47(43): 8277-8279.

34. Menner, A., Ikem, V., Salgueiro, M., Shaffer, M. S. P., Bismarck, A., *High internal phase emulsion templates solely stabilised by functionalised titania nanoparticles*. Chem. Commun., 2007: 4274-4276.

35. Colver, P. J., Bon, S. A. F., *Cellular polymer monoliths made via Pickering high internal phase emulsions*. Chem. Mater., 2007. 19(7): 1537-1539.

36. Vandezande, P., Gevers, L. E. M., Vermant, J., Martens, J. A., Jacobs, P. A., Vankelecom, I. F. J., *Solidification of emulsified polymer solutions via phase inversion (SEPPI): A generic way to prepare polymers with controlled porosity*. Chem. Mater., 2008. 20(10): 3457-3465.

37. Akartuna, I., Studart, A. R., Tervoort, E., Gauckler, L. J., *Macroporous ceramics from particle stabilized emulsions*. Adv. Mater., 2008. 20: 4714-4718.

38. Studart, A. R., Gonzenbach, U. T., Akartuna, I., Tervoort, E., Gauckler, L. J., *Materials from foams and emulsions stabilized by colloidal particles*. J. Mater. Chem., 2007. 17(31): 3283-3289.

39. Myers, D., *Surfaces, Interfaces and Colloids: Principles and Applications*. 1991, Weinheim: VCH Publishers.

40. Denkov, N. D., Ivanov, I. B., Kralchevsky, P. A., Wasan, D. T., *A possible mechanism of stabilization of emulsions by solid particles*. J. Colloid Interface Sci., 1992. 150(2): 589-593.

41. Akartuna, I., Studart, A. R., Tervoort, E., Gonzenbach, U. T., Gauckler, L. J., *Stabilization of oil-in-water emulsions by colloidal particles modified with short amphiphiles*. Langmuir, 2008. 24(14): 7161-7168.

7 General Route for the Assembly of Functional Inorganic Capsules*

Abstract

Semi-permeable, hollow capsules are attractive materials for the encapsulation and delivery of active agents in food processing, pharmaceutical and agricultural industries, and biomedicine. These capsules can be produced by forming a solid shell of close packed colloidal particles, typically polymeric particles, at the surface of emulsion droplets. However, current methods to prepare such capsules may involve multi-step chemical procedures to tailor the surface chemistry of particles or are limited to particles that exhibit inherently the right hydrophobic-hydrophilic balance to adsorb around emulsion droplets. In this work, we describe a general and simple method to fabricate semi-permeable, inorganic capsules from emulsion droplets stabilized by a wide variety of colloidal metal oxide particles. The assembly of particles at the oil-water interface is induced by the in situ hydrophobization of the particle surface through the adsorption of short amphiphilic molecules. The adsorption of particles at the interface leads to stable capsules comprised of a single layer of particles in the outer shell. Such capsules can be used in the wet state or can be further processed into dry capsules. The permeability of the capsules can be modified by filling the interstices between the shell particles with polymeric or inorganic species. Functional capsules with biocompatible, bioresorbable, heat resistant, chemical resistant, and magnetic

* *I. Akartuna, E. Tervoort, A. R. Studart, L. J. Gauckler, to be submitted.*

properties were prepared using alumina, silica, iron oxide, and tricalcium phosphate as particles in the shell.

7.1 Introduction

Semi-permeable capsules, also known as colloidosomes [1-4], can potentially be used in a broad range of applications for encapsulation and delivery of active agents in food, pharmaceutical and agricultural industries, and biomedicine [5-7]. These capsules are typically made by forming an elastic, solid shell of close packed colloidal particles at the interface of emulsion droplets. Colloidosomes are produced either by mechanical mixing of immiscible fluids [3, 4, 8-23] or by the controlled flow of immiscible fluids microfluidic devices [24-27]. Hollow dry capsules have also been obtained by evaporating the liquid phases of the wet capsules [3, 9, 14, 16, 18-20, 22, 23, 28]. The permeability of capsules is usually defined by the size of the interstices between the colloidal particles and can be tuned by changing, for example, the particle size. The permeability and the elasticity of the capsules can also be tailored by locking the particles together through attractive van der Waals force [3, 12], adsorbing a polymer or polyelectrolyte to the particle shell [3, 4, 9-12, 17], using particles of different sizes in the shell [22], coating of the capsule shell with additional layer of particles [11], fusing the particles together upon sintering [3, 12, 19], gelling or polymerizing the inner core of the capsules [13, 15, 16, 20, 22, 29-31] , or by swelling/contracting polymer-based particles upon changes in pH, ionic strength, and temperature [23, 30].

The capsule shell has been made using different types of colloidal particles, including for example inorganic [13, 15, 20-22, 24, 25, 29, 32], polymeric [3, 4, 9, 11, 12, 16, 17, 19, 22, 24, 25, 30, 31, 33-35], semiconducting [8, 14, 15], metallic [24, 25], and composite [36] particles. Inorganic particles, in particular, are attractive due to their intrinsic functional properties such as magnetic (Fe_3O_4), catalytic (TiO_2) and semi-conducting (SnO_2) behavior, biocompatibility (Al_2O_3, ZrO_2, SiO_2, and TiO_2), chemical and temperature resistance, and bioresorbability (calcium phosphates, bioglass).

Despite various previous investigations on inorganic-coated capsules, most of the current methods to prepare such capsules are limited to a few chemical compositions (e.g. latex and SiO_2 [4, 37]), usually involve multi-step chemical procedures to tailor the surface chemistry of particles (e.g. silanization [37, 38]) or are limited to particles that exhibit inherently the right hydrophobic-hydrophilic balance to adsorb around emulsion droplets [12, 24]. A general method to tailor the surface chemistry and control the

processing of inorganic particles of different sizes and surface chemistries into functional inorganic capsules is thus highly demanded.

We describe a simple, general method for the fabrication of semi-permeable, functional inorganic capsules by tailoring the surface chemistry of oxide particles of various sizes and chemical compositions. The in situ modified particles assemble at the surface of oil droplets dispersed in water to form stable inorganic capsules. Large quantities of wet and dry capsules are thus obtained directly from oil-in-water emulsions stabilized by inorganic particles. To illustrate the general nature of the method, we provide examples of capsules coated with oxide particles that are chemically inert and biocompatible (Al_2O_3, SiO_2), temperature-resistant (Al_2O_3, SiO_2), magnetic (Fe_3O_4), and bioresorbable (β-TCP).

7.2 Materials and methods

7.2.1 Materials

α-Al_2O_3 powder (Ceralox HPA-0.5, 99.99 % Al_2O_3) with d_{50} of 200 nm, specific surface area of 10 m^2/g, and density of 3.98 g/cm^3 was purchased from Sasol North America Inc. (Tucson, AZ, USA). Al_2O_3 powder, referred to as δ-Al_2O_3, a mixture of 70% δ- and 30% γ-phase, with d_{50} of 65 nm, specific surface area of 38 m^2/g, and density of 3.6 g/cm^3 was purchased from Nanophase Technologies Co. (Romeoville, IL, USA). SiO_2 powder (grade Snowtex ZL) with d_{50} ~ 80 nm, specific surface area of 25 m^2/g, and density of 2.1 g/cm^3 was purchased from Nissan Chemical (Houston, TX, USA). Fe_3O_4 powder (> 98% Fe_3O_4) with d_{50} of 20-30 nm, specific surface area of 60 m^2/g, and density of 4.95 g/cm^3 was purchased from Nanostructured & Amorphous Materials, Inc. (Houston, TX; USA). β-TCP powder (≥ 96% pure) with d_{50} of 500 nm, specific surface area of 1 m^2/g, and density of 3.14 g/cm^3 was purchased from Fluka AG (Buchs, Switzerland). Octane (97% pure, Boiling temperature T_b = 125 °C, Acros Organics, Belgium) and decalin (Decahydronaphthalene, cis/trans-isomers basis (GC), ≥ 98% pure, Boiling temperature T_b = 189-191 °C, Riedel-de Haën, Germany) were used as received from the manufacturers. The short amphiphilic molecules used for particle modification were butyric acid, hexyl amine and octyl gallate (> 99.5%, > 98%, and > 99% pure, respectively, Fluka AG, Buchs, Switzerland), and propyl gallate (≥ 98%, Sigma-Aldrich Chemie GmbH, Germany). Polyacrylic acid (PAA, M_W: 450 000, Sigma-

Aldrich Chemie GmbH, Germany), polyethyleneimine solution (PEI, M_W: 70 000, 30 wt% in water, Polyscience, Inc., Warrington, PA, USA), and poly-L-lysine solution (PLL, 0.1 w/v aqueous solution, Sigma-Aldrich Chemie GmbH, Germany) were used without purification. Double deionized water with an electrical resistance of 18 MΩcm was used in the experiments (Nanopure water system, Barnstead, USA). 2 M hydrochloric acid (HCl) and 1 M sodium hydroxide (NaOH) solutions (Titrisol, Fluka AG, Buchs, Switzerland) were used to adjust the pH.

7.2.2 Methods

Colloidal suspensions of α-alumina, δ-alumina, silica, iron oxide, and β-tricalcium phosphate particles were prepared by adding 35, 20, 35, 10, and 35 vol% of powder, respectively, into deionized water under steady mixing. The pH of these suspensions was adjusted by adding 1 M NaOH and/or 2 M HCl drop wise. It is important to note that the particle concentration indicated throughout this study refers to the solids content in the initial aqueous suspension and is not based on the emulsion total volume. In situ surface hydrophobization of initially hydrophilic particles was performed by de-agglomerating the powder for 22 h in a ball-mill using alumina milling balls (10 mm diameter) for α-alumina suspensions and zirconia balls (5, 10, and 20 mm diameter) for δ-alumina, silica, iron oxide, and β-tricalcium phosphate suspensions with a ball/powder weight ratio of 2.5, followed by a gradual addition of aqueous solutions containing the short amphiphiles (Table 7.1). After the preparation of suspensions, emulsification was performed by vigorously stirring the suspension and the oil for 3 min using a household mixer at 1040 rpm (Multimix 350 W, Braun, Spain). Surface charge and the isoelectric points (IEP) of the surface modified silica and δ-alumina particles were determined using the electroacoustic colloidal vibration technique (DT1200, Dispersion Technologies Inc., Mount Cisco, NY). Experiments were performed with 2 vol% suspensions of silica and δ-alumina particles initially surface modified with 2.27 mmol/L hexyl amine at pH 10.4 and 6.94 mmol/L butyric acid at pH 4.75, respectively.

To prepare wet capsules, the emulsions were diluted 10x with the continuous water phase at the pH of the initial suspensions (see Figure 11.7-A in Appendix), and centrifuged in 40 mL Eppendorf tubes for 1 hr at room temperature. The supernatant was then removed, and the creamed emulsion droplets were redispersed in water at

the pH of the initial suspension. This centrifugation-washing procedure was repeated five times. The centrifugation force for diluted emulsions containing δ-alumina, silica, and iron oxide particles was 400 rpm (19 g), 140 rpm (2 g), and 110 rpm (1 g), respectively. Following the washing step, creamed emulsions were further diluted with 1000 mL water at the pH of the initial suspensions (see Figure 11.7-A in Appendix).

Table 7.1: Conditions required for the preparation of particle stabilized oil-in-water emulsions with a wide range of metal oxide powders.

Metal Oxide	**pH**	**Suspension solids content (vol%)**	**Amphiphile**	**Amphiphile content (mmol/L)**	**Oil**	**Oil Content (vol%)**	**Number Fraction of Particles Adsorbed on the Capsule Surface**
δ-Al_2O_3	4.75	20	Butyric acid	85	Decalin	82	1.07
SiO_2	10.4	35	Hexyl amine	60	Octane	72	0.43
Fe_3O_4	9.9	10	Octyl gallate	44	Octane	79	0.42
β-TCP	9.9	35	Propyl gallate	130	Octane	72	1.35
α-Al_2O_3	4.75	35	Propionic acid	180	Octane	72	-

Strengthening of capsules was performed by first diluting the emulsions 10x with water at the pH of the initial suspensions and centrifuging the diluted emulsions 1x in 40 mL Eppendorf tubes at conditions mentioned above (see Figure 11.7-B in Appendix). The creamed droplets were then redispersed in aqueous polyelectrolyte solution having an opposite charge with respect to the particles. The dispersion of creamed droplets and polyelectrolyte solution was mixed gently for 2 h with a magnetic mixer to allow the adsorption of the polyelectrolyte on the particle shells. In the case of silica capsules suspended in water at pH 10.4, PEI (pK_a: 11) and PLL (pK_a: 10.5) solutions were used in concentrations of 5 and 1 mg/mL, respectively, (pH 8) to strengthen the particle shell. For δ-alumina capsules at pH 4.75, PAA (pK_a: 4.5) at a

concentration of 1 mg/mL (pH 7) was used for strengthening. To fully dissolve PAA in water, the PAA-water mixture was heated to ~50 °C. Following the adsorption of polyelectrolytes, excess polyelectrolyte and particles were removed by four repeated centrifugation and washing cycles at the same conditions as mentioned above. During each washing step, the pH of the final dispersion was maintained at pH 8 and 7 for silica and δ-alumina capsules, respectively. Creamed oil droplets (~5-10 mL) were finally diluted in 500-1000 mL water at pH 7-8.

To strengthen the capsules with inorganic ionic species, oil-in-water emulsions stabilized by inorganic particles were first diluted 5000-7000x with the continuous water phase at the pH of the initial suspensions (see Figure 11.7-C in Appendix). To produce capsules with inorganic-organic hybrid layers, emulsions were diluted 5000-7000x with 1 mg/mL aqueous polyelectrolyte solutions at the pH of the initial suspensions. For silica capsules, an aqueous solution of PLL was prepared at pH 10.4; while an aqueous solution of PAA at pH 4.75 was used for capsules with alumina shells. Strengthened dry hollow capsules were finally obtained by putting several drops of diluted wet capsules onto a clean aluminum SEM sample holder and drying them in air at room temperature for 1 day.

The morphology and size of the emulsions and wet capsules were examined by an optical microscope in transmission mode (Polyvar MET, Reichert-Jung, Austria) connected to a digital camera (DC 300, Leica, Switzerland). Droplet size distributions of emulsions were determined by evaluating a set of at least 5 optical microscope images for each sample using the linear intercept method (Software Lince, TU Darmstadt, Germany). Average droplet sizes and 68% confidence intervals were obtained by fitting log-normal distributions to the experimental data. Optical microscope images of wet capsules were taken by putting a droplet of diluted emulsion between a glass object slide and cover glass. Imaging with a confocal laser scanning microscope (Zeiss, LSM 510, Germany) was carried out using fluorescent silica particles (d_{50}: 500 nm) in a 20x diluted octane-in-water emulsion prepared according to the procedure described by Akartuna et al. [39]. The structure and morphology of dry hollow capsules were investigated by scanning electron microscopy (SEM, LEO 1530). SEM samples were prepared by sputtering samples with Pt for 55 s at 60 mA.

7.3 Results and discussion

The assembly of hydrophilic metal oxide particles at the oil-water interface was accomplished by the in situ hydrophobization of the particle surface through the adsorption of short amphiphilic molecules [4, 39, 40]. In contrast to the long-chain surfactants used in most previous studies to tailor particle wettability [41-49] (more than 8 carbons in the hydrocarbon chain), the short amphiphilic molecules used in our approach exhibit remarkably higher solubility and critical micelle concentrations in water, enabling fast surface modification of high concentration of submicrometer- and nano-sized particles in the continuous liquid phase. Moreover, short amphiphiles alone are not able to stabilize the emulsions, ensuring that stabilization is only achieved through the formation of a shell of modified particles around the droplets rather than solely by the adsorption of surface active molecules at the oil-water interface.

On the basis of our previous work [39], colloidal particles of δ-alumina, silica, iron oxide, and β-tricalcium phosphate were in situ surface hydrophobized in water upon adsorption of butyric acid, hexyl amine, octyl gallate, and propyl gallate, respectively. For δ-alumina and silica particles, surface modification was induced by the electrostatic attraction of butyic acid and hexyl amine molecules onto the oppositely charged alumina and silica particles, respectively, at pHs in the vicinity of the pK_a values of the short amphiphiles. In the case of iron oxide and β-tricalcium phosphate particles, the surface hydrophobization was achieved through a ligand exchange reaction between the hydroxyl groups of the gallate molecules and the hydroxyl groups on the particle surface [50].

Once the surface of the colloidal particles was in situ modified in water, mechanical shearing of a mixture of oil and the aqueous suspensions of modified particles led to formation of stable oil-in-water emulsions. Stabilization of the oil-water interface with surface modified δ-alumina, silica, iron oxide, and β-tricalcium phosphate particles enabled emulsification of 72 to 82 vol% of oil throughout the suspension (Table 7.1). Due to the very high particle concentrations in the initial aqueous suspensions, only a fraction of those particles (0.42 to 1.35) is required to form a monolayer coating on the surface of the newly formed oil droplets (Table 7.1).

Oil-in-water emulsions prepared from high concentrations of alumina, silica, iron oxide, and β-tricalcium phosphate particles in the initial suspensions showed remarkable stability against coalescence, Ostwald ripening, and creaming. No

significant change was observed in the droplet size distributions of the emulsions for more than four years after preparation. This is illustrated in Figure 7.1.a, b and Figure 11.8 in Appendix for the case of oil-in-water emulsions prepared with α-alumina particles modified with propionic acid. This long-term stability of the emulsions is based on the strong attachment of the modified colloidal particles onto the interface of emulsion droplets [51, 52]. Particles irreversibly adsorbed at the oil-water interface impede the rupture of the thin film between adjacent droplets and possibly also the shrinkage of droplets due to Ostwald ripening, allowing thus for the stabilization of emulsions over long periods of time [52].

The long-term stability enabled the production of stable wet capsules by simply diluting the particle-stabilized emulsions with the continuous water phase. To fabricate capsules comprising a solid shell of inorganic particles, the concentrated oil-in-water emulsions were first 10x diluted, then gently centrifuged and finally washed with water to separate the emulsion droplets from the non-adsorbed particles and amphiphiles (Figure 11.7-A in Appendix). After five centrifugation-washing cycles, stable wet capsules were obtained as exemplified in Figure 7.1.c for silica capsules. The particle-coated capsules did not coalesce under the high centrifuging forces arising during multiple centrifugation-washing cycles. Unruptured wet capsules of δ-alumina, silica, iron oxide, and β-tricalcium phosphate were easily obtained following this approach (Figure 11.9 in Appendix). The ability of the wet capsules to resist coalescence under high external forces results from the strong adsorption of particles at the oil-water interface, which ultimately protects the droplets against fusion.

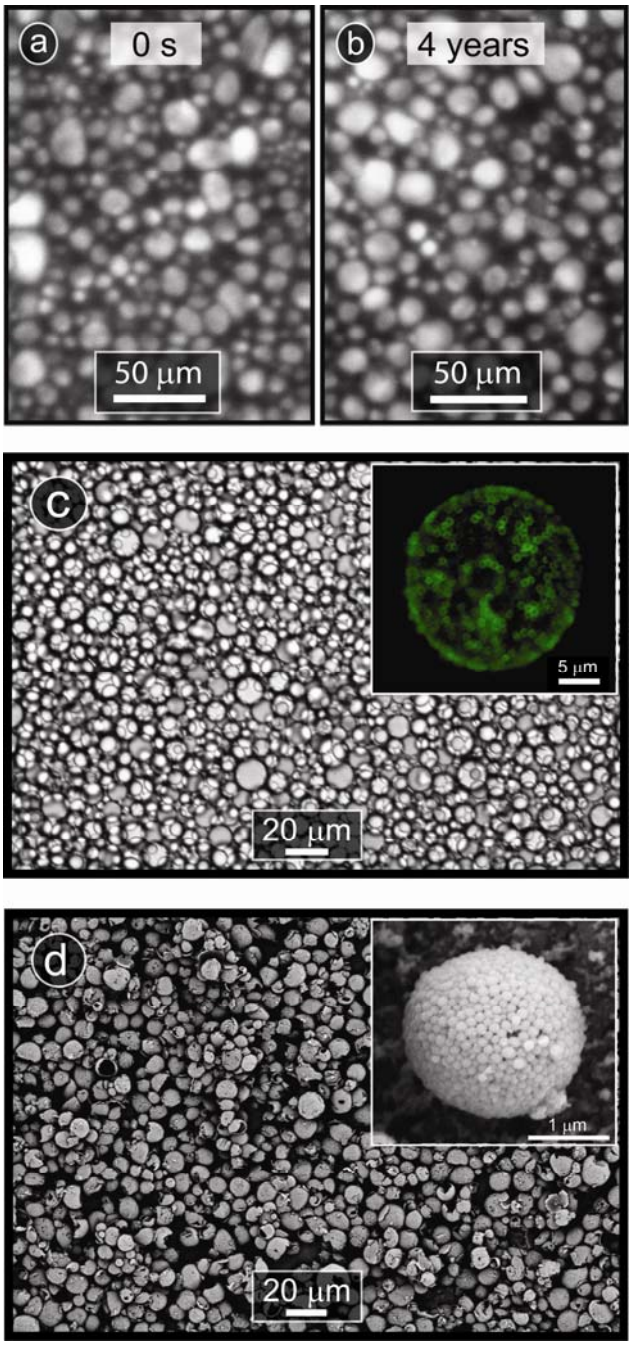

Figure 7.1: a) Optical microscope images of α-alumina stabilized-emulsions taken (a) just after emulsification and (b) 4 years after emulsification, c) Optical microscope image of wet capsules prepared with silica particles following five sequential centrifugation and washing cycles. Inset: Confocal scanning laser micrograph of a wet capsule composed of fluorescent silica particles, d) Hollow capsules obtained by drying of wet capsules in a. Inset: Scanning electron microscope image of a dry, hollow capsule comprised of a single layer of silica particles in the outer shell.

Dry capsules were also prepared by further diluting the wet capsules with water and afterwards evaporating the oil and the water phase at 23 °C in air. The as-prepared hollow capsules exhibited a single layer of colloidal inorganic particles in the shell, as shown in Figure 7.1.d in the case of silica capsules. Most of the capsules could not maintain their structural integrity under the high capillary forces developed during drying. Many capsules were either buckled or ruptured after evaporation of the liquid phases (Figure 7.1.d). Some of the capsules however did survive the drying step (Figure 7.1.d, inset). Dry hollow capsules with shells of different chemical compositions were obtained from emulsions stabilized by different inorganic particles, as shown in Figure 7.2. SEM images of broken hollow capsules clearly showed that the capsule walls were composed of single layer of particles (Figure 7.2.a, c). In general, we observed that the survival probability of the capsules was higher for smaller capsules. The higher resistance of smaller capsules against buckling and fracture is in agreement with the classic theory of shells, which predicts that the critical stress required to initiate buckling in thin spherical shells (σ_c) is given by [53]:

$$\sigma_c = \frac{2}{\sqrt{3(1-\nu^2)}} \frac{Et^2}{r^2} \qquad \text{Eq. 7.1}$$

where E is the Young's modulus, t is the shell thickness, ν is the Poisson ratio and r is the droplet radius. Even though Eq. 7.1 also predicts a dependence of the critical stress on the shell thickness, the thickness of the capsules did not vary significantly among the investigated systems to allow for a clear differentiation in buckling behavior.

Since buckling is caused by capillary forces on the droplet surface during drying, we estimated the critical shell stiffness E required to avoid buckling by simply equating the critical stress σ_c (in Eq. 7.1) to the capillary pressure developed across the droplet surface during drying, γ/r (where γ is the droplet interfacial tension). Assuming an interfacial tension of 0.050 N/m, a droplet radius of 5 µm, a Poisson ratio of 0.3 and a shell thickness of 100 nm, we obtained a capillary stress of 10 kPa and a critical shell stiffness (E_c) of the order of 5 GPa [54], our experimental results indicate that the stiffness of the monolayer of particles on the droplet surface was in general lower than this critical threshold value. Interestingly, we also observed that the particle layer forming the capsule shells exhibited different types of mechanical response after the critical

condition for buckling was achieved. Buckling of hollow capsules comprised of silica and alumina particles led to a brittle-like fracture of the outer shell, while buckling of capsules with iron oxide shells resulted in noticeable plastic deformation of the particle layer (Figure 7.2).

Strengthening of the particle layers at the droplet interface is essential to form wet capsules sufficiently stiff to withstand the high capillary stresses developed during drying ($E>E_c$). To increase the stiffness of the capsule shell, particles at the interface were locked together by adsorbing an oppositely charged polyelectrolyte to the particle shell through electrostatic interactions [3, 12, 26, 55, 56] (see Figure 11.7-B in Appendix). The pH values of the solutions were chosen so that the polyelectrolytes are highly ionized and exhibit high opposite charges with respect to the particles. Silica shells, for example, were strengthened using polycations, polyethyleneimine (PEI) or poly-L-lysine (PLL), in aqueous solutions at pH 8. Because modified silica particles are negatively charged at pH 8 (see Figure 11.10 in Appendix), both polycations can readily adsorb onto the particle layers. For alumina particles, polyacrylic acid (PAA) solutions were added to creamed capsules at pH 7. At this pH, highly negative PAA molecules can electrostatically assemble on the positively charged alumina particles (see Figure 11.10 in Appendix). No desorption of modified particles from the oil-water interface was observed after the addition of polyelectrolytes, confirming that these molecules are not sufficiently surface active to displace the particles from the droplet surface.

Strengthening of capsules with polyelectrolytes allowed for the production of hollow dry capsules with intact shells, as shown in Figure 7.3 for silica and δ-alumina capsules. As much as 95% of the original capsules had their structure preserved in the dried state. The polyelectrolyte layer covering the particle shells of the capsules were confirmed by electron microscopy of dry capsules, which indicated the formation of a smooth layer on the capsule outer surface (Figure 7.3). Increasing the polyelectrolyte concentration in the aqueous solution resulted in dry capsules with a denser polyelectrolyte layer around the particle shell, as shown in Figure 7.3.b, c for silica capsules strengthened by PLL. Furthermore, the formation of a polyelectrolyte layer onto the particle shells has been shown to decrease the permeability of the capsule by filling in the interstitial pores between the particles [26]. Thus, adjusting the molecular weight and the concentration of the polyelectrolyte should enable one to tune the strength and the permeability of the inorganic capsules in a controlled way.

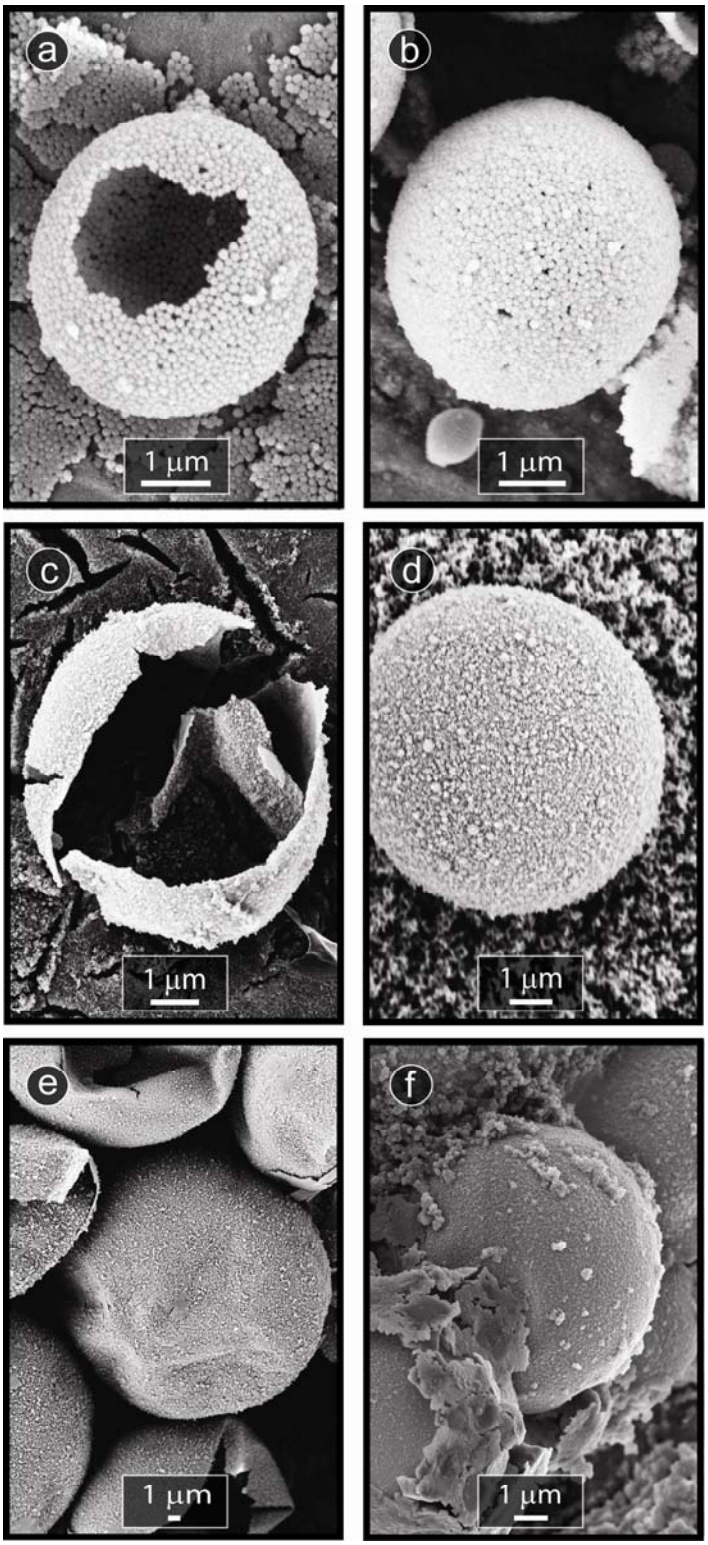

Figure 7.2: SEM images of dried capsules prepared after centrifugation and dilution of wet capsules formed by different inorganic particles. a) Broken silica capsule; b) Intact silica capsule; c) Broken, hollow capsule composed of δ-alumina particles; d) Intact δ-alumina capsule; e) Broken and stable capsules composed of magnetite particle shells; f) Dry β-TCP capsules obtained after dilution of wet capsules.

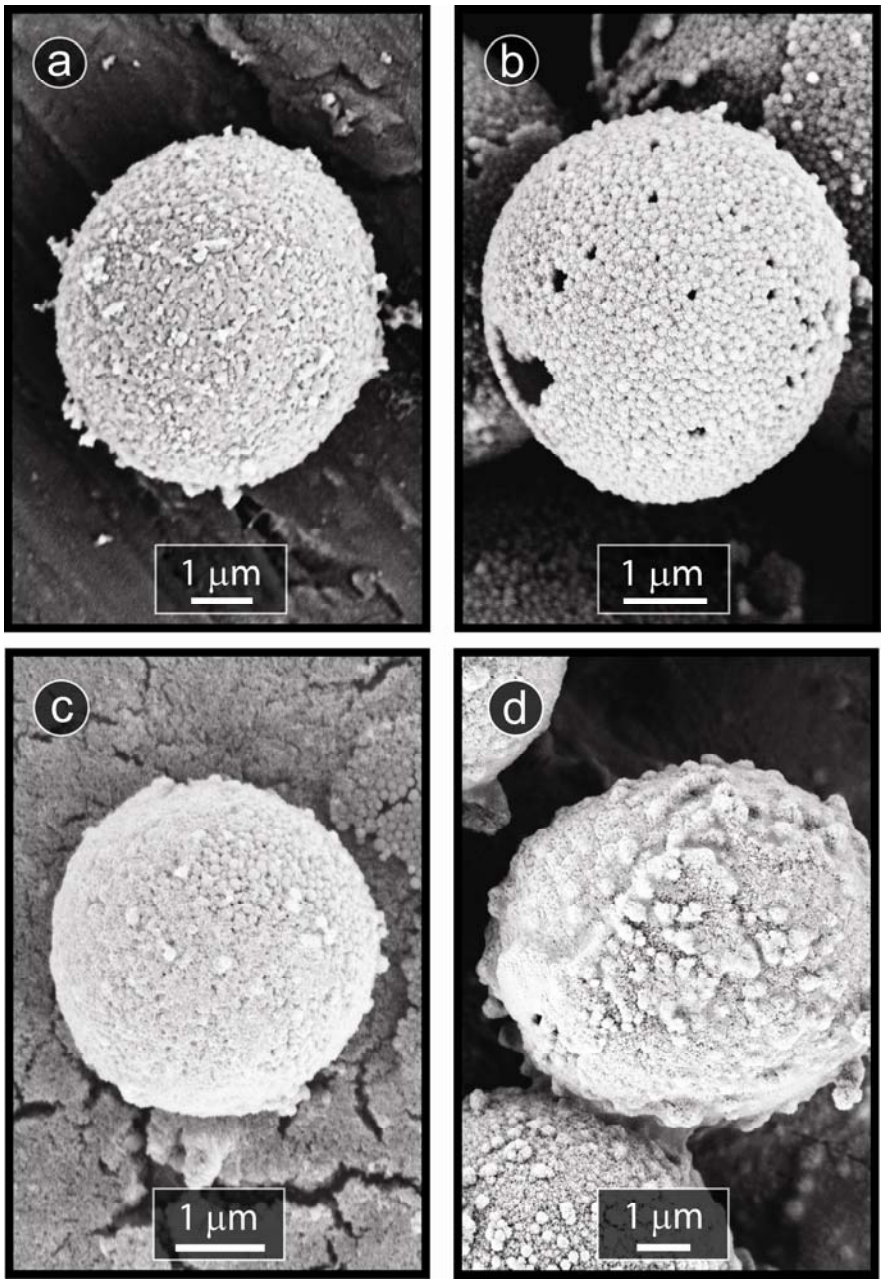

Figure 7.3: SEM images of dry capsules obtained after drying of centrifuged silica and δ-alumina stabilized wet capsules strengthened with different polyelectrolytes. a) Dry δ-alumina capsule strengthened with 1 mg/mL PAA at pH 7; b) Dry silica capsule strengthened with 0.3 mg/mL PLL at pH 8; c) Dry silica capsule strengthened with 1 mg/mL PLL at pH 8; d) Dry silica capsule strengthened with 5 mg/mL PEI at pH 8.

Besides the polyelectrolytes, we observed that the simple evaporation of the aqueous phase of highly diluted, unwashed emulsions also leads to the formation of a smooth dense layer on the capsule surface. Dilution of the particle stabilized oil-in-water emulsions with the continuous water phase at a pH in the vicinity of the pK_a

values of the amphiphiles, for example, resulted in intact, highly stable wet capsules with a smooth surface, as illustrated in Figure 7.4.a, b for δ-alumina and silica capsules. The smooth, dense layer formed on the capsule surface is considerably thinner than the particle diameter (80 nm) and probably results from the precipitation of Al^{3+} and SiO_4^{4-} ions initially dissolved from the particles into the continuous phase [57].

The morphology of these dense capsule shells could be further changed by adding polyelectrolytes into the continuous aqueous phase. The adsorption of the added polyelectrolytes onto the inorganic shells led to formation of hollow capsules with inorganic-organic hybrid layers of high roughness and surface area (Figure 7.4.c, d). Capsules with such rough surface might be advantageous in applications requiring fast dissolution of the hybrid wall or high density of adsorption/reaction sites on the capsule surface.

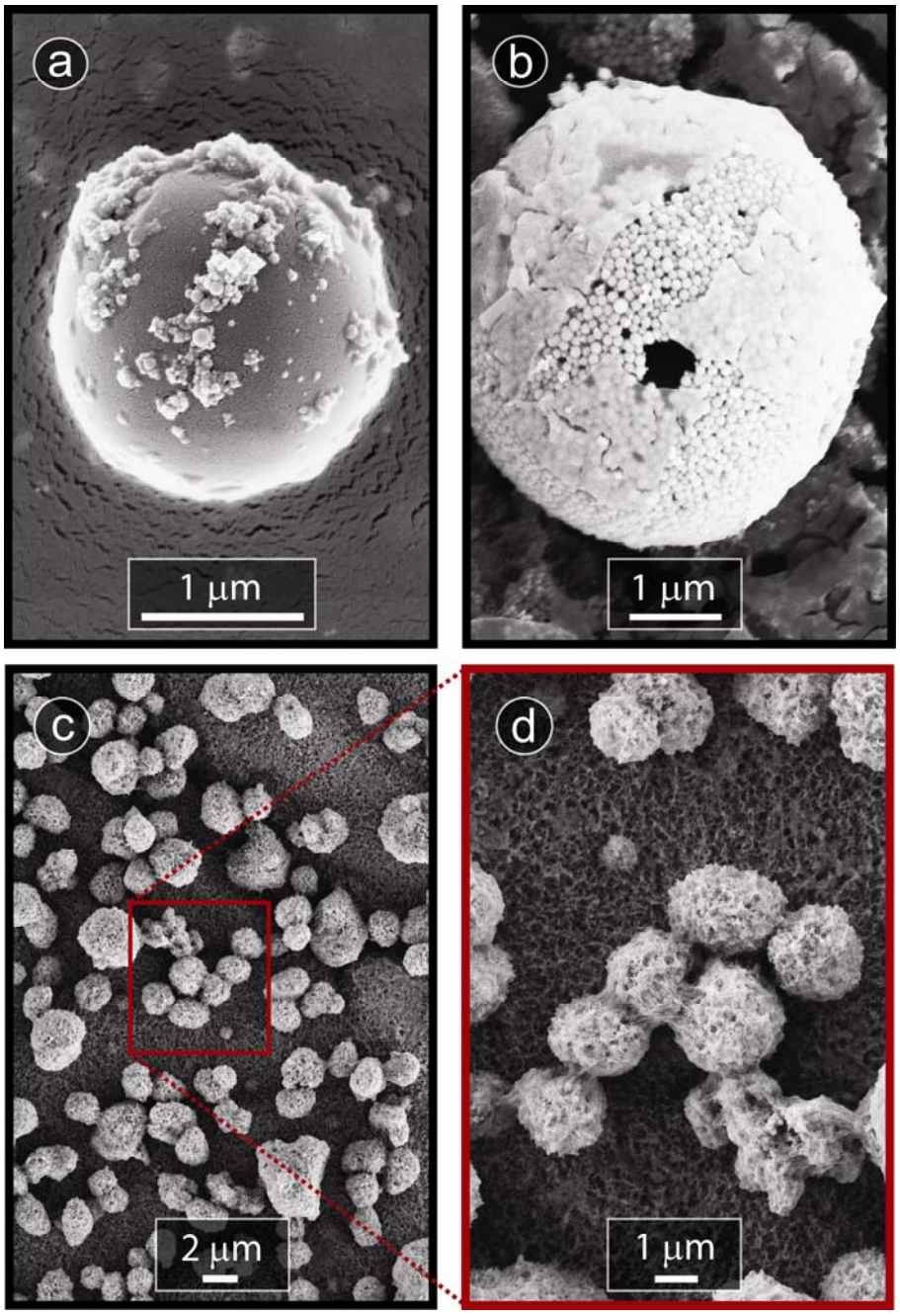

Figure 7.4: SEM images of dry inorganic capsules obtained after dilution of unwashed δ-alumina and silica stabilized wet capsules with the continuous water phase. a) Dry δ-alumina capsule after dilution 5000x with water at pH 4.75; b) Dry silica capsule after dilution 5000x with water at pH 10.4; c) Silica capsules strengthened with 1 mg/mL PLL following dilution 5000x with water at pH 10.4; d) Silica capsules in c at higher magnification.

7.4 Conclusions

The general and versatile method described here allows for the straightforward fabrication of large quantities of semi-permeable inorganic capsules with different functionalities. Stable wet capsules were formed through the assembly of in situ surface modified metal oxide particles onto the surface of oil droplets in an oil-in-water emulsion. Different amphiphiles were used for surface modification depending on the surface chemistry of the oxide particles, resulting in a powerful toolbox for the preparation of inorganic capsules of different chemical compositions. Although only oil-in-water emulsions were investigated in this work, the same set of amphiphilic molecules can also be used for the preparation of water-in-oil emulsions [58], which further extends the broad applicability of this method. Strengthening of particle shells through the adsorption of polyelectrolytes or the deposition of inorganic ionic species on the droplet surface enabled the fabrication of hollow, dry capsules with structural rigidity upon drying of the wet capsules. In addition to the strengthening effect, polyelectrolytes and inorganic species should also change the permeability and surface roughness of the capsule walls, and impart further versatility to this approach. The same concepts outlined here can also be extended to other oxide particles and potentially metallic particles with a surface oxide layer, following the rationale described in our earlier investigations [39, 59]. The biocompatibility, bioresorbability, heat resistance, chemical inertness and magnetic properties of the inorganic capsules produced by this simple route can potentially be explored for the fabrication of new, functional delivery systems in food, chemical and biochemical applications.

7.5 Acknowledgment

We thank Ciba Specialty Chemicals (Switzerland) for funding this study, as well as, Christina Pecnik, Joëlle Hofstetter, Lea Nowack, Adrian Marberger, and Basil Thalmann for their assistance in the experimental work.

7.6 References

1. Zeng, C., Bissig, H., Dinsmore, A. D., *Particles on droplets: From fundamental physics to novel materials*. Solid State Commun., 2006. 139(11-12): 547-556.

2. Manoharan, V. N., *Colloidal spheres confined by liquid droplets: Geometry, physics, and physical chemistry*. Solid State Commun., 2006. 139(11-12): 557-561.

3. Dinsmore, A. D., Hsu, M. F., Nikolaides, M. G., Marquez, M., Bausch, A. R., Weitz, D. A., *Colloidosomes: Selectively permeable capsules composed of colloidal particles.* Science, 2002. 298: 1006-1009.

4. Velev, O. D., Furusawa, K., Nagayama, K., *Assembly of latex particles by using emulsion droplets as templates. 1. Microstructured hollow spheres.* Langmuir, 1996. 12(10): 2374-2384.

5. Gouin, S., *Microencapsulation: Industrial appraisal of existing technologies and trends.* Trends Food Sci. Technol., 2004. 15(7-8): 330-347.

6. Tsuji, K., *Microencapsulation of pesticides and their improved handling safety.* J. Microencapsulation, 2001. 18(2): 137 - 147.

7. Park, J. K., Chang, H. N., *Microencapsulation of microbial cells.* Biotechnol. Adv., 2000. 18(4): 303-319.

8. Lin, Y., Skaff, H., Emrick, T., Dinsmore, A. D., Russel, T. P., *Nanoparticle assembly and transport at liquid-liquid interfaces.* Science, 2003. 299: 226-229.

9. Croll, L. M., Stöver, H. D. H., *Formation of tectocapsules by assembly and cross-linking of poly(divinylbenzene-alt-maleic anhydride) spheres at the oil-water interface.* Langmuir, 2003. 19: 5918-5922.

10. Croll, L. M., Stöver, H. D. H., *Mechanism of self-assembly and rupture of cross-linked microspheres and microgels at the oil-water interface.* Langmuir, 2003. 19: 10077-10080.

11. Gordon, V. D., Chen, X., Hutchinson, J. W., Bausch, A. R., Marquez, M., Weitz, D. A., *Self-assembled polymer membrane capsules inflated by osmotic pressure.* J. Am. Chem. Soc., 2004. 126: 14117-14122.

12. Hsu, M. F., Nikolaides, M. G., Dinsmore, A. D., Bausch, A. R., Gordon, V. D., Chen, X., Hutchinson, J. W., Weitz, D. A., Marquez, M., *Self-assembled shells composed of colloidal particles: Fabrication and characterization.* Langmuir, 2005. 21: 2963-2970.

13. Duan, H., Wang, D., Sobal, N. S., Giersig, M., Kurth, D. G., Möhlwald, H., *Magnetic colloidosomes derived from nanoparticle interfacial self-assembly.* Nano Lett., 2005. 5(5): 949-952.

14. Skaff, H., Lin, Y., Tangirala, R., Breitenkamp, K., Böker, A., Russell, T. P., Emrick, T., *Crosslinked capsules of quantum dots by interfacial assembly and ligand crosslinking.* Adv. Mater., 2005. 17(17): 2082-2086.

15. Wang, D., Duan, H., Möhlwald, H., *The water/oil interface: The imerging horizon for self-assembly of nanoparticles.* Soft Matter, 2005. 1: 412-416.

16. Bon, S. A. F., Cauvin, S., Colver, P. J., *Colloidosomes as micron-sized polymerisation vessels to create supracolloidal interpenetrating polymer network reinforced capsules.* Soft Matter, 2007. 3(2): 194-199.

17. Lawrence, D. B., Cai, T., Hu, Z., Marquez, M., Dinsmore, A. D., *Temperature-responsive semipermeable capsules composed of colloidal microgel spheres.* Langmuir, 2007. 23(2): 395-398.

18. Yi, H., Song, H., Chen, X., *Carbon nanotube capsules self-assembled by w/o emulsion technique.* Langmuir, 2007. 23(6): 3199-3204.

19. Laib, S., Routh, A. F., *Fabrication of colloidosomes at low temperature for the encapsulation of thermally sensitive compounds.* J. Colloid Interface Sci., 2008. 317(1): 121-129.

20. Chen, T., Colver, P. J., Bon, S. A. F., *Organic-inorganic hybrid hollow spheres prepared from TiO_2-stabilized pickering emulsion polymerization.* Adv. Mater., 2007. 19(17): 2286-2289.

21. Poortinga, A. T., *Microcapsules from self-assembled colloidal particles using aqueous phase-separated polymer solutions.* Langmuir, 2008. 24(5): 1644-1647.

22. Kim, S. H., Heo, C. J., Lee, S. Y., Yi, G. R., Yang, S. M., *Polymeric particles with structural complexity from stable immobilized emulsions.* Chem. Mater., 2007. 19(19): 4751-4760.

23. Kim, J.-W., Fernandez-Nievest, A., Dan, N., Utada, A. S., Marquez, M., Weitz, D. A., *Colloidal assembly route for responsive colloidosomes with tunable permeability.* Nano Lett., 2007. 7(9): 2876-2880.

24. Subramaniam, A. B., Abkarian, M., Stone, H. A., *Controlled assembly of jammed colloidal shells on fluid droplets.* Nat. Mater., 2005. 4: 553-556.

25. Subramaniam, A. B., Abkarian, M., Mahadevan, L., Stone, H. A., *Mechanics of interfacial composite materials.* Langmuir, 2006. 22(24): 10204-10208.

26. Lee, D., Weitz, D. A., *Double emulsion-templated nanoparticle colloidosomes with selective permeability.* Adv. Mater., 2008. 20(18): 3498-3503.

27. Nie, Z., Park, J. I., Li, W., Bon, S. A. F., Kumacheva, E., *An "inside-out" microfluidic approach to monodisperse emulsions stabilized by solid particles.* J. Am. Chem. Soc., 2008. 130(49): 16508-16509.

28. Russell, J. T., Lin, Y., Böker, A., Su, L., Carl, P., Zettl, H., He, J., Sill, K., Tangirala, R., Emrick, T., Littrell, K., Thiyagarajan, P., Cookson, D., Fery, A., Wang, Q., Russell, T. P., *Self-assembly and cross-linking of bionanoparticles at liquid-liquid interfaces.* Angew. Chem. Int. Ed., 2005. 44: 2420-2426.

29. Wang, C., Liu, H., Gao, Q., Liu, X., Tong, Z., *Facile fabrication of hybrid colloidosomes with alginate gel cores and shells of porous $CaCO_3$ microparticles.* ChemPhysChem, 2007. 8(8): 1157-1160.

30. Cayre, O. J., Noble, P. F., Paunov, V. N., *Fabrication of novel colloidosome microcapsules with gelled aqueous cores.* J. Mater. Chem., 2004. 14(22): 3351-3355.

31. Noble, P. F., Cayre, O. J., Alargova, R. G., Velev, O. D., Paunov, V. N., *Fabrication of "hairy" colloidosomes with shells of polymeric microrods.* J. Am. Chem. Soc., 2004. 126: 8092-8093.

32. Liu, H., Wang, C., Gao, Q., Liu, X., Tong, Z., *Fabrication of novel core-shell hybrid alginate hydrogel beads.* Int. J. Pharm., 2008. 351(1-2): 104-112.

33. He, X. D., Ge, X. W., Liu, H. R., Wang, M. Z., Zhang, Z. C., *Synthesis of cagelike polymer microspheres with hollow core/porous shell structures by self-assembly of latex particles at the emulsion droplet interface.* Chem. Mater., 2005. 17(24): 5891-5892.

34. Ngai, T., Auweter, H., Behrens, S. H., *Environmental responsiveness of microgel particles and particle-stabilized emulsions.* Macromolecules, 2006. 39(23): 8171-8177.

35. He, X. D., Ge, X. W., Liu, H. R., Deng, M. G., Zhang, Z. C., *Self-assembly of pH-responsive acrylate latex particles at emulsion droplets interface.* J. Appl. Polym. Sci., 2007. 105(3): 1018-1024.

36. He, Y. J., Li, T. H., Yu, X. Y., Zhao, S. Y., Lu, J. H., He, J., *Tuning the wettability of calcite cubes by varying the sizes of the polystyrene nanoparticles attached to their surfaces.* Appl. Surf. Sci., 2007. 253(12): 5320-5324.

37. Hong, L., Jiang, S., Granick, S., *Simple method to produce Janus colloidal particles in large quantity.* Langmuir, 2006. 22(23): 9495-9499.

38. Aveyard, R., Binks, B. P., Clint, J. H., *Emulsions stabilised solely by colloidal particles.* Adv. Colloid Interface Sci., 2003. 100-102: 503-546.

39. Akartuna, I., Studart, A. R., Tervoort, E., Gonzenbach, U. T., Gauckler, L. J., *Stabilization of oil-in-water emulsions by colloidal particles modified with short amphiphiles.* Langmuir, 2008. 24(14): 7161-7168.

40. Duan, H., Wang, D., Kurth, D. G., Möhwald, H., *Directing self-assembly of nanoparticles at water/oil interfaces.* Angew. Chem. Int. Ed., 2004. 43(42): 5639-5642.

41. Tambe, D. E., Sharma, M. M., *Factors controlling the stability of colloid-stabilized emulsions: I. An experimental investigation.* J. Colloid Interface Sci., 1993. 157(1): 244-253.

42. Schulman, J. H., Leja, J., *Control of contact angles at the oil-water-solid interfaces: Emulsions stabilized by solid particles ($BaSO_4$).* Trans. Far. Soc., 1954. 50(1): 598-605.

43. Tsugita, A., Takemoto, S., Mori, K., Yoneya, T., Otani, Y., *Studies on o/w emulsions stabilized with insoluble montmorillonite-organic complexes.* J. Colloid Interface Sci., 1983. 95(2): 551-560.

44. Gelot, A., Friesen, W., Hamza, H. A., *Emulsification of oil and water in the presence of finely divided solids and surface-active agents.* Colloids Surf., 1984. 12: 271-303.

45. Hassander, H., Johansson, B., Törnell, B., *The mechanism of emulsion stabilization by small silica (Ludox) particles.* Colloids Surf., 1989. 40: 93-105.

46. Binks, B. P., Desforges, A., Duff, D. G., *Synergistic stabilization of emulsions by a mixture of surface-active nanoparticles and surfactant.* Langmuir, 2007. 23(3): 1098-1106.

47. Binks, B. P., Rodrigues, J. A., *Enhanced stabilization of emulsions due to surfactant-induced nanoparticle flocculation.* Langmuir, 2007. 23(14): 7436-7439.

48. Binks, B. P., Rodrigues, J. A., Frith, W. J., *Synergistic interaction in emulsions stabilized by a mixture of silica nanoparticles and cationic surfactant.* Langmuir, 2007. 23(7): 3626-3636.

49. Menner, A., Ikem, V., Salgueiro, M., Shaffer, M. S. P., Bismarck, A., *High internal phase emulsion templates solely stabilised by functionalised titania nanoparticles.* Chem. Commun., 2007: 4274-4276.

50. Hidber, P. C., Graule, T. J., Gauckler, L. J., *Influence of the dispersant structure on properties of electrostatically stabilized aqueous alumina suspensions.* J. Eur. Ceram. Soc., 1997. 17: 239-249.

51. Pieranski, P., *Two-dimensional interfacial colloidal crystals.* Phys. Rev. Lett., 1980. 45(7): 569-572.

52. Binks, B. P., *Particles as surfactants--similarities and differences.* Curr. Opin. Colloid Interface Sci., 2002. 7(1-2): 21-41.

53. Ugural, A. C., *Mechanical Design: An Integrated Approach*. 2003, New York: McGraw Hill.

54. Balzer, B., Hruschka, M. K. M., Gauckler, L. J., *Coagulation kinetics and mechanical behavior of wet alumina green bodies produces via DCC.* J. Colloid Interface Sci., 1999. 216(2): 379-386.

55. Caruso, F., Möhlwald, H., *Preparation and characterization of ordered nanoparticle and polymer composite multilayers on colloids.* Langmuir, 1999. 15: 8276-8281.

56. Peyratout, C. S., Dähne, L., *Tailor-made polyelectrolyte microcapsules: From multilayers to smart containers.* Angew. Chem. Int. Ed., 2004. 43(29): 3762-3783.

57. Brinker, C. J., Scherer, G. W., *Sol-Gel Science: The Physics and Chemistry of Sol-Gel Processing*. 1990, San Diego: Acedemic Press, Inc.

58. Akartuna, I., Studart, A. R., Tervoort, E., Gauckler, L. J., *Macroporous ceramics from particle stabilized emulsions.* Adv. Mater., 2008. 20: 4714-4718.

59. Gonzenbach, U. T., Studart, A. R., Tervoort, E., Gauckler, L. J., *Stabilization of foams with inorganic colloidal particles.* Langmuir, 2006. 22(26): 10983-10988.

8 Rheology of Oil-in-Water Emulsions Stabilized by In Situ Modified Colloidal Particles

Abstract

The rheological properties of particle-stabilized oil-in-water emulsions such as viscosity, yield stress and storage modulus, and their dependence on amphiphile length, amphiphile concentration, solids content, and oil content is studied to describe possible mechanisms that determine the final droplet size of emulsions. High volume stable emulsions are prepared using in situ surface modified alumina particles. The surface modification of particles is accomplished by adsorption of short amphiphilic carboxylic acids on the particle surface. To evaluate the interrelation between the variables and the emulsion rheology, a model from literature is applied to the experimental data. In agreement with the model, the final droplet size of emulsions is tailored by the interfacial tension of the suspension-oil interface, the viscosity of emulsions, and the shear rate during mixing. The rheological properties such as viscosity, yield stress and storage modulus, and the interfacial tension of the suspension-oil interface are controlled by adjusting the amounts of short amphiphiles, particles, and oil phase.

8.1 Introduction

Emulsions are encountered in a widespread field of applications ranging from food products and pharmaceuticals to cosmetics and petroleum products. It is therefore important to control the emulsion properties such as droplet size, long-term stability, and rheological behaviour which would enable new possibilities for further applications.

Emulsions are complex fluids that can have a flow behaviour varying from Newtonian to highly viscoelastic, non-Newtonian. Despite being comprised solely of fluids, emulsions consisting of highly concentrated droplets can possess a remarkable shear rigidity that is characteristic of a solid [1, 2]. Such emulsions exhibit a plastic-like response to shear deformations; for small deformations they resist the shear elastically, with the stress being linearly proportional to the strain; and for large deformations they yield and flow [1, 3]. The change from linear to non-linear stress-strain relationship can be characterized by a yield stress and a yield strain, which mark the departure of the macroscopic droplet structure from its initial, unsheared configuration. For stresses higher than yield stress, the emulsion flows irreversibly; creating a residual deformation. During steady shear flow, the strain rate dependence of the stress reflects the interplay of dissipative mechanisms like fluid flow and droplet rearrangements with storage mechanisms like deformation. Thus, the flow properties of concentrated emulsions depend on the packing and deformation of the droplets, and on their intrinsic elasticity [3, 4].

The elasticity of droplets and the degree of deformation were first investigated in the theoretical treatments derived by Taylor [5]. Although other alternative approaches [6, 7] have been proposed since then, the adaptation of the Taylor's theoretical approach by Welch et al. [1] is the most suitable one for particle-stabilized emulsions.

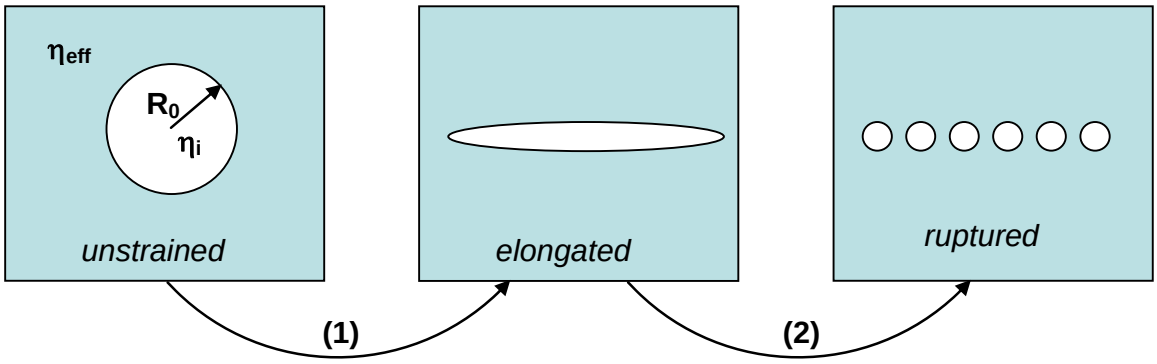

Scheme 8.1: Schematic of droplet rupture under shear.

According to this adapted Taylor model, when an undeformed spherical oil droplet as shown in Scheme 8.1 with viscosity η_i and radius R_o is sheared in a fluid (emulsion) of viscosity of η_{eff}, the droplet deforms into an ellipsoid or elongated cylinder if the applied shear stress $\eta_{eff}\dot{\gamma}$ overcomes the interfacial stress σ/R_o, where $\dot{\gamma}$ is the shear rate and σ is the interfacial tension (1). When the capillary number (Ca), the ratio between the shear stress and the interfacial stress, exceeds a critical value, Ca_{crit}, the elongated droplet will rupture into smaller droplets of average radius R (2). As shown by Taylor [5] and Grace [8], Ca_{crit} is a function of the ratio between viscosity of oil, η_i and the viscosity of emulsion, η_{eff}. Based on this adapted Taylor model, the trend in the final droplet size of emulsions (R) can be determined from Eq. 8.1 [1]:

$$R \propto Ca_{crit}\frac{\sigma}{\eta_{eff}\dot{\gamma}} \qquad \text{Eq. 8.1}$$

Using Eq. 8.1, the final droplet size can be defined directly proportional to the critical value Ca_{crit}, and the interfacial tension of oil-water interface (σ), and inversely proportional to the emulsion viscosity (η_{eff}) and shear rate ($\dot{\gamma}$).

When the maximum applied shear stress ($\eta_{eff}\dot{\gamma}$) is assumed to be equal to the yield stress (τ_{yield}) of the emulsion, Eq. 8.1 can be rewritten as

$$\tau_{Yield} = \frac{Ca_{crit}\sigma}{R} \qquad \text{Eq. 8.2}$$

and the influence of yield stress on the final droplet size can be described. Additionally, with Eq. 8.2, the elasticity of emulsions can be defined as a function of the interfacial stress (Laplace pressure, (σ/R)) of the droplet.

Here the rheological properties of particle stabilized oil-in-water emulsions such as viscosity, yield stress and storage modulus, and their dependence on amphiphile length, amphiphile concentration, solids content, and oil content are studied to describe possible mechanisms that determine the final droplet size of emulsions. High volume particle stabilized emulsions are prepared using in situ modification of alumina particles with short carboxylic acids. To evaluate the interrelation between the variables and the emulsion rheology, the Taylor model is applied to the experimental data.

8.2 Materials and methods

8.2.1 Materials

The α-alumina particles used were purchased from Sasol North America Inc. (Ceralox HPA-0.5, 99.99% Al_2O_3, Tucson, AZ, USA). They had an average particle diameter, d_{50}, of 200 nm, specific surface area of 10 m^2/g, and density of 3.98 g/cm^3. Octane (97% pure, boiling temperature T_b = 125 °C, Acros Organics, Belgium) was used as received for the preparation of the emulsions. The short carboxylic acids used for the experiments were propionic acid (99% pure, Sigma-Aldrich Chemie GmbH, Germany), butyric acid (> 99.5% (GC) pure, Fluka AG, Buchs, Switzerland), valeric acid (99% pure, Sigma-Aldrich Chemie GmbH, Germany). Double deionized water with an electrical resistance of 18 MΩcm was used in the experiments (Nanopure water system, Barnstead, USA). 2 M hydrochloric acid (HCl) and 1 M sodium hydroxide (NaOH) solutions (Titrisol, Fluka AG, Buchs, Switzerland) were used to adjust the pH.

8.2.2 Preparation of suspensions

Colloidal suspensions of 58 vol% alumina were prepared by dispersing alumina powder in double deionized water. For alumina particles to be modified with propionic acid concentrations of 131 mmol/L and higher, powders were added to aqueous solutions containing 54 mmol/L of propionic acid. In the case of other suspensions, pH was maintained at values below 5 by adding small aliquots of 2 N HCl solution.

To de-agglomerate the colloidal particles in the aqueous phase, suspensions were ball-milled in polyethylene bottles for 22 h using alumina milling balls (10 mm diameter, ball/powder weight ratio of 2.5). After ball-milling, the slurry was transferred to a glass beaker and the surface modifier, dissolved in a solution of double deionised water, and 1 N NaOH was added dropwise to the suspension. The suspension with the surface modifier was then stirred using a magnetic stirrer and the pH of the suspension was adjusted to 4.75 by adding 1 N NaOH and/or 2 N HCl dropwise.

8.2.3 Preparation and characterization of oil-in-water emulsions

Once the desired solids and amphiphile contents were set, the suspension was put in a polyethylene (PE) beaker. Emulsification was performed by vigorously stirring the suspension and the oil phase for 3 min, unless mentioned otherwise, using a household mixer at full power (Multimix 350 W, Braun, Spain). Droplet size distributions were determined by evaluating a set of at least five optical microscope images for each composition using the linear intercept method (software Lince, TU Darmstadt, Germany). Average droplet sizes and 68% confidence intervals were obtained by fitting log-normal distributions to the experimental data. Rheology measurements were performed at 25 °C using a stress-controlled rheometer (Bohlin-Rheometer CS-50, Bohlin, England) with profiled parallel-plate geometry (25 mm plate diameter). Experiments were carried out with a mechanically set gap of 1000 µm. A water trap was used to prevent evaporation during measurements. For each emulsion, measurements were performed three times. Oscillatory measurements were conducted at a constant frequency of 1 Hz by gradually increasing the maximum applied stress from 10 to 1000 Pa. Storage modulus (G') was determined by making a linear fit to the linearly decreasing part of the log G'-log shear rate curve. The yield stress was determined as the intersection point of the regression line obtained in the linearly decreasing part of the storage modulus curve and the one obtained in the linear viscoelastic regime. Steady-state experiments were carried out by progressively increasing the applied stress from 200 to 1000 Pa. For the evaluation of emulsion viscosity, the viscosity values were taken at a shear rate below the yield point where emulsion fracture does not take place [3, 4]. Hence the viscosities were determined at a shear rate of 0.0158 1/s as no yielding was observed at this point for all samples.

8.3 Results and discussion

All particle-stabilized emulsions show viscoelastic behavior with a noticeable yield stress. For small deformations, they resist the shear elastically and for larger deformations they flow irreversibly. The change from linear to non-linear character can be characterized by the yield stress. The typical example of an oil-in-water emulsion containing 35 vol% alumina particles modified with propionic acid is depicted in Figure 4.3, Chapter 4. Under steady-state conditions, emulsions stabilized with different types of the particles show a typical shear-thinning behavior with a decrease in apparent viscosity as the shear rate is increased (Figure 4.3, Chapter 4).

Table 8.1: Effect of amphiphile concentration on yield stress, storage modulus (G'), and viscosity (η_{eff}) of oil-in-water emulsions containing 72 vol% oil and aqueous suspensions of 35 vol% alumina particles at pH 4.75.

Propionic Acid (mmol/L)	Yield Stress (kPa)	G' (kPa)	η_{eff} (kPa.s)
29	0.13	2.36	8.2
87	0.23	14.48	15.8
131	0.49	48.37	70.7
180	0.43	40.44	26.9
206	0.45	33.06	26.1

Butyric Acid (mmol/L)	Yield Stress (kPa)	G' (kPa)	η_{eff} (kPa.s)
10	0.15	2.94	11.1
30	0.20	20.28	17.9
50	0.67	110.62	40.1
70	0.24	19.66	16.7
90	0.12	12.02	11.5

Valeric Acid (mmol/L)	Yield Stress (kPa)	G' (kPa)	η_{eff} (kPa.s)
10	0.21	19.21	17.0
20	0.30	42.91	17.3
25	0.40	70.83	28.0
30	0.19	29.39	15.1
40	0.21	33.31	19.1

8.3.1 Effect of amphiphile concentration

The influence of amphiphile concentration on the yield stress, storage modulus, and viscosity of oil-in-water emulsions containing 72 vol% oil and aqueous suspensions

of 35 vol% alumina particles are shown in Table 8.1 for different carboxylic acids. The emulsions exhibit the highest yield stress, storage modulus, and viscosity values at propionic acid, butyric acid, and valeric acid concentrations of 131, 50, and 25 mmol/L, respectively. For carboxylic acid concentrations lower and higher than these "optimum" amounts, the values of yield stress, storage modulus, and viscosity are decreasing.

The increase in the viscosity of emulsions with increasing amphiphile concentration below these optimum concentrations is mainly due to increased attraction forces between the particles. As the amount of amphiphiles in the initial suspension is increased, the thickness of the double layer around the particles is reduced due to the screening of the charge on the particle surface. Thus, the attractive forces are more effective than the repulsive forces, leading to higher viscosities. However, at concentrations above the optimum concentrations, the ionic strength of the external phase might decrease due to partitioning of the amphiphiles from the external phase to the oil phase, leading to a decrease in the viscosity of emulsions.

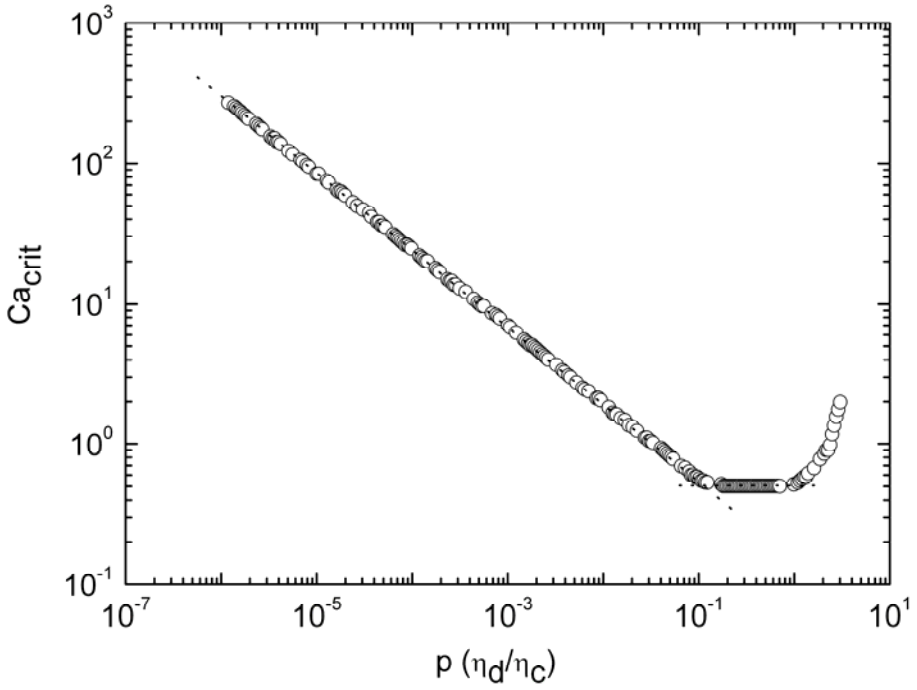

Figure 8.1: The dependence of the critical capillary number (Ca_{crit}) on the ratio (p) between the viscosity of the dispersed phase (η_d) and the viscosity of the continuous phase (η_c) based on the data obtained from the works of Grace et al. [8] and Janssen et al. [9].

According to Eq. 8.1, the final droplet size of emulsions should be proportional to the ratio $Ca_{crit}\sigma/\eta_{eff}$. Critical capillary numbers (Ca_{crit}) were calculated assuming simple shear conditions. The dependence of the Ca_{crit} values on the viscosity ratio p of the dispersed (η_d) and the continuous phase (η_c) is depicted in Figure 8.1 and was obtained based on the data from the works of Grace et al. [8] and Janssen et al. [9]. For p<0.12, the data was defined by Eq. 8.3:

$$Ca_{crit} = -0.5472\,p - 0.8029 \qquad \text{Eq. 8.3}$$

The viscosity of octane was taken as $5.42*10^{-4}$ Pas [10] and the interfacial tension values were taken from our previous work [11].

Table 8.2: Initial amphiphile concentration in the suspension, interfacial tension (σ) between octane-suspension, critical capillary number (Ca_{crit}), emulsion droplet size determined from the experiments (d_{50}, experimental) and the Taylor model (($Ca_{crit}\sigma)/\eta_{eff}$), and simplified Laplace pressure of the oil-in-water emulsions prepared with 72 vol% octane (oil to water volume ratio of 4) and 35 vol% particles in the aqueous phase (particle to water volume ratio of 0.54).

Propionic Acid (mmol/L)	σ (N/m)	Ca_{crit}	$d_{50,\,experimental}$ (μm)	$(Ca_{crit}\sigma)/\eta_{eff}$	σ/R
29	0.046	1338.16	22.69	0.0076	2058.77
87	0.041	1915.93	20.38	0.0049	1980.81
131	0.034	4350.00	11.62	0.0021	2909.29
180	0.033	2563.53	10.77	0.0032	3105.05
206	0.032	2521.53	13.35	0.0031	2430.71

Butyric Acid (mmol/L)	σ (N/m)	Ca_{crit}	$d_{50,\,experimental}$ (μm)	$(Ca_{crit}\sigma)/\eta_{eff}$	σ/R
10	0.049	1579.32	13.13	0.0070	3740.29
30	0.045	2051.33	15.94	0.0051	2808.03
50	0.041	3189.50	15.64	0.0032	2592.71
70	0.032	1974.90	15.94	0.0038	2012.55
90	0.028	1610.22	17.16	0.0039	1620.05

Valeric Acid (mmol/L)	σ (N/m)	Ca_{crit}	$d_{50,\,experimental}$ (μm)	$(Ca_{crit}\sigma)/\eta_{eff}$	σ/R
10	0.046	1994.23	19.92	0.0054	2332.00
20	0.041	2013.42	19.56	0.0047	2086.16
25	0.038	2620.38	16.43	0.0036	2337.29
30	0.031	1869.00	19.03	0.0039	1645.25
40	0.027	2125.48	15.22	0.0031	1808.30

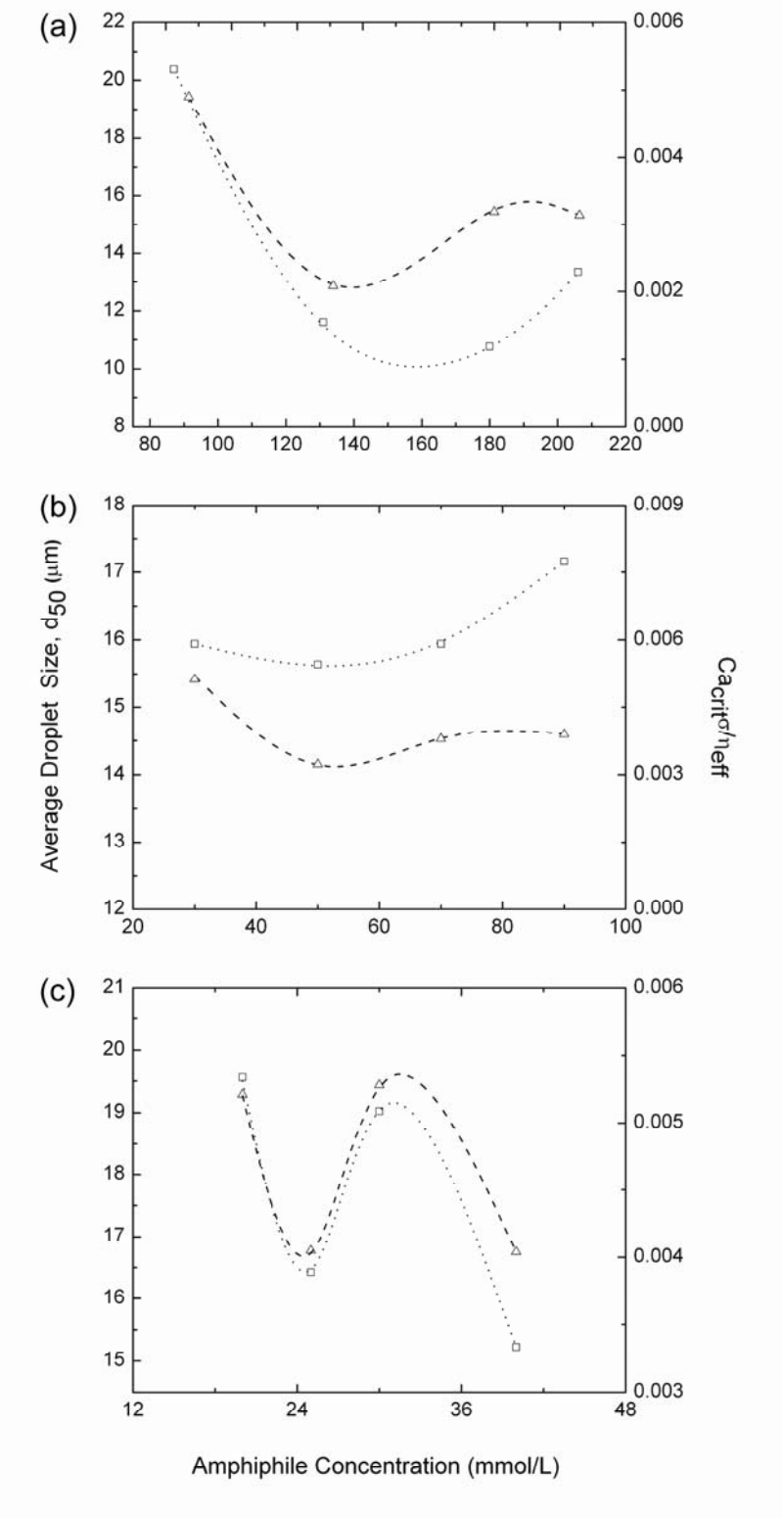

Figure 8.2 Effect of amphiphile concentration on the average droplet sizes (□) and the $(Ca_{crit}\sigma)/\eta_{eff}$ ratios (Δ) of oil-in-water emulsions prepared by mixing 72 vol% octane with 35 vol% alumina particles in situ surface modified with a) propionic acid, b) butyric acid, and c) valeric acid in the aqueous phase at pH 4.75.

The data for interfacial tension between octane-suspension, critical capillary number, and average droplet size determined from the experiments and the Taylor model for different carboxylic acid concentrations in suspensions are shown in Table 8.2. The experimentally measured droplet size, R and the calculated ratio, $Ca_{crit}\sigma/\eta_{eff}$ for emulsions with different carboxylic acids concentrations are compared in Figure 8.2. The trends in all curves demonstrate that the measured droplet sizes are consistent with the ratio $Ca_{crit}\sigma/\eta_{eff}$ for emulsions containing different amphiphile concentrations. The results show a good agreement between experimental data and theoretical predictions.

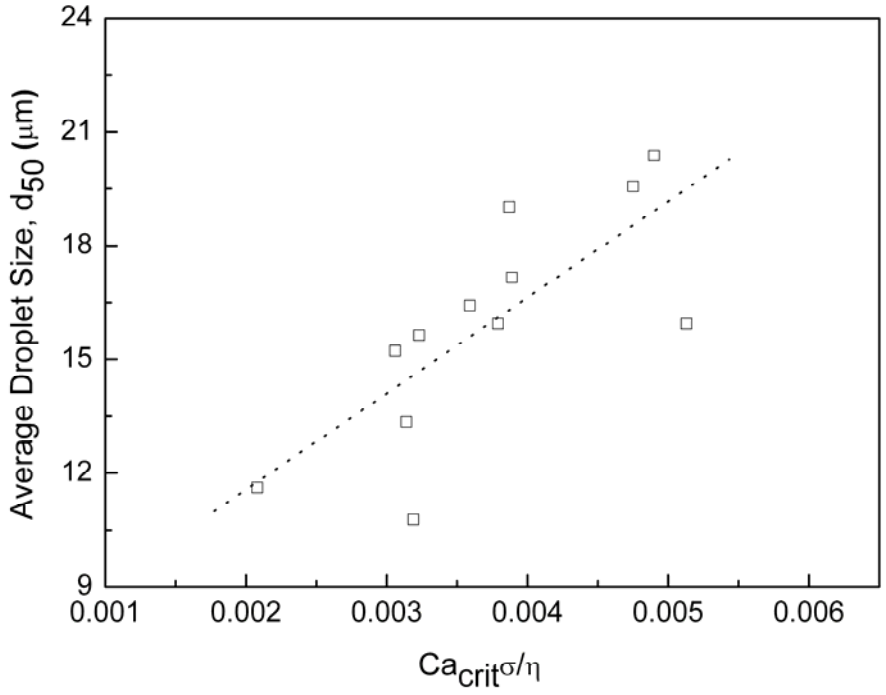

Figure 8.3: Average droplet size of oil-in-water emulsions as a function of $(Ca_{crit}\sigma)/\eta$eff ratios derived from the Taylor model for different carboxylic acids. The emulsions were prepared with 35 vol% alumina particles in the initial suspension and 72 vol% octane in the final emulsion.

The correlation between the measured final droplet size of emulsions and the calculated $Ca_{crit}\sigma/\eta_{eff}$ ratio can be demonstrated for different carboxylic acids in a master curve in Figure 8.3. The linear trend in the average droplet size-$Ca_{crit}\sigma/\eta_{eff}$ ratio curve (Figure 8.3) shows that the viscosity of the emulsions, the interfacial tension of the oil-water interface, and the critical capillary number play a significant role in

determining the final droplet size of emulsions. The average droplet size decreases with increasing emulsion viscosity and decreasing surface tension. Low critical capillary numbers also lead to much smaller emulsion droplet sizes.

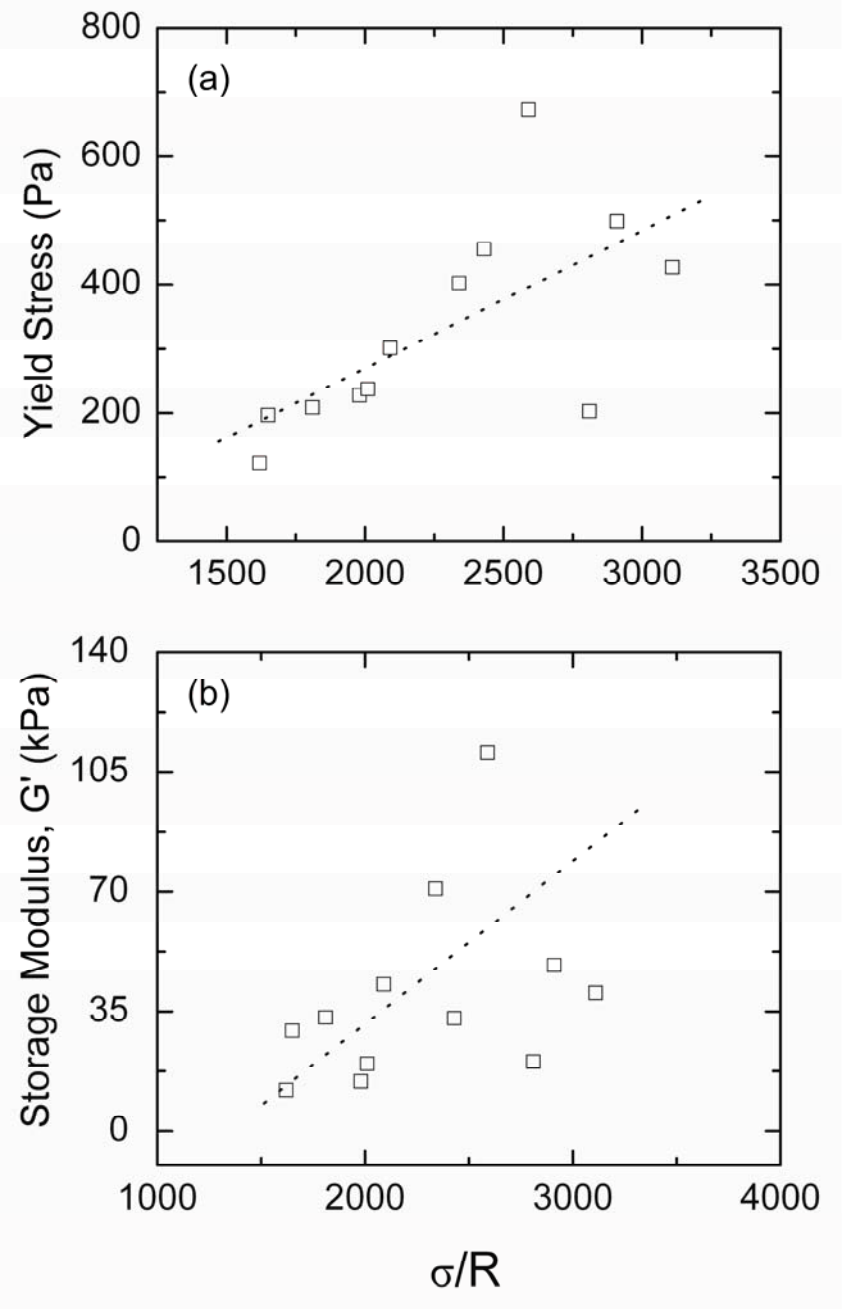

Figure 8.4: (a) Yield stress, (b) Storage modulus (G') of alumina-stabilized oil-in-water emulsions as a function of σ/R ratio derived from the Taylor model for different carboxylic acids. The emulsions were prepared with 35 vol% alumina particles in the initial suspension and 72 vol% octane in the final emulsion.

According to Eq. 8.2, the final droplet size decreases with decreasing surface tension and increasing applied yield stress of the emulsions. The experimentally measured yield stress of the emulsions containing different carboxylic acids amounts is plotted as a function of σ/R ratio derived from the Taylor model in Figure 8.4.a. The curve shows a good agreement with Eq. 8.2. High yield stresses correspond to higher σ/R ratios, which lead to much smaller droplet sizes. This consistency proves that the final droplet size of particle-stabilized emulsions can be controlled by the shearing of larger droplets during mixing.

The storage modulus of emulsions with different carboxylic acids amounts as a function of the Laplace pressure (σ/R) is shown in Figure 8.4.b. The observed scaling by the Laplace pressure confirms the essential role of the interfacial energy on the elasticity of emulsions. The storage moduli increase linearly with Laplace pressure for all carboxylic acid concentrations. At high Laplace pressures, the storage moduli increase with decreasing average droplet sizes.

Table 8.3: Effect of particle concentration on yield stress, storage modulus (G'), and viscosity (η_{eff}) of oil-in-water emulsions prepared at a fixed oil to water ratio of 4 and with a propionic acid concentration of 0.45 wt% relative to the weight of alumina at pH 4.75.

Particle Concentration (vol%)	Yield Stress (kPa)	G′ (kPa)	η_{eff} (kPa.s)
15	0.21	7.87	13.12
25	0.18	8.87	12.22
35	0.49	48.37	70.70
40	0.93	83.44	57.14

8.3.2 Effect of particle concentration

The yield stress, storage modulus, and viscosity values at different particle concentrations were investigated for oil-in-water emulsions prepared at a fixed oil to water ratio of 4 with a 0.45 wt% propionic acid. Rheological properties of octane-in-water emulsions are shown in Table 8.3 for different particle concentrations. The yield stress, storage modulus, and viscosity of emulsions increase with increasing particle amount in the initial suspension.

Table 8.4: Effect of oil content on yield stress, storage modulus (G'), and viscosity (η_{eff}) of oil-in-water emulsions prepared by mixing octane with 35 vol% alumina suspensions containing an initial propionic acid concentration of 131 mmol/L at pH 4.75. The amount of oil phase was calculated with respect to the emulsion total volume (water + particles + oil).

Oil Content (vol%)	Yield Stress (kPa)	G′ (kPa)	η_{eff} (kPa.s)
30	0.16	6.36	12.25
50	0.15	8.01	11.65
72	0.49	48.37	70.70

8.3.3 Effect of oil content

The yield stress, storage modulus, and viscosity values at different oil concentrations were investigated for oil-in-water emulsions containing 35 vol% alumina particles and 131 mmol/L propionic acid in the initial suspension, and 30, 50, and 72 vol% octane in the final emulsion. The data in Table 8.4 shows that an increase in the oil content leads to higher yield stress, storage modulus, and viscosity values for the emulsions.

8.4 Conclusions

Average droplet size of particle-stabilized emulsions is determined by the rheological behaviour of emulsions and the interfacial tension between the suspension and the oil phase. These properties are tailored by adjusting the amount of carboxylic acids, particles, and oil phase. This interrelation between the average droplet size, rheological properties, and interfacial tension is described with the Taylor model. In agreement with the model, the final droplet sizes of emulsions are adjusted by the interfacial tension of the suspension-oil interface, the viscosity of the emulsions, and the shear rate during mixing. An increase in the emulsion viscosity and a decrease in the interfacial tension lead to emulsions with smaller average droplet sizes. The emulsions with small droplet sizes exhibit higher stiffness and yield stress values.

8.5 Acknowledgment

We are very thankful to Lars Fleig for his assistance in the experimental work.

8.6 References

1. Welch, C. F., Rose, G. D., Malotky, D., Eckersley, S. T., *Rheology of high internal phase emulsions.* Langmuir, 2006, 22(4), 1544-1550.

2. Binks, B. P., Clint, J. H., Whitby, C. P., *Rheological behavior of water-in-oil emulsions stabilized by hydrophobic bentonite particles.* Langmuir, 2005, 21, 5307-5316.

3. Mason, T. G., Bibette, J., *Emulsification in viscoelastic media.* Phys. Rev. Lett., 1996, 77(16), 3481-3484.

4. Mason, T. G., Bibette, J., *Shear rupturing of droplets in complex fluids.* Langmuir, 1997, 13(17), 4600-4613.

5. Taylor, G. I., *The viscosity of a fluid containing small drops of another fluid.* Proc. Roy. Soc. London A, 1932, 138, 41-48.

6. Princen, H. M., Kiss, A. D., *Rheology of foams and highly concentrated emulsions. 4. An experimental study of the shear viscosity and yield stress of concentrated emulsions.* J. Colloid Interface Sci., 1989, 128(1), 176-187.

7. Otsubo, Y., Prudhomme, R. K., *Rheology of oil-in-water emulsions.* Rheol. Acta, 1994, 33(1), 29-37.

8. Grace, H. P., *Dispersion phenomena in high viscosity immiscible fluid systems and application of static mixers as dispersion devices in such systems.* Chem. Eng. Commun., 1982, 14, 225-277.

9. Janssen, J. M. H., Meijer, H. E. H., *Droplet breakup mechanisms-Stepwise equilibrium versus transient dispersion.* J. Rheol., 1993, 37(4), 597-608.

10. Iloukhani, H., Rezaei-Sameti, M., Basiri-Parsa, J., Azizian, S., *Studies of dynamic viscosity and Gibbs energy of activation of binary mixtures of methylcyclohexane with n-alkanes (C5-C10) at various temperatures.* J. Mol. Liquids, 2006, 126, 117-123.

11. Akartuna, I., Studart, A. R., Tervoort, E., Gonzenbach, U. T., Gauckler, L. J., *Stabilization of oil-in-water emulsions by colloidal particles modified with short amphiphiles.* Langmuir, 2008, 24(14), 7161-7168.

9 Conclusions

A simple and general approach is developed for the preparation of stable particle-stabilized emulsions through the in situ surface modification of a high concentration of particles with different surface chemistries and for the application of these emulsions as templates to fabricate colloidal capsules and macroporous materials.

Oil-in-water and water-in-oil emulsions are formed using colloidal inorganic particles that are in situ surface hydrophobized through the adsorption of short amphiphiles. The high solubility and critical micelle concentrations of short amphiphiles in liquid phases allow the in situ surface hydrophobization of high concentration of initially hydrophilic particles. The type of the emulsions is determined by the original location of the particles prior to emulsification. The continuous phase of the emulsions is comprised of the liquid in which the particles are originally dispersed and surface modified. The microstructure of the particle-stabilized emulsions is tailored by adjusting the composition of the initial suspensions and the amount of the dispersed phase. Droplet size distributions and average droplet sizes of particle-stabilized emulsions are determined by the rheological behaviour of emulsions and the interfacial tension between the suspension and the oil phase. An increase in the emulsion viscosity and a decrease in the interfacial tension lead to emulsions with smaller average droplet sizes. Preparation of emulsions using this new approach enables the long-term stability of emulsions. For instance, octane-in-water emulsions containing alumina particles surface hydrophobized with short carboxylic acids show remarkable stability against coalescence, Ostwald ripening, and creaming for more than two years after emulsification.

The particle-stabilized emulsions exhibit viscoelastic behavior with a high yield stress. The liquid-like behavior at stresses higher than the yield stress enables the injection or the deposition of the emulsions into molds or onto substrates using conventional technologies such as injection molding, extrusion, robocasting, ink-jet printing, and screen-printing. The elastic behavior obtained when the stresses are ceased after deposition allows for the emulsion to keep its shape without requiring any

further gelation or strengthening reaction. Furthermore, slight dilution of the emulsions with the continuous phase enables the preparation of fluid emulsions that can be easily poured or used for dip coating, spin coating, or spray deposition on substrates.

The long-term stability of emulsions also allows the fabrication of colloidal capsules that can be interesting for the encapsulation and delivery of active agents in food processing, pharmaceutical and agricultural industries, and biomedicine. Dilution of wet emulsions leads to large number of wet colloidal capsules, which can be further dried to harvest single inorganic hollow capsules. The structural rigidity of the capsules is achieved by the close-packed particle shell surrounding each droplet. The permeability of the inorganic capsules is defined by the interstices between the particles and is controlled by the size of the particles at the interface. Stabilization of the particle shells through the adsorption of polyelectrolytes to the capsule outer shell further allows for the fine tuning of the capsule permeability and results in hollow capsules with rigid walls.

In addition to the high stability of emulsions, their viscoelastic behavior allows the processing of particle-stabilized emulsions into porous structures of various shapes and chemical compositions. The microstructure and the porosity of macroporous ceramics are tailored from homogeneous to hierarchical pore structures by changing the oil content in the initial emulsions. This variation in the pore structure and porosity is attained upon incorporation of air bubbles into the matrix of oil droplets during shearing of the particle-oil-water mixtures. Sintering of such mixtures result in macroporous structures with pore distributions at length scales differing by one order of magnitude. The sintered porous ceramics exhibit either completely closed pores or pores with interconnectivity. The interconnectivity in the pore structure is adjusted by changing the type of the inorganic particles or the amount of particles in the original suspension. Moreover, tuning the microstructure of the porous ceramics allows porosities within the range of 72%–96% and mechanical strength levels between 1-13 MPa.

The use of colloidal polymeric particles instead of inorganic particles leads to preparation of stable water-in-oil emulsions and macroporous polymers in the absence of any chemical reaction. The adsorption of polymeric particles at the oil-water interface is accomplished by slightly reducing the wettability of the particles in the oil continuous phase where they are initially dispersed. The high stability of the wet

polymeric emulsions also allows the harvesting of single hollow microcapsules composed of close-packed shells of polymeric particles.

The method described in this thesis can be applied for the stabilization of emulsions with a large variety of metal oxide and polymeric particles as well as metallic particles. This versatile approach should thus allow for the preparation of stable emulsions that can be of interest in a variety of applications, including materials manufacturing, food, cosmetics, and pharmaceutical and agricultural products. Macroporous materials fabricated by this approach can be attractive as low-weight structural components, porous media for chemical and biological separation, thermal and electrical insulating materials, catalyst supports, refractory filters for gases, electrets and scaffolds for tissue engineering, and medical implants or vehicles for encapsulation and delivery of active agents.

10 Outlook

10.1 Monosized particle-stabilized emulsions

Emulsions are important in a variety of applications, ranging from food and pharmaceuticals to cosmetics and materials manufacturing. In contrast to surfactant-stabilized emulsions, stabilization of the emulsions with colloidal particles leads to the enhanced stability of emulsions. However, emulsions stabilized by particles often exhibit highly polydisperse droplet size distributions. Their polydispersity limits their use in applications that require precise control over the cell size.

Uniformity (monodispersity) in the droplet size distribution is one of the main challenges in emulsion production. So far, the most viable method has been the Fractionation procedure developed by Bibette [1]. But, this method was originally developed for surfactant-stabilized emulsions and requires repeated fractionation of emulsions. The other alternative methods are the membrane extrusion and microfluidic devices. However, these methods are not appropriate for mass production. There is no general and simple method for producing monosized particle-stabilized emulsions. Precise control over the cell size distribution can enable fabrication of macroporous materials for applications such as catalytic surfaces and supports, adsorbents, chromatographic materials, filters, light-weight structural materials, and thermal, acoustic and electrical insulators, and capsules for the delivery and release of active materials. Thus, a new and simple method for the production of monosized particle-stabilized emulsions that could be easily applied to different types of emulsions would be highly desirable.

10.2 Open porous materials

One of the main of objectives of this thesis was developing a simple and versatile approach to produce macroporous ceramics of various shapes and chemical compositions. As described in previous chapters, the emulsion templating method has allowed tailoring the microstructure and porosity of the porous components in a single step process. Macroporous ceramics produced from emulsion templates exhibit mainly

closed pore structures due to the coating of the emulsion droplet surface with particles. The windows and the pore interconnectivity were achieved by changing the type of the inorganic particles used and the amount of particles in the original emulsions.

In addition to these closed and interconnected pore structures; it will be also interesting to produce ceramics with open pore microstructures. Open pore structures have become very attractive as catalyst supports, filters for gases and molten metals, and scaffolds for tissue engineering and medical implants materials. To obtain materials with open pores, one possibility can be using less concentration of surface modified inorganic particles together with polymeric particles in the original suspension. The non-adsorbed short amphiphiles present in the suspension might decrease the interfacial tension of the oil-water interface and thus induce the adsorption of polymeric particles at the interface. The inorganic particles in the continuous phase of the emulsions might form the three dimensional particle networks. Adjusting the ratio between the polymeric and inorganic particles might allow controlling the size of the openings in the pores of the sintered emulsions.

Alternatively, open pore ceramics can be produced from polymer emulsions loaded with colloidal inorganic particles. Water-in-oil emulsions stabilized with polymeric particles can be additionally loaded with inorganic particles. Due to the high stability of the particle-stabilized emulsions, such emulsions can be dried and sintered without any chemical reactions. During sintering, the polymeric particles coating the emulsion droplets and present in the continuous phase can be burned away, leaving behind open pores, while the inorganic particles in the continuous phase of the emulsion can form the three dimensional inorganic matrix as a result of densification.

10.3 Functional colloidal capsules

In chapter 7 of this thesis, a method for producing colloidal inorganic capsules from particle-stabilized emulsions is described. As a follow up for this chapter, the release of these inorganic capsules can be investigated and the properties of the capsules can be further adjusted based on the possible potential applications.

10.3.1 Possible Release Mechanisms

Functional inorganic capsules described in this thesis can be very attractive materials for the encapsulation of active molecules due to various possible release mechanisms that can be selected depending on each specific application.

The interstitial pores between the particles forming the capsule shell and the possibility of tuning the pore size by locking the particles via adsorption of polyelectrolytes can allow for sustained release through the controlled pores. In the case of wet capsules, the selective permeability through the interstitial pores can be achieved by removing the interface between the dispersed and the continuous phase either via co-solvent addition or centrifugation [2]. Reducing the pore size upon decreasing the particle size or increasing the concentration of the polyelectrolyte, or coating the polyelectrolyte layer with smaller particles could help to control the permeability and release through the particle shells.

Alternatively, the elasticity of the capsule shells can allow for controlled release triggered by mechanical load or shear stress. Increasing the elasticity of the capsule shells by adsorbing polyelectrolytes can increase the capsule resilience and help to withstand much higher stresses. Moreover, using colloidal particles with different deformation characteristics, brittle or plastic rupture, can further control the response of the capsules to shear stresses.

The use of colloidal particles and polyelectrolytes for the formation of the capsule shells can also provide additional release strategies. For instance, by changing the ionic strength the permeability through the polyelectrolyte layer can be finely tuned. As described in previous studies [3, 4], increasing the ionic strength leads to increased permeability and release rate of the polyelectrolyte layers as a result of the weakening of the electrostatic interactions between the polyelectrolyte molecules in the presence of salt ions, whereas decreasing the amount of salt ions reverses the condition, making them less permeable again. Similarly, the permeability and the release of the capsules can be adjusted by changing the pH. At pH values where the interactions between the polyelectrolyte molecules or between the polyelectrolyte and the underlying particle shell, or between the interfacially adsorbed particles and the surface modifiers on the particle surfaces are expected to be less favorable, the permeability of the capsule walls can be increased [3, 4]. At completely unfavorable pH conditions, the release can be achieved upon destabilization of the capsule wall.

Alternatively, addition of charged molecules either inside the capsules or to the outside solution can create an internal/external osmotic pressure which can trigger the deflation and collapse of the capsules [3, 5].

Additionally, the release in the case of magnetic capsules comprised of iron oxide particle shells can be triggered upon application of external magnetic field. As previously shown [6], an increase in the applied magnetic field can induce destabilization of the capsules, which could then provide controlled release of the encapsulated molecules.

As an alternative to the stimuli responsive release mechanisms, the release of the inorganic capsules can be further controlled by adsorbing self-degradable polyelectrolytes to strengthen the capsule wall [4]. The use of biodegradable polyelectrolytes that can degrade in vivo can open up new possibilities for biomedical applications of the inorganic capsules.

10.3.2 Potential Applications

This simple and flexible approach described here can be easily applied to a wide variety of other metal oxide particles. Owing to their controllable permeability and elasticity, inorganic capsules can be used for the encapsulation of active agents such as drugs, proteins, vitamins, nutrients, flavors, fragrances, and pesticides. The use of inorganic particles to form the capsule shells can bring additional advantages compared to polymeric capsules. In applications where the encapsulated molecules should be protected against harsh conditions such as high temperatures and corrosive environments, inorganic particle shells can serve as inert, rigid shields isolating the encapsulated molecule from the capsule environment. Thus, inorganic capsules can prevent degradation or loss of the encapsulated agents during processing, delivery, and storage and provide improved handling [7-9].

Inorganic capsules encapsulating active agents can be of interest as potential vehicles for drug and vaccine delivery [10]. They can address a variety of needs for both oral [11, 12] and pulmonary drug delivery [13]. For instance, in the case of dry capsules ($d > 1\ \mu m$), the low mass density attained as a result of the capsule porosity can permit efficient aerosolization and increased bioavailability of therapeutics, making the porous capsules attractive carriers for inhalation therapies [13-16]. The sustained or controlled release of the therapeutic agents encapsulated by the inhaled or orally administered

capsules can occur either through the controlled pores or in response to external stimuli such as an electric or magnetic field or mechanical load, or to changes in the capsule environment (pH, ionic strength, internal/external osmotic pressure). Furthermore, direct specific targeting to tissues or antigen-presenting cells can be achieved by conjugating a targeting ligand or an antibody on the capsule surface [12, 17].

Additionally, the chemical inertness and the nontoxic character of the inorganic particle shells could allow for the viability of capsules as bioreactors [7, 18]. Immobilization of cells, hormones, enzymes, and antibodies inside the inorganic capsules can provide better protection and handling of biomolecules in various bioprocesses [7].

Another important application possibility for inorganic capsules can be radiotherapy and hyperthermia treatments for cancer. Capsules with iron oxide particle shells can be useful as thermoseeds for inducing hyperthermia in cancers. Once they are injected into tumors, they can heat the cancerous cells locally by the hysteresis loss under an alternating applied magnetic field [19-21]. Similarly, formation of capsule shells from a radioactive material can also allow for the production of radioactive microcapsules that could be used to in situ irradiate the cancerous cells during radiotherapy of cancer [19].

Dry inorganic capsules with their structural rigidity can also become attractive materials for powder processing. The choice of different inorganic particles and the controllable pore structure of the dry hollow capsules can enable the production of porous granules and particles in different size ranges. Moreover, these porous particles can be further used for the consolidation of bulk porous materials [22] which might be used as thermal or acoustic insulators, catalytic supports, filters, separation membranes, scaffolds for tissue engineering, and porous electrodes for fuel cells.

10.4 References

1. Bibette, J., *Depletion interactions and fractionated crystallization for polydisperse emulsion purification*. J. Colloid Interface Sci., 1991, 147(2), 474-478.

2. Hsu, M. F., Nikolaides, M. G., Dinsmore, A. D., Bausch, A. R., Gordon, V. D., Chen, X., Hutchinson, J. W., Weitz, D. A., Marquez, M., *Self-assembled shells composed of colloidal particles: Fabrication and characterization*. Langmuir, 2005, 21, 2963-2970.

3. Peyratout, C. S., Dähne, L., *Tailor-made polyelectrolyte microcapsules: From multilayers to smart containers*. Angew. Chem. Int. Ed., 2004, 43(29), 3762-3783.

4. De Geest, B. G., Sanders, N. N., Sukhorukov, G. B., Demeester, J., De Smedt, S. C., *Release mechanisms for polyelectrolyte capsules*. Chem. Soc. Rev., 2007, 36(4), 636-649.

5. Gordon, V. D., Chen, X., Hutchinson, J. W., Bausch, A. R., Marquez, M., Weitz, D. A., *Self-assembled polymer membrane capsules inflated by osmotic pressure*. J. Am. Chem. Soc., 2004, 126, 14117-14122.

6. Melle, S., Lask, M., Fuller, G. G., *Pickering emulsions with controllable stability*. Langmuir, 2005, 21, 2158-2162.

7. Park, J. K., Chang, H. N., *Microencapsulation of microbial cells*. Biotechnol. Adv., 2000, 18(4), 303-319.

8. Madene, A., Jacquot, M., Scher, J., Desobry, S., *Flavour encapsulation and controlled release - a review*. Int. J. Food Sci. Technol., 2006, 41(1), 1-21.

9. Tsuji, K., *Microencapsulation of pesticides and their improved handling safety*. J. Microencapsulation, 2001, 18(2), 137 - 147.

10. Hanes, J., Cleland, J. L., Langer, R., *New advances in microsphere-based single-dose vaccines*. Adv. Drug Deliv. Rev., 1997, 28(1), 97-119.

11. Desai, M. P., Labhasetwar, V., Amidon, G. L., Levy, R. J., *Gastrointestinal uptake of biodegradable microparticles: Effect of particle size*. Pharm. Res., 1996, 13(12), 1838-1845.

12. Keegan, M. E., Whittum-Hudson, J. A., Saltzman, W. M., *Biomimetic design in microparticulate vaccines*. Biomaterials, 2003, 24, 4435-4443.

13. Edwards, D. A., Hanes, J., Caponetti, G., Hrkach, J., Ben-Jebria, A., Eskew, M. L., Mintzes, J., Deaver, D., Lotan, N., Langer, R., *Large porous particles for pulmonary drug delivery*. Science, 1997, 276(5320), 1868-1872.

14. Service, R. F., *Biomedicine: Drug delivery takes a deep breath*. Science, 1997, 277(5330), 1199-1200.

15. Tsapis, N., Bennett, D., Jackson, B., Weitz, D. A., Edwards, D. A., *Trojan particles: Large porous carriers of nanoparticles for drug delivery*. Proc. Natl. Acad. Sci. U. S. A., 2002, 99(19), 12001-12005.

16. Tsapis, N., Bennett, D., O'Driscoll, K., Shea, K., Lipp, M. M., Fu, K., Clarke, R. W., Deaver, D., Yamins, D., Wright, J., Peloquin, C. A., Weitz, D. A., Edwards, D. A., *Direct lung delivery of para-aminosalicylic acid by aerosol particles*. Tuberculosis, 2003, 83, 379-385.

17. Wang, X., Yang, L., Chen, Z., Shin, D. M., *Application of nanotechnology in cancer therapy and imaging*. CA Cancer J Clin, 2008, 58(2), 97-110.

18. Dinsmore, A. D., Hsu, M. F., Nikolaides, M. G., Marquez, M., Bausch, A. R., Weitz, D. A., *Colloidosomes: Selectively permeable capsules composed of colloidal particles*. Science, 2002, 298, 1006-1009.

19. Kawashita, M., *Ceramic microspheres for biomedical applications*. Int. J. Appl. Ceram. Technol., 2005, 2(3), 173-183.

20. Kawashita, M., Tanaka, M., Kokubo, T., Inoue, Y., Yao, T., Hamada, S., Shinjo, T., *Preparation of ferrimagnetic magnetite microspheres for in situ hyperthermic treatment of cancer*. Biomaterials, 2005, 26(15), 2231-2238.

21. Kawashita, M., Domi, S., Saito, Y., Aoki, M., Ebisawa, Y., Kokubo, T., Saito, T., Takano, M., Araki, N., Hiraoka, M., *In vitro heat generation by ferrimagnetic maghemite microspheres for hyperthermic treatment of cancer under an alternating magnetic field*. J. Mater. Sci.: Mater. Med., 2008, 19(5), 1897-1903.

22. Grader, G., Shter, G., *Method for preparation of bulk shaped foam articles*. USP 6.869.563 B2, 2005.

11 Appendix

This chapter entails the additional graphs, tables, and information from the previous chapters.

11.1 Stabilization of oil-in-water emulsions by colloidal particles modified with short amphiphiles

11.1.1 Particle characterization

The particle size of the investigated powders was characterized by scanning electron microscopy (SEM; LEO 1530, LEO, Oberkochen, Germany) and X-ray disc centrifuge sedigraph (XDC; Brookhaven Instruments Corp., Holtsville, NY, USA). The specific surface area was determined using a Brunauer-Emmett-Teller (BET) gas-adsorption apparatus (Nova 1000, Quantachrome, Odelzhausen, Germany). The isoelectric points (IEP) of the particles were measured using the electroacoustic colloidal vibration technique [1] (DT-1200, Dispersion Technology, Inc., Mount Kisco, NY, USA). Isoelectric points at pH values 9, 9.2, 1.5, and 7.8 were obtained for the α-Al_2O_3, δ-Al_2O_3, SiO_2, and Fe_3O_4 powders, respectively.

11.1.2 Confocal laser scanning microscopy

Fluorescent silica particles and the amphiphile hexyl amine were used for the confocal laser scanning microscopy images. Fluorescently-labeled silica particles (d_{50} ~ 500 nm) were synthesized following the procedure described by van Blaaderen and Vrij [2]. The final particles consisted of a silica core of approximately 400 nm, a fluorescent layer around the core of about 10 nm and an outer silica rim of 100 nm. Concentrated emulsions were prepared by mixing octane and a 30 vol% silica suspension containing 50 mmol/L of hexyl amine. Emulsification was carried out at pH 10.2 using a hand mixer (Bodum Schiuma 3040, Bodum AG, Switzerland). Oil droplets covered with silica particles were obtained by diluting 20× the initial concentrated emulsions with water.

The silica-coated droplets could be easily harvested for imaging in the confocal laser scanning microscope (Zeiss, LSM 510, Germany). To improve the quality of the optical images, the oil droplets were immobilized by gelling the continuous aqueous phase via the free radical polymerization of methoxy polyethylene glycol monomethacrylate using the initiator ammonium persulphate and the catalyst N,N,N',N'-tetramethylethylenediamine, as described elsewhere in the literature [3].

11.1.3 Determination of the partition coefficient of short carboxylic acids between water and octane

The partition of amphiphiles between two immiscible liquid phases occurs when the molecules are soluble in both liquids, as is the case for carboxylic acids in octane-water mixtures. At equilibrium, the ratio between the concentration of molecules in the oil and the aqueous phases ($C_{oil}^{eq}/C_{H_2O}^{eq}$) is equal to the solubility ratio of these molecules in the respective phases (S_{oil}/S_{H_2O}). The solubility ratio S_{oil}/S_{H_2O} is usually referred to as the partition coefficient, K_p.

To calculate K_p, aqueous solutions of short amphiphiles (100 mL) were gently mixed with an equal volume of octane (100 mL) for 24 h using a magnetic stirrer to avoid vortex mixing. After partitioning the aqueous amphiphile solutions were titrated with 0.05 N KOH solution and the partition coefficient was calculated from the relation

$$K_P = \frac{1}{Q}\left(\frac{C_{H_2O}^{i}}{C_{H_2O}^{eq}} - 1\right) \qquad \text{Eq. 11.1}$$

where Q is the ratio between the volume of oil and water (V_{oil}/V_{H_2O}), $C_{H_2O}^{i}$ is the initial concentration of amphiphiles in water and $C_{H_2O}^{eq}$ is the concentration of amphiphiles in the aqueous phase after equilibration with octane. The K_p value was determined by taking the average partition coefficient for a series of experiments at different amphiphile concentrations.

11.1.4 Partition of amphiphiles during emulsification

On the basis of Eq. 11.1, one can estimate the final equilibrium concentration of molecules in the aqueous phase ($C^{eq}_{H_2O}$), as follows [4]:

$$K_P = \frac{1}{Q}\left(\frac{C^{i}_{H_2O}}{C^{eq}_{H_2O}} - 1\right) \qquad \text{Eq. 11.2}$$

Using Eq. 11.2, we estimated the amount of free amphiphiles transferred from the initial suspensions to the oil phase in the oil-in-water emulsions prepared in this study. For these calculations, we used the experimentally obtained partition coefficients of 0.173, 0.310, and 0.880 for propionic, butyric, and valeric acids. The results of the calculations are displayed in Table 11.1 for initial amphiphile concentrations (C_{add}) within the range required for emulsification of mixtures containing 72 vol% octane prepared from 35 vol% alumina suspensions.

The free amphiphile concentration initially present in the aqueous phase ($C^{i}_{H_2O}$) was estimated from previously published data on the adsorption behavior of carboxylic acids on alumina surfaces (Γ in Table 11.1) [5]. In these calculations, we also assumed that the amounts of amphiphile adsorbed at the oil-water interface and desorbed from the particle surface during partition are negligible compared to the amphiphile concentration in the bulk phases.

Table 11.1: Estimated equilibrium concentrations of free amphiphiles in the octane (C^{eq}_{Oil}) and aqueous phases ($C^{eq}_{H_2O}$) for mixtures containing 72 vol% octane prepared from 35 vol% alumina aqueous suspensions. C_{Added}, Γ, C_{ads}, $C^{i}_{H_2O}$ and f_{diff} are the concentration of amphiphiles initially added to the suspension, the amount of amphiphiles adsorbed on the alumina surface per unit surface area [5], the concentration of amphiphiles initially present in water that adsorb on the alumina surface, the initial concentration of free amphiphiles left in the aqueous phase after surface adsorption ($C_{Added} - C_{Ads}$), and the fraction of amphiphiles initially present in the aqueous phase that diffuses into the oil, respectively. Under emulsification conditions, the initial concentration of amphiphiles in octane (C^{i}_{Oil}) is null.

C_{Added} (mM)	Surface Coverage, Γ ($\mu mol/m^2$)	C_{Ads} (mM)	Free Amphiphiles			
			$C^{i}_{H_2O}$ (mM)	$C^{eq}_{H_2O}$ (mM)	C^{eq}_{Oil} (mM)	f_{diff}
Propionic acid						
29	1.21	25.93	3.07	1.81	1.26	
87	2.90	62.15	24.85	14.69	10.16	
131	3.50	75.01	55.99	33.09	22.90	0.41
180	3.80	81.44	98.56	58.25	40.31	
206	3.90	83.58	122.42	72.35	50.07	
Butyric acid						
10	0.41	8.79	1.21	0.54	0.67	
30	1.12	24.00	6.00	2.68	3.32	
50	1.75	37.50	12.50	5.58	6.92	0.55
70	2.17	46.50	23.50	10.49	13.01	
90	2.49	53.36	36.64	16.36	20.28	
Valeric acid						
10	0.45	9.64	0.36	0.08	0.28	
20	0.80	17.14	2.86	0.63	2.23	
25	0.95	20.36	4.64	1.02	3.62	0.78
30	1.01	21.65	8.35	1.84	6.52	
40	1.41	30.22	9.78	2.15	7.63	

11.1.5 Partition of amphiphiles during interfacial tension measurements

The equilibrium concentration of amphiphiles after partition between immiscible phases depends strongly on the oil to water volume ratio of the mixture (Q), as indicated in Eq. 11.2. The oil-in-water emulsions investigated in this work (72 vol% oil) have a Q ratio of 4. In contrast, the Q ratios that can be achieved in the pendant drop

technique used for the interfacial tension measurements are typically at least two orders of magnitude higher than that of the oil-in-water emulsions. As a result of such higher *Q* values, diffusion of free amphiphiles from the alumina suspensions towards the oil phase is markedly stronger during the interfacial tension measurements than during the emulsification process. For a *Q* ratio of 1133 used here for the interfacial tension analysis of alumina suspensions, more than 99.5, 99.7, and 99.9 % of the free amphiphiles initially present in the aqueous phase are transferred to the oil phase during measurements with propionic, butyric, and valeric acids, respectively. This contrasts with the fractions of, respectively, 41, 55, and 78 % expected for these molecules during the emulsification process (*Q* = 4).

To reduce the strong partition effect that occurs during the interfacial tension analysis and thus reproduce the conditions encountered during the emulsification process, we deliberately added amphiphiles to the oil phase prior to the pendant drop measurements so that the fraction of free molecules that diffuse towards the oil phase is the same as that observed during emulsification. The concentration of amphiphiles initially added to the oil phase to obtain such conditions (C_{Oil}^{i}) was estimated based on the *Q* ratio used in the interfacial tension analysis, the amphiphile partition coefficient K_p, the initial concentration of amphiphiles in the aqueous phase $C_{H_2O}^{i}$ and the equilibrium concentration of amphiphiles in the aqueous phase under emulsification conditions ($C_{H_2O}^{eq}$ in Table 11.1). Taking into account mass conservation during partition, one can estimate the concentration C_{Oil}^{i} needed to achieve an equilibrium concentration $C_{H_2O}^{eq}$ in the aqueous phase, as follows:

$$C_{Oil}^{i} = \frac{C_{H_2O}^{eq}\left(K_p Q + 1\right) - C_{H_2O}^{i}}{Q} \qquad \text{Eq. 11.3}$$

The above equation reduces to Eq. 11.2 when no amphiphile is initially present in the oil phase ($C_{Oil}^{i} = 0$), as is the case for the real emulsions.

The amphiphile concentrations, C_{Oil}^{i}, added to the oil phase before the interfacial tension measurements were obtained from Eq. 11.3 taking into account the *Q* ratios used for the interfacial tension measurements with amphiphile aqueous solutions (*Q* = 486) and amphiphile-containing alumina suspensions (*Q* = 1133). Using

this procedure, we were able to characterize the oil-water interfacial tension under the same conditions given in the emulsification process.

Table 11.2: Parameters of the log-normal probability density function (Eq. 2.1, Chapter 2) used to describe the droplet size distributions of emulsions obtained after different mixing times. Emulsions were prepared with 72 vol% octane, 40 vol% alumina particles in the aqueous phase and 0.45 wt% propionic acid relative to the weight of alumina at pH 4.75.

	Mixing time (min)		
	1	***2***	***3***
N^{ber} of peaks	1	1	1
d_c (μm)	19.8	7.9	7.0
σ	0.64	0.36	0.32
A	1	1	1
68 % confidence interval (μm)	10.4 – 37.5	5.5 – 11.3	5.1 – 9.6

11.1.6 Effect of mixing time on the emulsion microstructure

The effect of mixing time on the emulsion droplet size distribution was investigated on emulsions containing 72 vol% oil, 40 vol% alumina in the aqueous suspensions and 0.45 wt% propionic acid relative to the weight of alumina. Figure 11.1 and Table 11.2 show that the emulsion droplet size distribution is noticeably narrowed and the average droplet size is decreased by increasing the mixing time up to 2 min. No significant difference in the droplet size distributions were observed between emulsions prepared after 2 and 3 min of mixing. A similar behavior was observed for other emulsions prepared at the conditions indicated in the emulsification region of Figure 2.5 (see Chapter 2). Therefore, a standard mixing time of 3 min was used for the emulsification of most of the compositions evaluated in this study. Emulsions prepared using too short amphiphiles or with insufficient amphiphile concentrations required

more time for complete emulsification. These compositions are indicated by the open symbols in Figure 2.5 of Chapter 2.

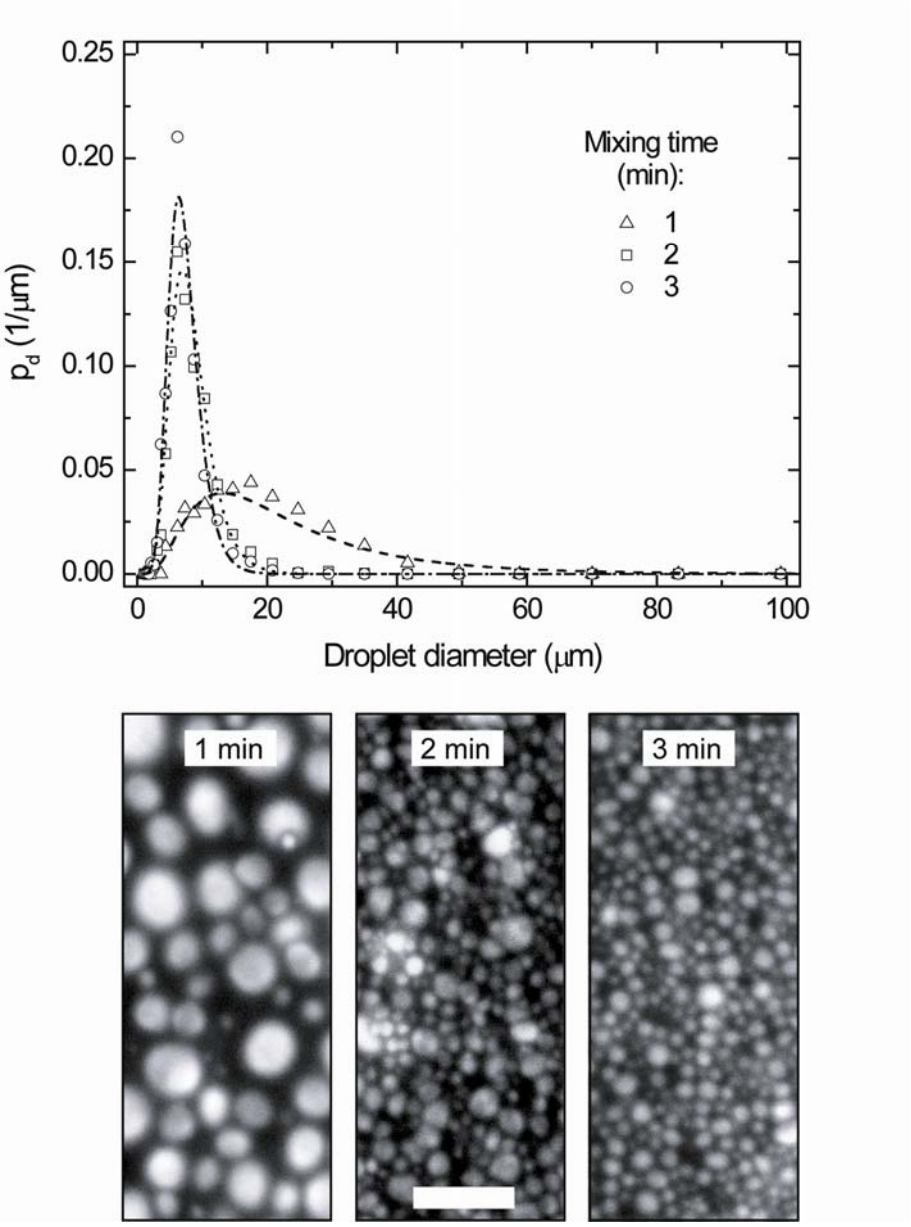

Figure 11.1: Droplet size distributions (top) and optical microscope images (bottom) of oil-in-water emulsions obtained after different mixing times. Emulsions were prepared with 72 vol% octane, 40 vol% alumina particles in the aqueous phase and 0.45 wt% propionic acid relative to the weight of alumina at pH 4.75. The continuous lines correspond to the probability density functions used to describe the droplet size distributions. Scale bar: 50 μm.

11.2 Simple and double emulsions stabilized by colloidal particles and short amphiphiles

11.2.1 Additional graphs

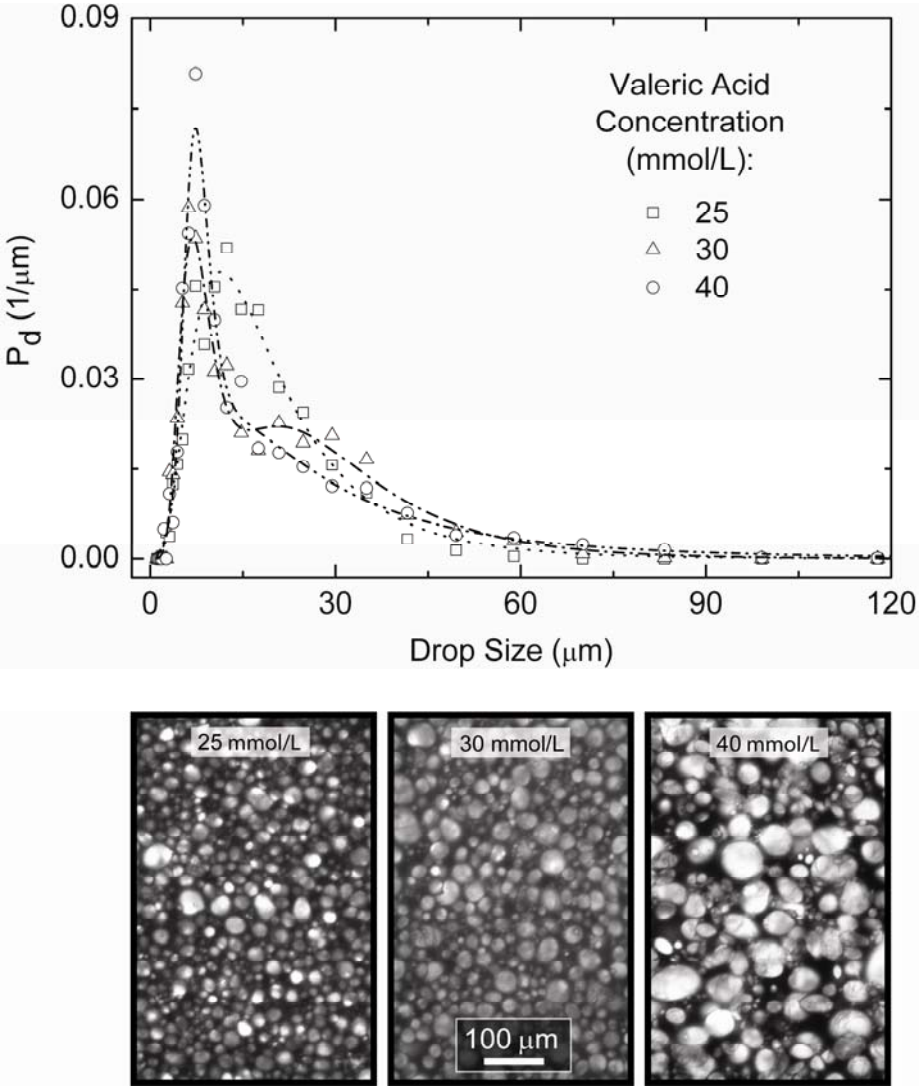

Figure 11.2: Droplet size distributions (top) and optical microscope images (bottom) of oil-in-water emulsions prepared with α-alumina particles and different concentrations of valeric acid. Emulsions were prepared with 72 vol% octane and 35 vol% particles in the aqueous phase at pH 4.75.

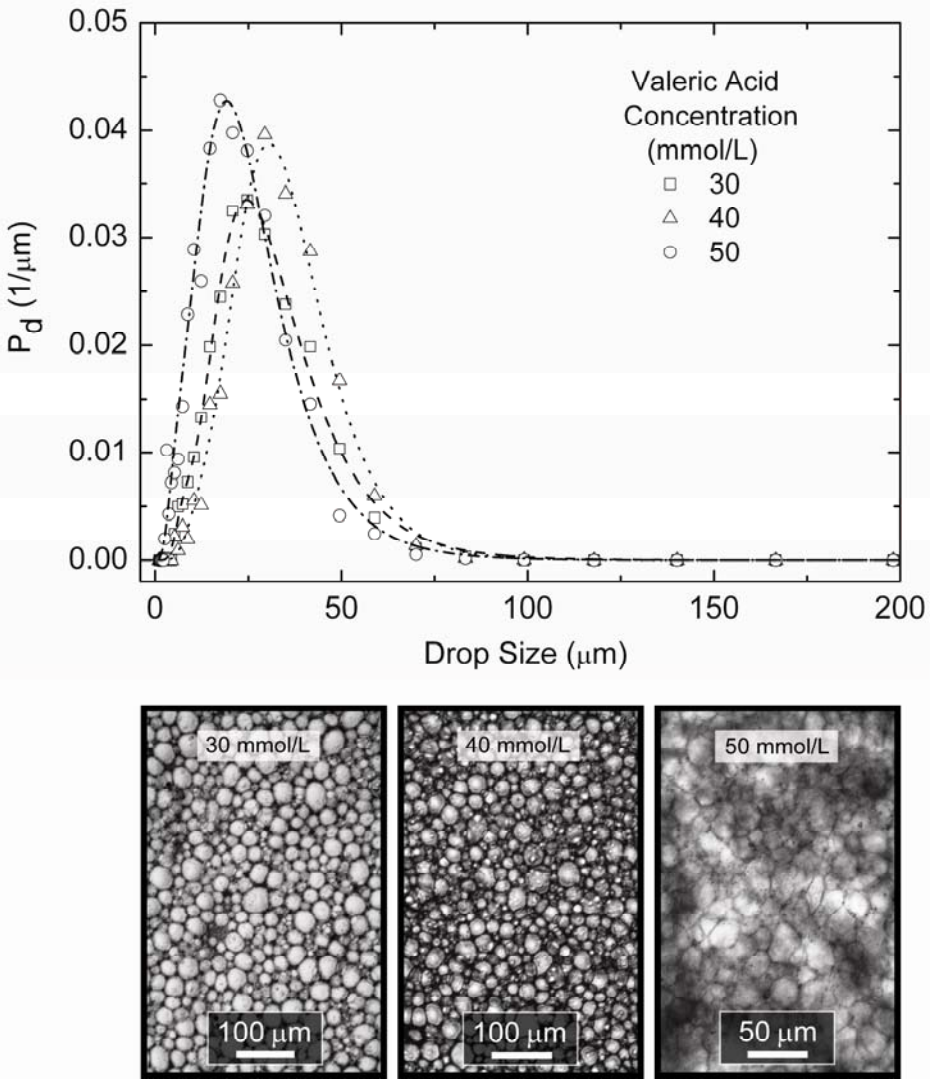

Figure 11.3: . Droplet size distributions (top) and optical microscope images (bottom) of oil-in-water emulsions prepared with δ-alumina particles and different concentrations of valeric acid. Emulsions were prepared with 81.9 vol% octane and 20 vol% particles in the aqueous phase at pH 4.75.

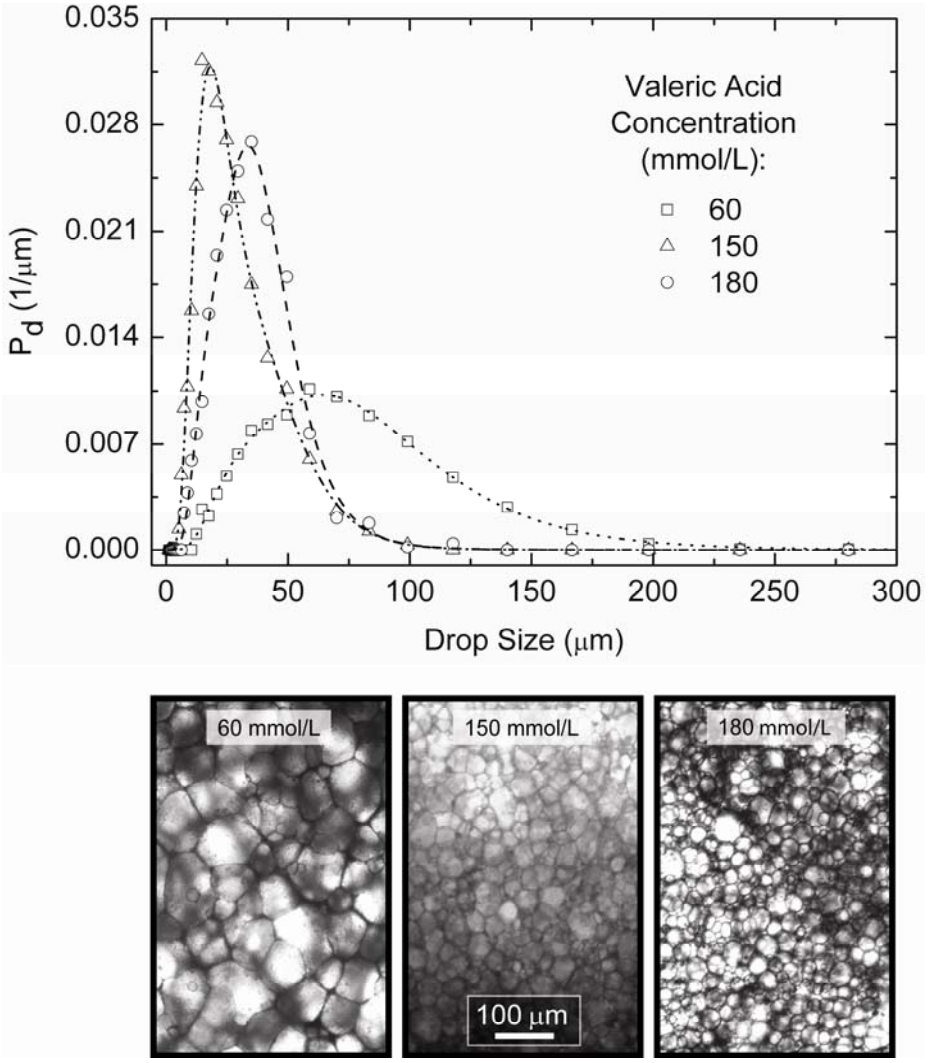

Figure 11.4: Droplet size distributions (top) and optical microscope images (bottom) of water-in-oil emulsions prepared with α-alumina particles and different concentrations of valeric acid. Emulsions were prepared by mixing 83.6 vol% water with suspensions of 10 vol% alumina in oil.

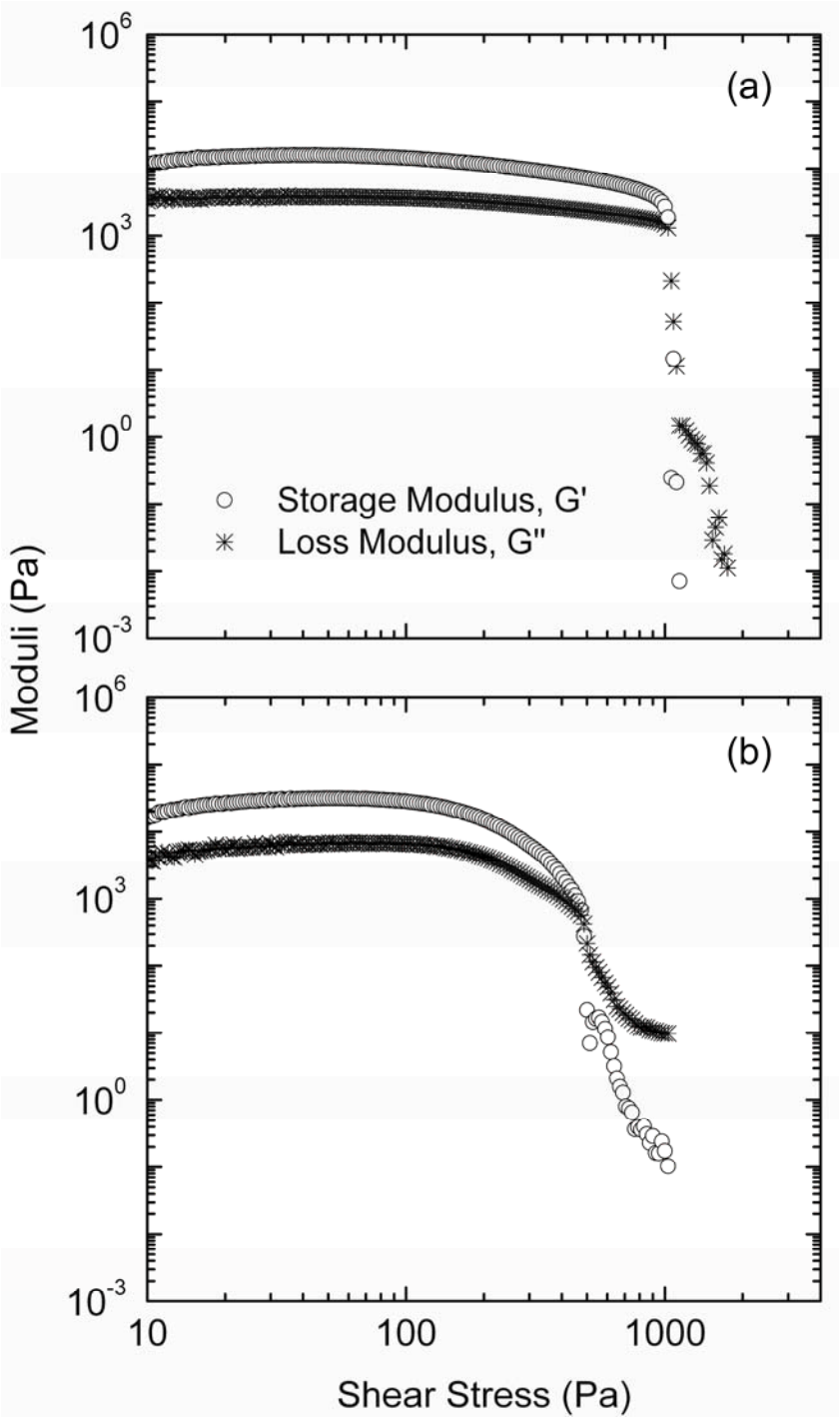

Figure 11.5: Storage (G', ○) and loss (G", ∗) moduli as a function of applied shear stress for (a) octane-in-water emulsion containing 20 vol% δ-alumina particles, 50 mmol/L valeric acid and 81.9 vol% octane, (b) water-in-oil emulsion containing 10 vol% δ-alumina particles, 400 mmol/L valeric acid and 83.6 vol% water.

11.3 Macroporous ceramics from particle-stabilized emulsions

11.3.1 Additional graphs

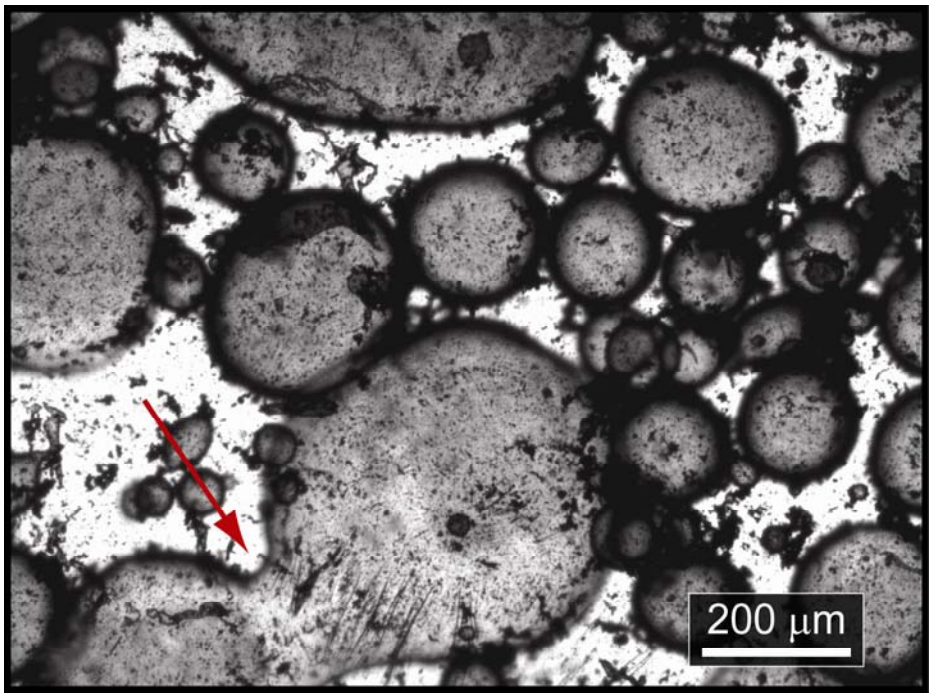

Figure 11.6: Optical microscope image of a wet water-in-oil emulsion showing the partial coalescence of two adjacent droplets (indicated by the arrow). Partial coalescence results in the formation of a “connecting neck” between the droplets. Emulsion was prepared by mixing 70 vol% water with an oil suspension of 1 vol% iron oxide particles and 5 mmol/L octyl gallate for 3 min.

11.4 General route for the assembly of functional inorganic capsules

11.4.1 Estimation of number fraction of particles initially dispersed in the suspension that adsorb onto the capsule surface

We use a simple geometrical analysis to estimate the number fraction of particles initially dispersed in the suspension that afterwards adsorb on the capsule surface. Assuming spherical droplets and particles of average diameters d_{drop} and d_{part}, respectively, one can show that the number fraction of particles adsorbed on the droplet surface f is given by:

$$f = \frac{4x\phi_{oil}d_{part}}{d_{drop}\phi_{part}(1-\phi_{oil})} \qquad \text{Eq. 11.4}$$

where x is the surface coverage of droplets by particles, ϕ_{oil} is the volume fraction of oil in the emulsion, and ϕ_{part} is the volume fraction of particles in the initial suspension.

Assuming hexagonal close packing of particles on the droplet surface (x = 0.90) and average droplet diameters of 5, 5, 10, and 10 μm for emulsions stabilized with alumina, silica, iron oxide and tricalcium phosphate, respectively, we obtained f values varying from 0.42 to 1.35 for the systems investigated in this study (Table 7.1, see Chapter 7).

11.4.2 Additional graphs

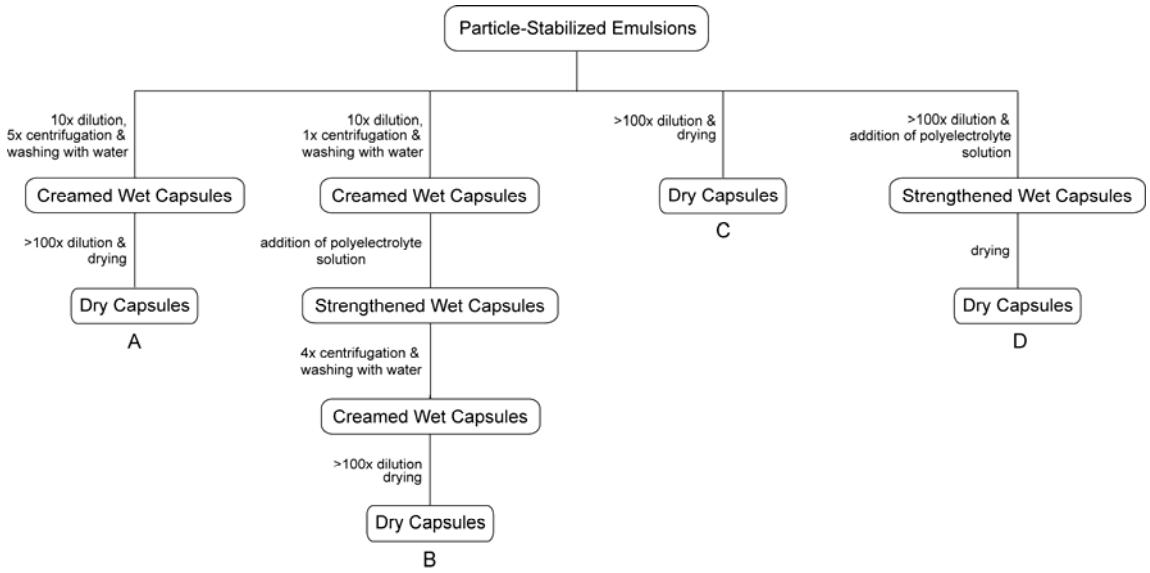

Figure 11.7: Processing flowchart for the fabrication of wet and dry inorganic capsules from particle-stabilized emulsions. Fabrication of capsules via A: centrifugation of emulsions; B: centrifugation in the presence of polyelectrolytes; C: dilution of emulsions without centrifugation; D: dilution of emulsions without centrifugation in the presence of polyelectrolytes.

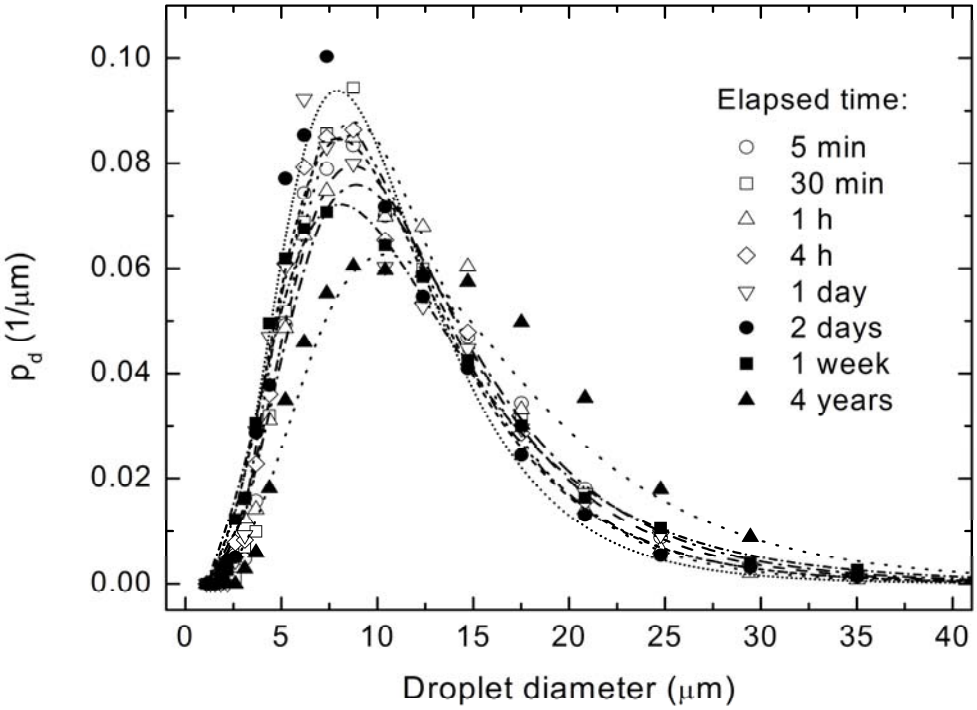

Figure 11.8: Droplet size distribution of oil-in-water emulsions (72 vol% octane) stabilized by α-alumina particles as a function of time after emulsification. The emulsions were prepared by mixing octane with 35 vol% α-alumina suspensions containing an initial propionic acid concentration of 180 mmol/L at pH 4.75.

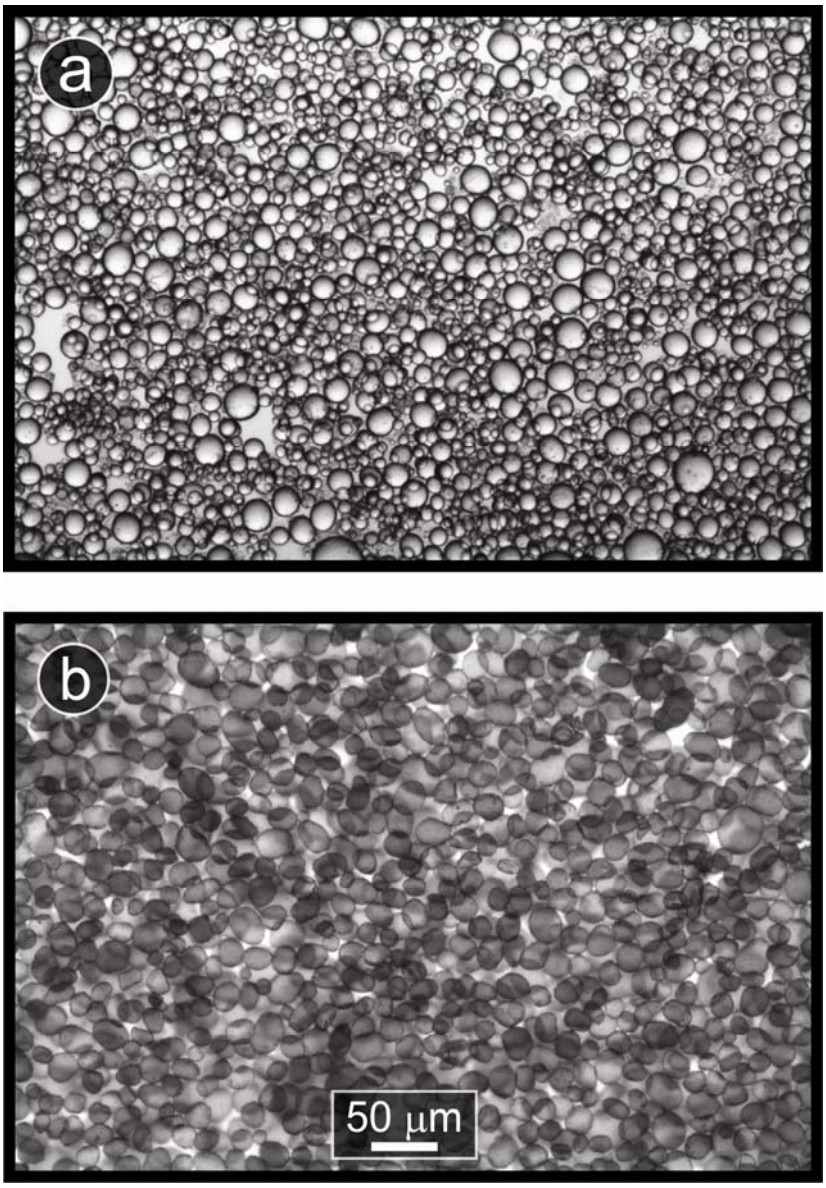

Figure 11.9: Optical microscope images of wet capsules prepared from different inorganic particles following five sequential centrifugation and washing cycles. a) Wet capsules prepared with δ-alumina particles, b) Wet capsules composed of magnetite particle shells.

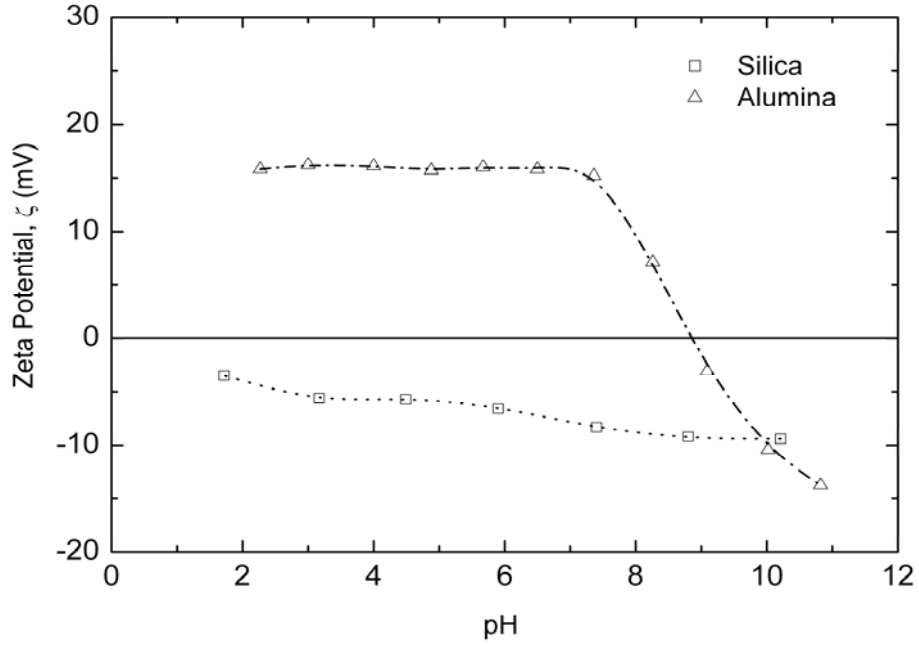

Figure 11.10: Zeta potentials of silica and δ-alumina particles after surface modification with short amphiphilic molecules. All suspensions were prepared with 2 vol% particles. Silica and δ-alumina particles were surface modified with 2.27 mmol/L hexyl amine at pH 10.4 and 6.94 mmol/L butyric acid at pH 4.75, respectively. The zeta potential data for silica indicate that the isoelectric point of this oxide is lower than pH 2, which is in agreement with the range of values reported in the literature [6].

11.5 References

1. Dukhin, A. S., Shilov, V. N., Ohshima, H., Goetz, P. J., *Electroacoustic phenomena in concentrated dispersions: New theory and CVI experiment*. Langmuir, 1999. 15: 6692-6706.

2. van Blaaderen, A., Vrij, A., *Synthesis and characterization of colloidal dispersions of fluorescent, monodisperse silica spheres*. Langmuir, 1992. 8(12): 2921-2931.

3. Janney, M. A., Omatete, O. O., Walls, C. A., Nunn, S. D., Ogle, R. J., Westmoreland, G., *Development of low-toxicity gelcasting systems*. J. Am. Ceram. Soc., 1998. 81(3): 581-591.

4. Ferrari, M., Liggieri, L., Ravera, F., Amodio, C., Miller, R., *Adsorption kinetics of alkylphosphine oxides at water/hexane interface: 1. Pendant drop experiments*. J. Colloid Interface Sci., 1997. 186(1): 40-45.

5. Gonzenbach, U. T., Studart, A. R., Tervoort, E., Gauckler, L. J., *Ultrastable particle-stabilized foams*. Angew. Chem. Int. Ed., 2006. 45(21): 3526-3530.

6. Parks, G. A., *Isoelectric points of solid oxides, solid hydroxides and aqueous hydroxo complex systems*. Chem. Rev., 1965. 65(2): 177-198.